UNIVERSITY OF CALIFORNIA,
IRVINE

HMGB2 regulation of effector, memory, and exhausted $CD8^+$ T cells during viral infection and cancer

DISSERTATION

submitted in partial satisfaction of the requirements
for the degree of

DOCTOR OF PHILOSOPHY

in Biological Sciences

by

Emily N. Neubert

Dissertation Committee:
Assistant Professor Roberto Tinoco, Chair
Professor Melissa Lodoen
Associate Professor Matthew Inlay
Assistant Professor Lisa Wagar

2023

DEDICATION

To my wonderful family:

Amy, Dave, and Maddie

Thank you for the endless love and support, I could not have done this without you

TABLE OF CONTENTS

LIST OF FIGURES

ACKNOWLEDGEMENTS

There are many who have helped me throughout this journey, and I want to take a moment to thank them.

First, I'd like to thank my thesis advisor, Dr. Roberto Tinoco, for his guidance and feedback throughout this project. I'm thankful for his support and for providing me the endless resources to progress my project and allow me to become a better scientist. I would also like to thank my committee members, Dr. Melissa Lodoen, Dr. Matt Inlay, and Dr. Lisa Wagar for their time, thoughtful insights on this project, and for always supporting me both personally and professionally.

I would especially like to thank Vanessa Scarfone at the UCI Sue and Bill Gross Stem Cell Research Center, Dr. Melanie Oakes and Dr. Jenny Wu at the UCI Genomics Core, and Dr. Jennifer Atwood at the UCI Institute for Immunology for technical support and use of core facilities. I would also like to thank the laboratories of Dr. Ilhem Messaoudi and Dr. Rémi Buisson, with special thanks to Dr. Sloan Lewis and Dr. Pedro Ortega for their invaluable collaborations on this project. I would especially like to thank Sloan for being so patient while teaching me how to code and interpret omics data.

Thank you to the staff at the UCI University Laboratory Animal Resources (ULAR) McGaugh Hall facility for all their efforts towards making this project possible. Specifically, Chris Gadegbeku and Catherine Regnier for taking such amazing care of the mice, who I would also be remised not to thank.

I would also like to thank the UCI Center for Virus Research (CVR) and National Institutes of Health for the financial support through the T32 training grant (T32AI007319).

I would like to thank Nature Portfolio for permission to include Chapters 2 and 3 of my dissertation, which were originally published in *Nature Communications*.

Thank you to my amazing lab mates. Specifically, thank you to Julia, Karla, and Melissa for helping me through the hardest experimental days and for being a wonderful support system and sounding board over these last five years.

I am so incredibly grateful for the friends I have made during graduate school. Thank you to Julia, Makena, and Will for being my best friends throughout this whole experience. I can't begin to express how much your friendship has meant to me. You three have provided continued support, laughter, and have been a necessary outlet through the ups and downs of graduate school. I can't imagine a better group for our pandemic bubble. Thank you for sharing in all the memories, food, tears, and reality TV.

Julia, I am so thankful housing randomly placed us together. I could not have survived graduate school without you by my side both in lab and our apartment. Thank you for being my go-to person for experimental help and for being my voice of reason. Also, thank you for adopting Jazz and bringing him into my life. I can't imagine surviving the pandemic and graduate school without him.

Patrick, thank you for believing in me when I didn't believe in myself. You have gone above and beyond in every way over these last five years. I am grateful for your unwavering support no matter how many time zones were between us. I am so thankful that we've been able to help each other succeed in graduate school, and I couldn't be prouder of us.

Lastly, I would like to thank my family. You have all shown me unconditional love, support, and encouragement throughout my entire life and I am extremely thankful. To

my parents and sister, for whom this work is dedicated, I have no way of expressing how much I love you and how influential you were to the completion of this journey. Thank you for believing in me and shaping me into the person I have become.

VITA

Emily N. Neubert

University of California, Irvine

EDUCATION

University of California, Irvine 2018 - 2023
Ph.D. Biological Sciences, emphasis Immunology
Advisor: Dr. Roberto Tinoco

California Polytechnic State University, San Luis Obispo 2014 - 2018
B.S. Cellular and Molecular Biology, *summa cum laude*
B.S. Microbiology, *summa cum laude*

RESEARCH EXPERIENCE

University of California, Irvine 2018 - 2023
Doctoral Candidate
Dr. Roberto Tinoco, Department of Molecular Biology and Biochemistry
Dissertation: "HMGB2 regulation of effector, memory, and exhausted $CD8^+$ T cells during viral infection and cancer"

Seattle Genetics Summer 2018
Research Intern
Department of Experimental Pharmacology
Bothell, WA

California Polytechnic State University, San Luis Obispo 2016 - 2018
Undergraduate Research Assistant
Dr. Edward Himelblau, Department of Biological Sciences

PUBLICATIONS

Neubert EN, DeRogatis JM, Lewis SA, Viramontes KM, Ortega P, Henriquez ML, Buisson R, Messaoudi I and Tinoco R (2023) HMGB2 Regulates the Differentiation and Stemness of Exhausted $CD8^+$ T Cells During Chronic Viral Infection and Cancer. *Nature Communications*.

DeRogatis JM, **Neubert EN**, Viramontes KM, Henriquez ML, Nicholas D and Tinoco R (2023) Cell-intrinsic CD38 Expression Sustains Exhausted $CD8^+$ T cells by Regulating Their Survival and Metabolism During Chronic Viral Infection. *Journal of Virology.* doi:10.1128/jvi.00225-23

Viramontes KM, **Neubert EN**, DeRogatis JM and Tinoco R (2022) PD-1 Immune Checkpoint Blockade and PSGL-1 Inhibition Synergize to Reinvigorate Exhausted T Cells *Front. Immunol.* 13:869768. doi: 10.3389/fimmu.2022.869768

DeRogatis JM, **Neubert EN**, Viramontes KM and Tinoco R (2022) Targeting the PSGL-1 Immune Checkpoint Promotes Immunity to PD-1 Resistant Melanoma. *Cancer Immunol Res*. doi: 10.1158/2326-6066.CIR-21-0690

DeRogatis JM, **Neubert EN**, Viramontes KM and Tinoco R (2021) PSGL-1 Immune Checkpoint Inhibition for $CD4^+$ T Cell Cancer Immunotherapy. *Front. Immunol*. 12:636238. doi: 10.3389/fimmu.2021.636238

Tinoco R, **Neubert EN**, Stairiker C, Henriquez M and Bradley LM (2021) PSGL-1 is a T cell Intrinsic Inhibitor that Regulates Effector and Memory Differentiation and Responses During Viral Infection. *Front. Immunol*. 12:677824. doi: 10.3389/fimmu.2021.677824

AWARDS, HONORS, AND GRANTS

Edward Wagner Award – School of Biological Sciences, UCI	2023
The AAI Young Investigator Award – Immunology Fair, UCI	2022
Best Oral Presentation Award – MB&B Department Retreat, UCI	2022
T32 Virology Predoctoral Training Fellowship, NIH (AI007319)	2020 - 2023
School of Biological Sciences Dean's Graduate Fellowship, UCI	2018
Microbiology Student of the Year, Cal Poly	2018
Brandon D. Huang Memorial Scholarship, Cal Poly	2018

MENTORING

Jonathan Luu, Undergraduate Researcher, UCI	2022 - 2023
Amber Keith, PhD Student, UCI	2022 - 2023
Melissa Thone, Postdoctoral Researcher, UCI	Fall 2022
Jon Salazar, PhD Student, UCI	Spring 2021
Karla Viramontes, PhD Candidate, UCI	Fall 2019

TEACHING EXPERIENCE

University of California, Irvine

Molecular Biology	Spring 2020
General Microbiology and Lab	Winter 2020, Spring 2020
Immunology with Hematology	Winter 2020

PROFESSIONAL DEVELOPMENT

Data Science: R Basics Certification, Harvard University	Spring 2021
Introduction to R Certification, DataCamp	Spring 2021
Adobe Illustrator and Photoshop Certification, Udemy	Spring 2021
Advanced Immunology Course, AAI	Summer 2020

SKILLS

Immunology: Extensive experience in mouse immunology – isolation and preparation of single cell suspensions from spleen, blood, lymph nodes, and tumors, T cell stimulation

and characterization, multi-parameter flow cytometry and panel design (10+ colors), cell sorting (FACS), imaging flow cytometry, surface, intracellular and intranuclear staining, tissue culture.

Genomics: Interpretation and visualization of RNA (Bulk RNA-Seq) and chromatin (ATAC-Seq) profiling.

Software: Adobe Illustrator, FlowJo, GraphPad Prism, R, MacOS, MS Office and Excel.

Communication: Public speaking, collaboration, technical writing, peer-reviewed publication, teaching, and mentoring.

ABSTRACT OF THE DISSERTATION

HMGB2 regulation of effector, memory, and exhausted CD8$^+$ T cells during viral infection and cancer

by

Emily N. Neubert

Doctor of Philosophy in Biological Sciences

University of California, Irvine, 2023

Assistant Professor Roberto Tinoco, Chair

CD8$^+$ T cells are a critical component of adaptive immune responses, mediating the clearance of viral infections and cancers while providing long-term protection. In response to infection, CD8$^+$ T cells enter a range of differentiation states dictated by antigen strength and other environmental cues. These extrinsic signals induce a network of transcriptional regulators that further specify the CD8$^+$ T cell fate decision. The significant impact of extrinsic signals on the quality of T cell responses and the subtypes of T cells produced is highlighted by the drastic differences in phenotype and function of T cells arising during acute and chronic infections. During acute infections, antigen-specific CD8$^+$ T cells differentiate into cytotoxic effector T cells that clear the infection before a small subset differentiate into memory T cells for long-lived immunity. These effector and memory T cell differentiation programs are altered during chronic viral infections and cancers due to persistent antigen stimulation, resulting in antigen-specific CD8$^+$ T cells entering a state of exhaustion. Exhausted CD8$^+$ T cells are dysfunctional compared to the effector and memory T cells that arise during acute infections, resulting in impaired immune responses to chronic infections and diminished long-term protection.

As with effector and memory differentiation, exhaustion is accompanied by specific transcriptional and epigenetic programs that reinforce this terminal cell fate. However, the complete characterization of the cellular and molecular mechanisms underlying effector, memory, and exhausted $CD8^+$ T cell differentiation are still unknown.

We investigated the role of HMGB2, a chromatin modifier, on the transcriptional and epigenetic networks that modulate terminal differentiation of antigen-specific $CD8^+$ T cells during acute and chronic infections. During acute LCMV Armstrong infection, we found HMGB2 was critical for the differentiation and maintenance of memory $CD8^+$ T cells, and more specifically the central memory T cell (Tcm) subset. Tcm cells are critical for secondary immune responses to reinfections, and correspondingly, memory *Hmgb2*$^{-/-}$ $CD8^+$ T cells were unable to mount a response to a secondary challenge. We showed that HMGB2 regulated the accessibility of memory and stem cell associated genes that were required for memory T cell differentiation and recall responses. We also found that HMGB2 expression was dispensable for effector $CD8^+$ T cell responses, as WT and *Hmgb2*$^{-/-}$ $CD8^+$ T cells had equivalent frequencies, numbers, and cytotoxic function during Arm infection. In contrast, we found a critical role for HMGB2 in the maintenance of exhausted $CD8^+$ T cells during chronic LCMV Cl13 infection and cancer. We found that HMGB2 was required for the differentiation and survival of progenitor exhausted (Tpex) T cells, which are critical for seeding the exhausted T cell pool and re-expansion to immune checkpoint blockade therapies. Therefore, exhausted *Hmgb2*$^{-/-}$ $CD8^+$ T cells were lost during Cl13 infection and within melanoma tumors, with an inability to re-expand upon secondary acute infection. We found HMGB2 regulated the accessibility and expression of Tpex associated genes, while inhibiting the accessibility and expression of

genes associated with terminally exhausted (Tex) T cells. The decline of these more terminally exhausted *Hmgb2*$^{-/-}$ CD8^{+} T cells resulted in diminished viral and tumor control using both *in vivo* adoptive transfer T cell models and *Hmgb2*$^{-/-}$ mice. Together, this dissertation details the critical role for HMGB2 in regulating the transcriptional and epigenetic networks of memory and exhausted CD8^{+} T cell differentiation. This work is an important contribution to our current understanding of CD8^{+} T cell fate decisions during acute and chronic infections, with various implications for vaccination and immunotherapeutic strategies.

CHAPTER 1

Introduction

1.1 T Cell Activation

After maturation, naïve $CD8^+$ T cells exit the thymus and continuously migrate throughout secondary lymphoid organs. Within this population of naïve T cells, a small proportion are able to respond to infection by any given pathogen. Effective T cell activation requires three signals to produce a productive response to an infection, with only the first signal being antigen-specific. First, naïve $CD8^+$ T cells scan the cell surface of antigen presenting cells (APCs), which are immune cells that display antigen in the form of processed peptides on their major histocompatibility complexes (MHC). Once the T cell receptor (TCR) of a naïve $CD8^+$ T cell encounters its cognate antigen presented by an MHC class I molecule, this interaction serves as the first signal required for optimal T cell activation. The final two signals are from co-stimulation molecules (CD80/86 and CD28) and cytokines (Il-12, Type-I interferons). Combined, these three signals generate intracellular TCR signaling pathways that cause antigen-specific $CD8^+$ T cells to rapidly proliferate and acquire effector functions. However, each signal can individually influence the effector T cell response: TCR signal strength and duration impacts the proliferation and differentiation of activated T cells; the surface molecules providing co-stimulation result in unique downstream signaling and gene expression; cytokines initiate distinct signaling and transcriptional pathways[1, 2, 3]. Therefore, the pathogen and resulting inflammation determines the cell fate and longevity of the responding T cell pool. Additionally, the transition from naïve to effector T cells is accompanied by dynamic transcriptional and epigenetic changes which ultimately impact the fundamental identity of effector T cells. These changes are regulated by upstream transcription factors that initiate early effector gene expression and epigenetic modifications that impact chromatin

accessibility. The subsequent CD8$^+$ T cell response after activation differs depending on the type of infection encountered; acute infections (those cleared quickly) result in the differentiation of effector and memory T cells while chronic infections (those persisting long-term) initiate the T cell exhaustion program and prevent memory T cell development. The differences between CD8$^+$ T cell responses to acute and chronic infections will be discussed further in subsequent chapters. Together, the activation of naïve CD8$^+$ T cells involves multiple signals, which impact the cell fate decision, survival, and accumulation of effector T cells during acute and chronic infections.

1.2 CD8$^+$ T Cell Responses to Acute Viral Infections

The immune response to viral infections centers around the differentiation of cytotoxic CD8$^+$ T cells from their naïve precursors. Acute viral infections usually result in effective anti-viral T cell responses, with the robust proliferation and expansion of differentiated effector CD8$^+$ T cells that specialize in killing infected cells. Once the virus is cleared from the host, effector T cells experience reprieve from antigen and functional memory CD8$^+$ T cells develop, providing long-term protection from reinfection. Overall, the CD8$^+$ T cell response can be characterized by three distinct phases: (i) expansion; (ii) contraction; and (iii) memory differentiation (**Fig. 1.1**). In the following sections, I will provide a summary of the foundational literature and regulation surrounding effector and memory CD8$^+$ T cell responses.

1.2.1: Effector T cell differentiation

As described in the previous section, antigen-specific naïve CD8$^+$ T cells that are activated will proliferate and differentiate into effector CD8$^+$ T cells. These effector T cells migrate to peripheral sites of infection and kill infected cells through expression of effector

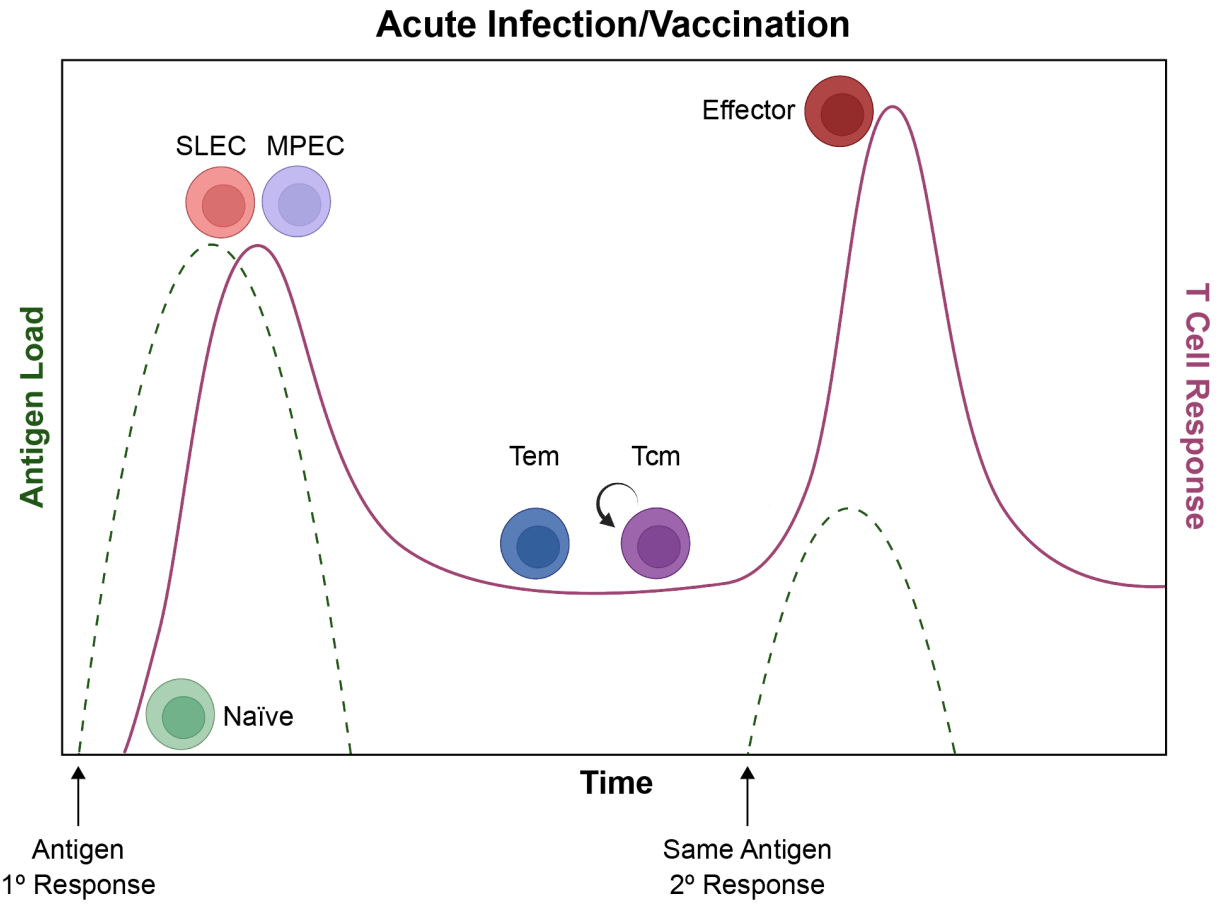

Figure 1.1 T cell differentiation in response to acute infection or vaccination. Upon activation by cognate antigen, naïve $CD8^+$ T cells differentiation into SLECs and MPECs, subsets within the Teff pool, to control peak antigen load. The majority of Teff cells die, with remaining cells differentiating into Tmem cells (Tem and Tcm). Following secondary antigen exposure, Tmem cells are reactivated and differentiate into secondary Teff cells to control the infection. Abbreviations: SLEC, short-lived effector T cell; MPEC, memory precursor effector T cell; Teff, effector T cell; Tem, effector memory T cell; Tcm, central memory T cell.

molecules, including perforin, granzymes and anti-viral cytokines. During this expansion, antigen-specific effector $CD8^+$ T cells further differentiate and form a heterogenous population, consisting of two major subsets: short-lived effector T cells (SLECs) and memory precursor effector T cells (MPECs)[4]. SLECs are terminally differentiated cytotoxic T cells with increased KLRG-1 expression and reduced expression of CD127, which have full cytotoxic capacity and are mainly responsible for eliminating infected cells. Comparatively, MPECs make up a much smaller subset of the effector T cell pool and retain CD127 expression and downregulate KLRG-1. These cells are precursors to the memory T cell compartment since they have greater potential to survive long-term after pathogen clearance. The bifurcation of these two subsets is regulated by both extracellular and intracellular signals that are not fully understood, although a few lineage-specifying transcription factors have been identified. Known transcription factors crucial for the initial expansion and differentiation of SLECs are IRF4, STAT1, TBET, BLIMP1, ID2 and ZEB2, while EOMES, TCF-1, FOXO1, ID3, BACH2, and STAT3 promote MPEC differentiation[1, 2, 5, 6, 7, 8, 9, 10, 11, 12, 13, 14]. Additionally, epigenetic differences between SLECs and MPECs may mechanistically explain the divergence in their gene expression profiles. For example, DNMT3A and TET2 inhibit MPEC formation by methylating genes (repressing transcription) associated with memory T cell differentiation and function[15, 16]. Additionally, SLECs have repressive histone modifications at genes required for survival and memory T cell formation[17], while MPECs have more open regulatory regions at genes related to naïve and memory properties[18]. Once the pathogen is cleared, only 5-10% of effector T cells surviving to form the long-lived memory T cell pool[19, 20]. The majority of SLECs undergo apoptosis while the MPECs survive this contraction and transition to

memory CD8$^+$ T cells[8, 21]. Contraction of the effector T cell pool is critical because this prevents stimulated CD8$^+$ T cells from damaging healthy cells and tissues after the resolution of infection.

1.2.2: Memory T cell differentiation

Memory CD8$^+$ T cell differentiation is critical for effective and rapid responses upon reinfections with the same pathogen. Importantly, memory T cells are more efficient than naïve T cells in mounting effector responses and combating infection. Not only are there significantly increased numbers of antigen-specific memory T cells compared to antigen-specific naïve T cells, but memory T cells are also capable of circulating peripheral tissues, allowing them to localize to different sites of re-infection. Furthermore, memory T cells have a unique epigenetic state compared to naïve T cells that supports a more accelerated antigen-specific response[22, 23]. Memory CD8$^+$ T cell differentiation is progressive after antigen clearance, resulting in unique genotypic, phenotypic, and functional properties[24, 25, 26]. Memory T cells downregulate effector molecules but can quickly reacquire cytotoxic activity with pathogen re-exposure. They are also maintained long-term via homeostatic proliferation that preserves the memory T cell pool in the absence of antigen. Within the memory CD8$^+$ T cell compartment, there are distinct subsets defined by effector function, proliferative potential, transcriptional program, and contribution to protection from reinfection[26, 27, 28, 29, 30, 31, 32]. The classic memory T cell subsets are effector memory (Tem) and central memory (Tcm) T cells. Tem cells are more cytotoxic with constitutive effector functions and migrate to peripheral tissues within the host[1, 28, 30, 33, 34]. Comparatively, Tcm cells are long-lived, have enhanced self-renewal and proliferative capacity, traffic through lymphoid tissues, and facilitate the maintenance

of long-term memory T cell responses[29, 30, 35, 36, 37, 38, 39]. Tcm cells are also capable of differentiating into effector T cells after reinfection. Despite having decreased proliferation upon re-infection, Tem cells quickly produce effector molecules and serve as the first line of defense, while Tcm cells are considered the critical memory subset for robust, long-term protection.

The heterogeneity within the $CD8^+$ memory T cell pool allows for the maintenance of a stable T cell population capable of producing rapid, effective responses upon re-infections. The differentiation of memory T cells is regulated by a specific network of transcription factors that modulate gene expression. Additionally, these transcription factors can also alter chromatin structure through recruitment of chromatin modifying enzymes or through their intrinsic activity. Specific transcription factors critical for memory T cell identity include FOXO1, RUNX3, BCL-6, LEF1, and TCF-1. FOXO1 is critical for memory T cell development and maintenance, with decreased quantity and self-renewal capacity of memory T cells without *Foxo1* expression[40, 41, 42, 43]. FOXO1 directly promotes the expression of pro-memory and pro-survival genes, including *Il7r, Bcl2, Sell, Ccr7, Tcf7, Eomes,* and *Bach2*, and may do so through shielding these loci from repressive chromatin modifications[17, 44, 45]. RUNX3 and BCL-6 also drive memory T cell formation, with RUNX3 directly modulating the accessibility of memory T cell *cis*-regulatory elements and BCL-6 binding regulatory regions of memory genes, including *Tcf7*[46, 47]. The epigenetic program of memory T cells also allows them to rapidly reacquire effector functions upon reinfection and be long-lived. Specifically, memory $CD8^+$ T cells are demethylated at promoters of effector genes (including *Ifng*, *Gzmb*, and *Prf1*) and survival genes (including *Bcl2* and *Il7r*)[48, 49, 50, 51].

TCF-1 is a critical regulator of memory T cell differentiation, self-renewal, and recall responses. TCF-1 is a key transcription factor of the Wnt signaling pathway, plays a crucial role in T cell fate specification, and is a well-established regulator of $CD8^+$ T cell self-renewal[52, 53]. The expression of TCF-1 is downregulated in effector T cells but reacquired in memory, with TCF-1 expression required for the formation and survival of MPECs and Tcm cells, but not for effector T cell responses[7, 54, 55, 56, 57]. In addition to its role as a transcription factor, TCF-1 also has intrinsic histone deacetylase activity, thereby condensing chromatin and repressing gene transcription[58, 59]. More specifically, TCF-1 is required for preprogramming a transcriptional program in memory T cells that supports their rapid recall responses upon secondary challenge[60]. TCF-1 also induces the deacetylation of effector genes, including *Prdm1*, in favor of memory T cell formation[7, 59]. Furthermore, TCF-1 deficient memory $CD8^+$ T cells have compromised self-renewal and differentiation into secondary effectors upon reinfection[7, 54, 55].

Overall, there is a complex network of transcription factors and epigenetic modifying proteins that regulate the effector vs. memory fate decision in activated $CD8^+$ T cells. Despite some characterization, the majority of these proteins involved still need to be identified. Moreover, the relationships between regulators and how they may interact to drive T cell subset-specific differentiation are still unknown. It is imperative to identify the critical regulators of memory T cell formation as this understanding could help reprogram terminally differentiated $CD8^+$ T cells and contribute to the design of T cell-based therapies and vaccines.

1.3 $CD8^+$ T Cell Responses to Chronic Infections

During acute infections, naïve $CD8^+$ T cells are activated and undergo robust proliferation and differentiate into effector $CD8^+$ T cells. Following antigen clearance, a small subset of activated $CD8^+$ T cells differentiate into memory T cells which are critical for recall responses upon reinfections. However, in cases of chronic viral infections and cancer where the pathogen is not cleared, $CD8^+$ T cells are persistently stimulated by antigen. This continued TCR stimulation alters effector and memory T cell differentiation, inducing a hyporesponsive state of dysfunction in antigen-specific T cells called exhaustion (**Fig. 1.2**). T cell exhaustion is characterized by high co-expression of multiple inhibitory molecules, diminished effector function, altered transcriptional, epigenetic and metabolomic programs, and overall ineffective viral and tumor control. Despite an inability to eliminate chronic infections, exhausted T cells prevent continued activation of effector T cells that would induce T cell-mediated pathology and mortality of the host. Therefore, exhaustion is an intrinsic regulatory mechanism that prevents immune system overactivation. Since exhausted T cells are a unique immune cell type with central roles in chronic viral infections and cancer, they have become a critical target for immunotherapies, which target the immune systems of chronically infected patients for therapeutic benefit. However, these therapies are not robustly effective and fail in the majority of patients. In order to improve upon current immunotherapies, it is clinically important to have a better understanding of the development, molecular mechanisms, and transcriptional and epigenetic programs of exhausted T cells.

1.3.1: Exhausted T cell characteristics

T cell exhaustion was first used to described persistent but functionally compromised $CD8^+$ T cells in mice with chronic lymphocytic choriomeningitis virus

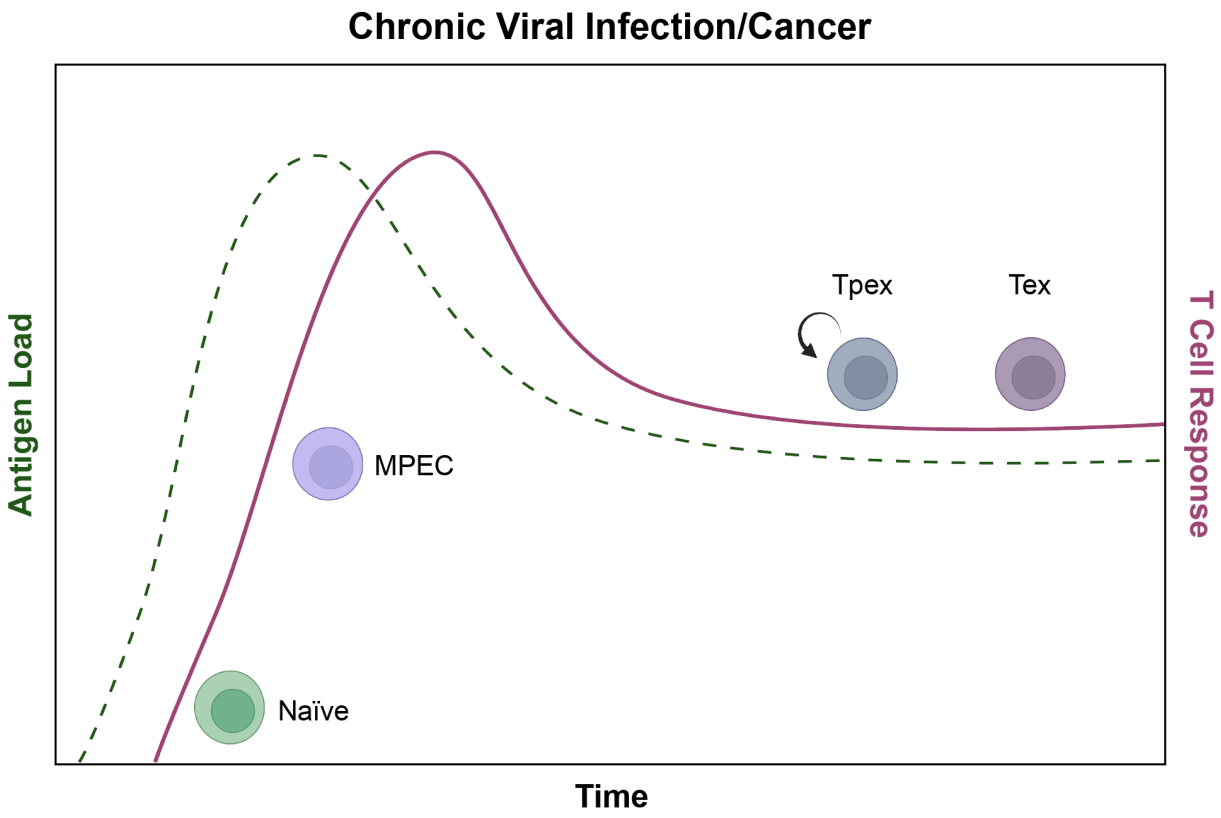

Figure 1.2 T cell differentiation in response to chronic infection or cancer. Upon activation by cognate antigen, naïve $CD8^+$ T cells differentiation into MPECs and eventually fully differentiate into Tex cells. During chronic infection or cancer, Tex cells are unable to clear antigen and develop into Tpex and then terminal Tex cells, before being deleted entirely. Abbreviations: MPEC, memory precursor effector T cell; Tex, exhausted T cell; Tpex, progenitor exhausted T cell.

(LCMV) infection[61]. These antigen-specific T cells were unable to control the viral infection due to diminished cytotoxicity and cytokine production[62, 63]. Since their initial discovery decades ago, exhausted T cells have been identified as a unique T cell population, functionally distinct from effector and memory T cells. Exhausted T cells are characterized by their hierarchical loss of effector functions, decreased proliferative capacity, upregulation of inhibitory receptors, and altered transcriptome and epigenetic program (**Fig. 1.3**)[64]. T cells enter this exhaustion program during chronic viral infections and cancers due to high load and long duration of antigen exposure. Additionally, severity of exhaustion correlates to inhibitory receptor expression, anti-inflammatory signals from immunomodulatory cells and cytokines, and decreased $CD4^+$ T cell help[65]. Exhausted T cell responses have been identified in many human chronic viral infections, including human immunodeficiency virus (HIV), hepatitis B virus (HBV), and hepatitis C virus (HCV)[66, 67, 68].

Exhausted T cells begin losing effector functions at early stages of chronic infection, which becomes progressively more severe as the infection progresses. First, exhausted $CD8^+$ T cells lose the ability to produce IL-2 and have reduced proliferation capacity[69]. Exhausted T cells then lose TNF-α and IFN-γ production, as well as cytotoxicity, which combined results in severely defective effector function. Finally, the responding exhausted T cells die via apoptosis and are physically eliminated in the host. Together, this promotes pathogen persistence but prevents immune-mediated pathology. Exhausted $CD8^+$ T cells are also characterized by their co-expression of multiple inhibitory receptors, surface molecules that regulate the overactivation of T cells. At late stages of acute infections, effector T cells begin expressing inhibitory receptors to

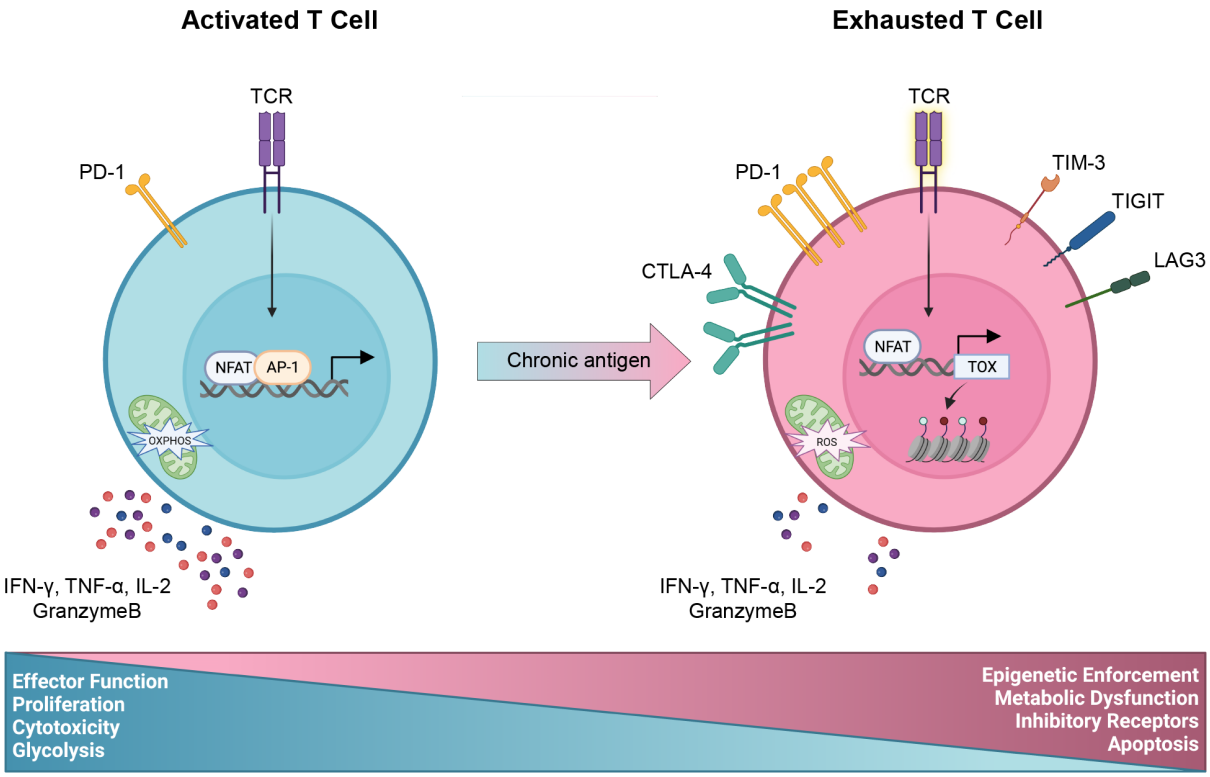

Figure 1.3 Characteristics of functional and exhausted T cells.
Chronic antigen exposure drives T cell exhaustion in chronic viral infections and cancer. Exhausted T cells have increased expression of inhibitory receptors, increased TOX expression which drives the fixed exhaustion epigenetic program, decreased production of effector molecules, and metabolic dysfunction. Together, these alterations result in diminished cytotoxicity and prevents effective viral and tumor control. Abbreviations: OXPHOS, oxidative phosphorylation; ROS, reactive oxygen species; TCR, T cell receptor.

attenuate T cell activation and limit immune function to prevent immunopathology. In contrast, exhausted T cells have elevated and prolonged expression of multiple inhibitory receptors, including PD-1, TIM-3, LAG3, CTLA-4, and TIGIT, which dampen positive costimulatory signals in these cells[70]. These inhibitory receptors utilize various mechanisms to damped exhausted T cell function, including competitive binding and reduction of TCR signaling. Despite being dysfunctional compared to effector $CD8^+$ T cells arising during acute infections, exhausted $CD8^+$ T cells maintain some antiviral function; depletion of exhausted $CD8^+$ T cells from mice infected with chronic LCMV[71, 72] or from macaques with simian immunodeficiency virus (SIV)[73, 74] results in increased viral loads. Exhausted T cells are also characterized by metabolic dysfunction. Compared to effector and memory T cells which utilize aerobic glycolysis and elevated oxidative phosphorylation (OXPHOS) respectively, exhausted T cells have suppressed mitochondrial respiration and glycolysis, with increased reactive oxygen species (ROS)[75, 76, 77, 78]. Underlying the phenotypic and functional differences between exhausted T cells and other T cell subsets are unique epigenetic and transcriptional changes that will be discussed in a subsequent section.

Tumor-specific $CD8^+$ T cells also have hallmarks of T cell exhaustion, with these dysfunctional T cells identified in patients with melanoma[79, 80, 81, 82, 83], chronic myeloid and lymphocytic leukemia[84, 85, 86], ovarian cancer[87], non-small cell lung cancer[88, 89], and Hodgkin lymphoma[90]. The tumor microenvironment exacerbates chronic stimulation of tumor-specific T cells through the presence of abundant ligands for co-inhibitory receptors, inhibition of aerobic glycolysis, and downregulation of MHCI expression[91, 92]. These mechanisms of immune evasion allow for the long-term persistence of cancer

cells, similar to that seen during chronic viral infections, and result in tumor-specific T cells entering the exhaustion-specific differentiation program.

1.3.2: Exhausted T cell subsets

Exhausted T cell (Tex) differentiation is a dynamic and progressive process with heterogeneity in the responding T cells. The differentiation and cell fate of exhausted T cell subsets are defined by specific transcriptional programs, which are enforced at the epigenetic level. Additionally, these subsets are further defined by functionality. Although memory and exhausted T cells arise from the same pool of naïve T cells, the persistent antigen stimulation during chronic infections drives the exhaustion fate decision, resulting in the progressive loss of their memory potential[93, 94].

Recently, there is a proposed linear differentiation process of T cell exhaustion, which consists of progenitor, intermediate, and terminally exhausted subsets (**Fig. 1.4**)[95, 96]. Progenitor exhausted T cells (Tpex) express TCF-1, CXCR5, Slamf6, ID3, and BACH2, with low expression of TIM-3[97, 98, 99, 100, 101]. Tpex cells continuously proliferate and are referred to as “stem-like” because they self-renew and generate the more terminal exhausted subsets[98, 102]. However, Tpex cells are not multipotent in that their differentiation is limited to the generation of exhausted subsets. In this way, Tpex and memory T cells have functional similarities, but are transcriptionally and epigenetically distinct[100]. The formation, maintenance, and function of Tpex cells require the transcription factor TCF-1[52, 102, 103, 104, 105, 106]. TCF-1 stabilizes Tpex cells by promoting the expression of EOMES, BCL-6, cMyb, and BCL-2, which antagonize terminal differentiation and promote survival[97, 98, 100, 101]. The Tpex population is of clinical importance, as immune checkpoint blockade (ICB) therapies specially target their

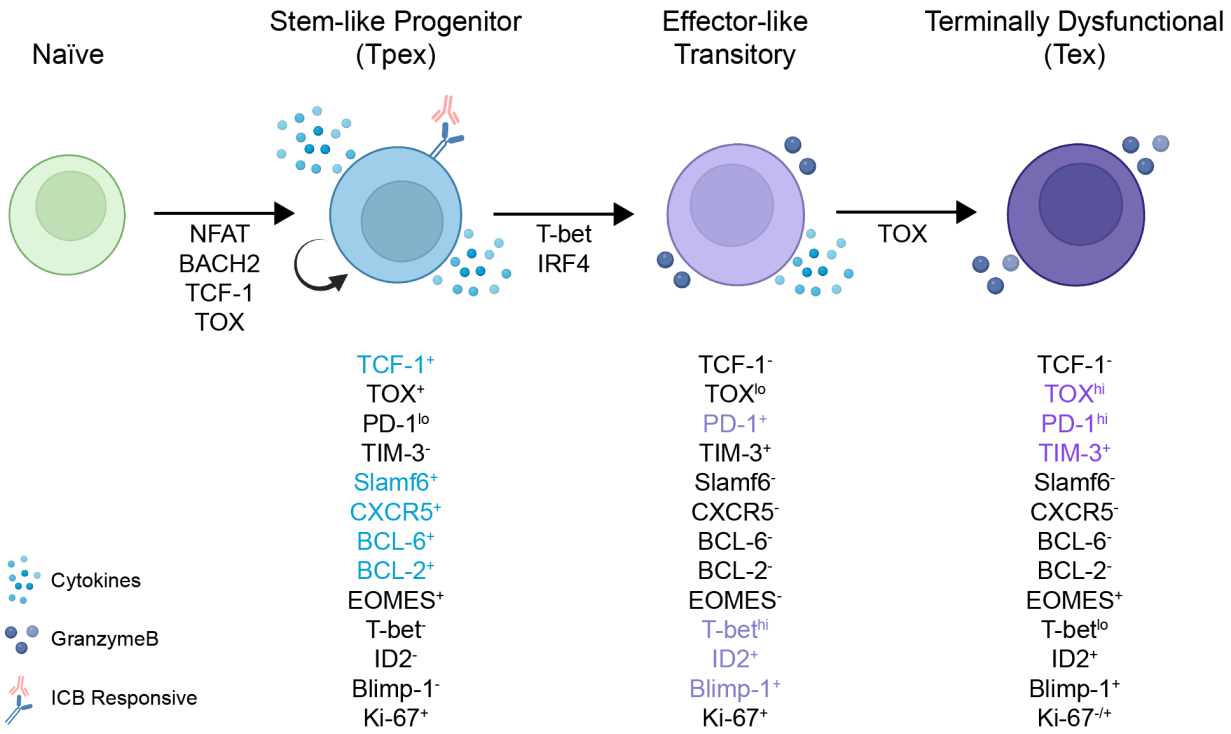

Figure 1.4 Subsets of exhausted T cells.
Proposed linear model of exhausted T cell differentiation during chronic viral infections and cancer. Transcription factors and surface markers defining progenitor exhausted (Tpex), transitory effector-like exhausted, and terminally exhausted (Tex) T cell subsets.

expansion and proliferation to reinvigorate adaptive immune responses in chronically infected patients, which will be discussed in greater detail in a subsequent section.

The intermediate subset is an effector-like transitory exhausted population that is characterized by downregulation of TCF-1, upregulation of TOX, and surface expression of PD-1 and CX3CR1[107, 108]. Transitory exhausted T cells represent an intermediate cell state between Tpex and terminal Tex cells, with retained proliferative capacity and the initiation of GranzymeB production[107]. Compared to Tpex cells, transitory Tex cells have increase effector function. Transcriptionally, transitory Tex cells are defined by their expression of BATF, IRF4, T-bet, Blimp-1, and ID2[92]. Although transitory Tex cells are similar in function and transcription factor expression to effector $CD8^+$ T cells arising during acute infections, the two subsets are epigenetically distinct[109].

Finally, terminal Tex cells are short-lived and have the most severe functional defects; although they have increased effector function compared to the other subsets, they have the lowest proliferation capacity, polyfunctionality, and are unamenable to reinvigoration[110]. Terminal Tex cells do not express TCF-1, and instead overexpress TOX, which transcriptionally and epigenetically reinforces the exhaustion program[95]. They also have high co-expression of the inhibitory receptors PD-1, TIM-3, LAG3, and CD38, with low expression of CXCR5, CD44, and Slamf6[110]. The terminal exhausted state of this subset prevents their reinvigoration, while Tpex and transitory Tex cells are both reinvigorated with ICB therapy[111].

1.3.3: Epigenetic and transcriptional profile of exhaustion

Cell fate is largely determined by transcriptional programs, where the expression of specific genes is regulated by networks of transcription factors and chromatin

accessibility. Exhausted $CD8^+$ T cells are a distinct T cell lineage compared to naïve, effector, and memory, and as such, have a unique profile of transcriptional and epigenetic factors that drive and reinforce this state of dysfunction (**Fig. 1.5**). The majority of phenotypic and functional differences between these distinct T cell subsets can be explained by differences in their epigenetic landscapes. The overall epigenetic state of exhaustion is not only unique to exhausted T cells but is extremely stable with a temporal link between the establishment of the exhaustion-specific epigenetic signature and the commitment to exhaustion. Epigenetic programs are associated with changes in histone modifications, DNA methylation, chromatin accessibility, and expression of transcription factors (discussed in subsequent section). Importantly, recent epigenetic analyses in mouse and human chronic viral infections and cancers have shown a conserved exhausted T cell epigenetic profile between species and across chronic infections[111, 112, 113, 114]. These exhausted T cells have common differentiation programs, regulatory mechanisms, and epigenetic modifications, thereby suggesting that exhausted T cell epigenetic regulation is mainly driven by chronic TCR signaling. Some of these conserved epigenetic signatures unique to exhausted T cells include decreased accessibility of genes associated with effector T cell differentiation (*Ifng, Tnfa, Il2, Klrg1*) and increased accessibility of genes associated with exhaustion (*Pdcd1, Havcr2, Lag3, Tigit, Tox, Tcf7*)[44, 109, 115, 116]. The common differentiation program across species and infection types suggests the transcriptional and epigenetic programs unique to exhaustion are regulated by a common network of transcription factors and chromatin modifiers. However, the complete regulatory network underlying the exhaustion-specific program is unknown.

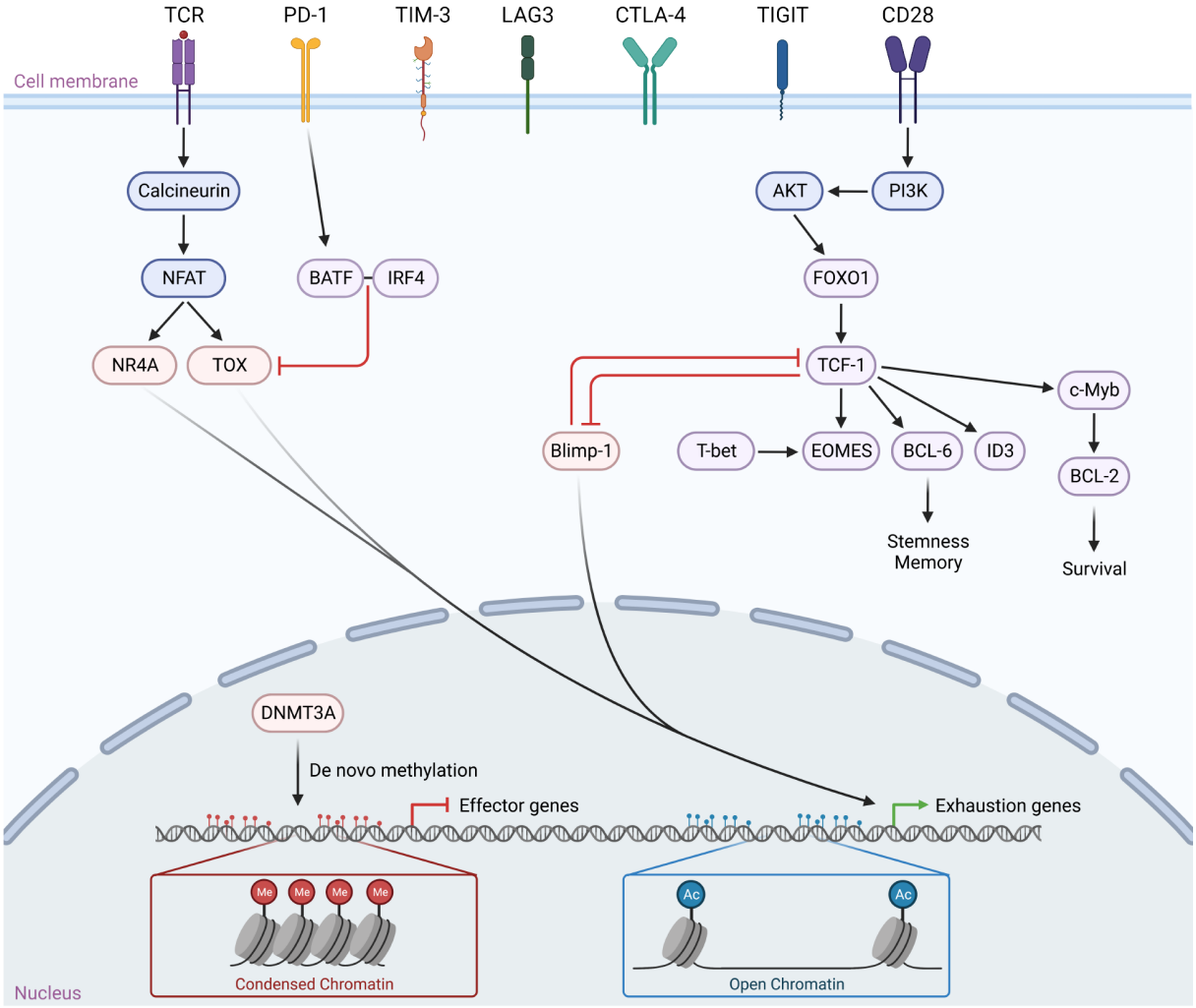

Figure 1.5 Regulatory network of exhausted T cells.
Chronic TCR signaling drives exhaustion, activating NFAT and its downstream molecules (mainly NR4A and TOX) through calcineurin, thereby upregulating expression of inhibitory receptors. TOX and NR4A promote and maintain Tex cells through epigenetic and transcriptional modifications. Transcription factor TCF-1 is activated by CD28 and the FOXO1 signaling network, driving the formation and survival of Tpex cells through promoting expression of EOMES, BCL-6, and BCL-2. Blimp-1 and TCF-1 repress each other, with Blimp-1 promoting Tex cells through inhibiting expression of memory T cell genes. DNMT3A epigenetically reinforces the exhaustion program through silencing effector and memory T cell genes.

One notable epigenetic signature of exhausted T cells is an additional enhancer upstream of the *Pdcd1* (PD-1) loci. Although $CD8^+$ T cells activated during acute and chronic infections express PD-1, this enhancer is only found in exhausted T cells and not effector or memory[116, 117]. Additionally, the *Pdcd1* promoter and two proximal enhancer elements are fully demethylated, whereas these regions are methylated, and thus *Pdcd1* expression is repressed, after acute LCMV clearance[118]. Another important regulator of the exhausted T cell epigenetic program is the methyltransferase DMNT3A, which catalyzes methylation events during exhausted T cell differentiation[119]. When DNMT3A is deleted, there is an increase in the expression of memory associated genes, including *Tcf7*, suggesting it enforces the differentiation of terminally exhausted T cells[119]. Significantly, the epigenetic state of exhausted T cells is fixed and irreversible, even with reactivation or ICB therapy. These exhaustion-specific epigenetic features are initiated early on during chronic infections, with the fixed epigenetic state developing over time. This stepwise acquisition of the exhausted epigenetic program was highlighted in adoptive transfer experiments of tumor-specific $CD8^+$ T cells, where two distinct phases of chromatin remodeling were identified that enforce the differentiation of exhausted T cells after activation instead of effector or memory T cells[94]. Furthermore, exhausted T cells experience epigenetic imprinting, where core exhaustion epigenetic features are propagated to progeny[94, 100, 119, 120, 121]. Despite ICB therapy inducing robust reinvigoration of exhausted T cells in patients, the epigenetic state of antigen-specific exhausted T cells changes only slightly, preventing robust therapeutic responses in the majority of patients[117]. The unique epigenetic program of exhausted T cells helps explain their

altered network of transcription factors and the exhaustion-specific gene regulation of these cells.

As with the epigenetic program, the transcriptional signature of exhausted T cells has been investigated, with numerous important regulators identified. Of note, many exhausted T cell features are associated with the altered use of transcription factors commonly used by functional effector and memory T cells[122, 123]. These transcription factors are expressed in exhausted T cells but form distinct transcriptional networks unique to exhausted T cell differentiation and function. Overall, there is a temporally regulated hierarchy of transcription factors that establish and maintain exhaustion during chronic infections: first, chronic TCR signaling after activation results in partnerless NFAT inducing the expression of inhibitory genes (*Pdcd1, Havcr2, Tox*)[124, 125]; second, TCF-1 and BACH2 enforce the differentiation of Tpex cells, as well as their self-renewal, proliferation and survival[100]; third, T-bet drives the transition from Tpex to the transitory effector exhausted state[8]; finally, TOX, EOMES, and NR4A drive terminal Tex cell differentiation and support their persistence during later stages of chronic infection[95, 126, 127]. During this temporal regulation of the exhaustion-specific transcriptional program, key regulators have been identified with similar roles in exhausted T cells from chronic viral infections and cancers. Transcription factors supporting Tpex differentiation and function include TCF-1, FOXO1, BACH2, ID3, BCL-2, and BCL-6[41, 43, 100, 123, 128], while those associated with terminal Tex cells include TOX, EOMES, NFAT, and Blimp-1[98, 123, 124, 129]. Of these transcription factors, TCF-1 and TOX are the two most important regulators of the exhaustion cell fate decision and the differentiation of Tpex and terminal Tex cells.

1.3.4: TCF-1 and TOX

TCF-1 is a key transcription factor of the Wnt signaling pathway, with a critical role in T cell fate decisions[130]. In $CD8^+$ T cells, TCF-1 regulates stemness with a significant role in memory T cell and Tpex cell self-renewal and long-term survival[98, 106]. In addition to its function as a transcription factor, TCF-1 also has intrinsic histone deacetylase activity and thus can remodel chromatin accessibility[59]. As discussed earlier, TCF-1 is critical for the differentiation, function, and maintenance of Tpex cells during both chronic viral infections and cancers. The binding motifs of TCF-1 are enriched in Tpex cells, emphasizing the importance of TCF-1 in regulating the Tpex-specific transcriptional and epigenetic programs[95, 131, 132]. More specifically, TCF-1 increases the expression of BCL-2 and EOMES to enhance Tpex cell survival[97], increases BCL-6 expression to maintain Tpex cell stemness[130], and inhibits Blimp-1 expression to enhance the expression of memory genes (*Ccr7, Il7ra, Sell, Cxcr5*)[130]. When TCF-1 is overexpressed in $CD8^+$ T cells, there is an overall increase in exhausted T cell function, and thus increased viral and tumor control. TCF-1 overexpression reprogrammed exhausted T cells to adopt phenotypic and functional features of Tpex cells through increasing accessibility of genes associated with effector function (*Foxo1, Zeb2, Id3, Eomes*)[133] and decreasing accessibility of *Prdm1* (Blimp-1) and *Bcl2l11* (BIM) loci[132]. Furthermore, overexpression of TCF-1 promotes the formation of Tpex cells in both chronic viral infections and cancer[44, 97, 98, 132, 133]. Similarly to chronic viral infections, TCF-1 expression in tumors is exclusively associated with the Tpex population[52, 104, 111, 134]. Moreover, the presence of intratumoral $TCF\text{-}1^+$ $CD8^+$ T cells has a positive correlation with responses to ICB therapy, progression-free survival, and overall survival of cancer patients[111, 135]. Together, further elucidating how TCF-1 supports stem-like functions of exhausted $CD8^+$ T cells will help

improve therapeutic strategies. Importantly, the interplay between TCF-1 and other regulators in programming exhausted T cell stemness is poorly described. Since TCF-1 binding sites do not necessarily have TCF-1 consensus binding motifs, it has been suggested that TCF-1 can be indirectly recruited to chromatin by other transcriptional regulators[58]. Therefore, identifying proteins that enhance TCF-1 binding and/or activity in exhausted T cells will improve our understanding of how the differentiation of these cells is regulated, which has important clinical implications.

Another critical regulator of exhausted T cell differentiation is TOX. Recent studies emphasize the role of TCF-1 as a fate-decision transcription factor in maintaining Tpex cells during chronic infections, but they also highlight TOX as further imprinting the dysfunctional epigenetic program in exhausted T cells. TOX is a transcription factor that epigenetically programs exhausted T cell fate commitment early during chronic infections, with roles in regulating both induction and maintenance of exhaustion[125, 126, 127, 136, 137]. TOX levels are induced by NFAT transcription factors downstream chronic TCR signaling, with the highest levels in exhausted T cells and low levels in effector and memory subsets[127, 136]. Throughout the progression towards terminal exhaustion, there is a transition from high TCF-1 expression to high TOX expression, which defines exhausted subsets[128140]. TOX promotes T cell exhaustion through chromatin remodeling at promoters and enhancers of various genes; TOX decreases the accessibility of genes associated with terminal effector functions (*Klrg1, Gzma, Gzmb, Zeb2, Nr4a1*) and increases the accessibility of exhaustion-specific genes (*Pdcd1, Cd38, Lag3, Ctla4,Tcf7, Bach2*)[127]. This TOX-driven epigenetic regulation is achieved in part through acetylation of histone H3 and H4, as well as global DNA methylation[138]. Although TOX is critical for

the formation of exhausted T cells and their terminal differentiation in chronic viral infections and cancer, deleting TOX results in increased immunopathology to the host[126]. Thus, the exhausted phenotype TOX induces is important for lessening tissue damage from overactive T cells during chronic infection[126]. Without TOX, exhausted T cells are at very low frequencies, with decreased inhibitory receptor expression, increased cytotoxicity and decreased Tpex cell differentiation[126, 127]. Of note, TOX is not required for effector or memory T cell differentiation, as without TOX, both of these subsets are generated during acute infection. TOX has a similar role in promoting exhaustion in tumor-infiltrating lymphocytes (TILs), as TOX expression in TILs positively correlates with markers of exhaustion and TOX-deficient TILs have an inhibited exhaustion program in both phenotype and function[125, 127, 139].

Exhausted T cells are a distinct cell type from effector and memory T cells, with unique epigenetic and transcriptional programs driving their fate commitment. The regulatory network promoting initial epigenetic events in exhausted T cells is still not well characterized, especially proteins that function alongside TCF-1 and TOX. Currently, the fixed epigenetic state of exhausted T cells is a large hurdle to current immunotherapies, with limited responses in patients. Therefore, a better understanding of the epigenetic regulators of exhausted T cell differentiation will reveal new targets and therapeutic opportunities against chronic viral infections and cancers.

1.3.5: Immunotherapies

The dysfunctional response of exhausted T cells prevents effective immunological control of chronic viral infections and cancers in both animal models and human diseases[140, 141]. As a result, current therapeutic strategies against chronic infections are

aiming to reinvigorate exhausted T cells. The discovery and use of immunotherapies, particularly immune checkpoint inhibitors and adoptive T cell transfers, have revolutionized the treatment of chronic infections. However, the majority of patients still fail to respond, requiring further investigation into improving current or discovering new immunotherapies. Current immunotherapies are unable to fully restore the function of exhausted T cells because the fixed epigenetic state of exhaustion prevents reversion of these cells into fully functional effector or memory T cells[44, 93, 142, 143]. Given this major efficacy limitation, it is critical to better understand exhausted T cell differentiation in hopes of redirecting T cells away from this dysfunctional cell fate. With this in mind, researchers are now combining current immunotherapy strategies with the modulation of transcriptional and epigenetic regulators of exhausted T cells.

T cell function is tightly controlled by co-inhibitory molecules, serving as intrinsic regulatory mechanisms that prevent overactive immune responses. The expression of co-inhibitory receptors on effector T cells ensures their effective contraction after antigen clearance and maintain self-tolerance in the context of autoimmune diseases. However, they are constitutively expressed on T cells during chronic viral infections and cancers, exacerbating exhaustion and dampening effector T cell responses. Some of the well-studied co-inhibitory molecules on exhausted T cells include PD-1, CTLA-4, LAG3, and Tim-3[144, 145]. To improve anti-viral and anti-tumor T cell responses by reinvigorating exhausted T cells, these negative regulators are clinically targeted through various immunotherapies termed immune checkpoint inhibitors (ICIs). ICIs work by interrupting the inhibitory signals of endogenous T cells, thus reinvigorating T cell immune responses[146, 147]. Initial immunotherapies directed against PD-1 and CTLA-4 had amazing

efficacy in patients with melanoma, and then subsequently in several other cancers[148, 149]. Despite these successes, many patients still fail to respond, and several types of solid tumors are resistant to ICI therapies[150]. One explanation for the brief re-expansion of T cells in chronically infected patients after ICI therapy is the fixed epigenetic state of exhausted T cells. After either ICI therapy or antigen clearance, exhausted T cells revert back to their exhausted state with little to no changes in global chromatin accessibility and gene transcription[44, 94, 109, 116, 119, 120, 142, 143]. This suggests the functional defects of exhausted T cells are imprinted and their epigenetic state is “scarred”, emphasizing the inability of ICIs to sufficiently rewire exhausted T cells. Since T cells entering late stages of exhaustion do not respond as well to therapeutic intervention as those at earlier stages, finding strategies to interrupt the exhaustion program early may be most effective in improving immunity to chronic viral infections and cancers. Additionally, combining ICIs with epigenetic modulation may help reprogram T cells away from the exhausted fate, allowing for more durable and effective reinvigoration of these cells.

Understanding the differentiation of exhausted T cells is also critical for another therapeutic strategy, genetically engineered chimeric antigen receptor (CAR) T cells. The use of these adoptively transferred CAR-T cells has transformed therapy for patients with cancers refractory to ICIs[151, 152]. Unlike using ICIs to block negative signaling in endogenous T cells, CAR-T cells are autologous T cells with precise antigen-specificity for that patient’s malignancy. For example, using CAR-T cells in patients with CD19-expressing B cell malignancies has high clinical response rates, with some patients experiencing cure[153, 154]. However, just like with ICIs, the disease relapse of CAR-T cell therapy remains a challenge for clinicians and researchers. As with endogenous T cells

experiencing chronic antigen stimulation, CAR-T cell responses are limited as they enter the exhaustion differentiation program and ultimately become terminally differentiated[155, 156]. Thus, similar approaches are being investigated where CAR-T cell therapy is combined with both ICIs and epigenetic modifications in hopes of preventing terminal exhaustion differentiation early on during therapy.

Given the fixed epigenetic state of exhausted T cells, the use of epigenetic and transcriptional modifiers for preventing terminal exhaustion has become more enticing. As mentioned previously, the state of exhaustion is enforced by a network of transcriptional regulators and a "scarred" epigenetic program. This epigenetic reinforcement of exhaustion limits overactivation of effector T cells and immune pathology during immune responses, but as such, prevents effective T cell responses to chronic viral infections and cancer. Using epigenetic modifiers to prevent exhaustion requires complete understanding of the stages of T cell differentiation during chronic infections, in hopes of identifying when T cells become committed to the exhausted fate. A promising new use of epigenetic modifiers is in combination with CAR-T cells. For example, when DNMT3A, an epigenetic reinforcer of exhaustion-specific DNA methylation, was deleted in CAR-T cells prior to adoptive transfer, these CAR-T cells had preserved functional capacity with improved proliferation, cytokine production and an overall increase in anti-tumor ability[157, 158].

Together, the clinical efficacy of the aforementioned immunotherapies relies on developmental plasticity of the antigen-specific T cells. Previous works highlighting the fixed state of terminally exhausted T cells emphasize the need for immunotherapies that prevent T cells from initially entering the terminal exhaustion differentiation trajectory. One

such strategy is epigenetically reprogramming T cells prior to the induction of exhaustion, which has shown some success in combination with other immunotherapies. However, a more complete characterization of the molecular mechanisms driving the differentiation of exhausted T cells is required to improve upon both immunotherapies and overall responses of patients with chronic infections.

1.4 HMGB2 overview

HMGB2 is a member of the High Mobility Group (HMG) superfamily, which are non-histone nuclear proteins that modulate chromatin to regulate many genomic processes. HMGB proteins bind DNA, impacting the accessibility of chromatin and therefore regulating replication, transcription, chromatin remodeling, and DNA repair. In doing so, HMGB proteins are critical regulators of many cellular programs, including senescence and self-renewal. Despite the myriad of research into the HMGB protein family, the majority of studies have focused on HMGB1, a closely related family member of HMGB2. Therefore, although HMGB2 is important in regulating many biological processes through chromatin remodeling, nothing is known of its role in adaptive immune responses, and its role in $CD8^+$ T cells has not been investigated.

1.4.1: Structure

In mice and humans, there are three canonical HMGB proteins: HMGB1, HMGB2 and HMGB3[159]. HMGB proteins are evolutionary conserved with more than 80% identity shared in both structure and amino acid sequence[159, 160]. HMGB1-3 all have a molecular mass of ~25 KDa, with the only major difference being the lengths of their acidic C-tails[161]. In addition to their C-tails, HMGB proteins also consist of a short N-terminal region and have two DNA-binding domains, referred to as HMG-box A and B. HMGB proteins are

able to both bind and bend DNA with their HMG-boxes, but do so without DNA sequence specificity[162]. There is another subgroup of proteins within the HMGB family that only have one DNA-binding domain and are able to recognize specific DNA sequences (such as TCF-1/LEF1 and TOX)[159]. Despite the high degree of homology between HMGB1-3, these family members have different secondary structures and are non-redundant. In studies with *Hmgb1*$^{-/-}$ mice, the loss of HMGB1 cannot be substituted with endogenous HMGB2 expression and these mice die shortly after birth, suggesting these two proteins have distinct functional roles[163, 164].

1.4.2: Function

HMGB proteins modulate chromatin structure through direct DNA binding, influencing the binding of other regulatory proteins and impacting various genomic processes, including transcription and DNA repair (**Fig. 1.6**). HMGB proteins do not bind DNA in a sequence specific manner but have high affinity for noncanonical DNA structures. HMGB1 and HMGB2 preferentially bind DNA that is single-stranded, bent, unwound, cruciform, and/or supercoiled[159, 165, 166, 167, 168, 169]. In addition to binding DNA, HMGB proteins can also interact with histone proteins to influence chromatin structure. Through binding DNA and histones, HMGB proteins are able to influence the binding of transcription factors. The ability of HMGB proteins to bend DNA also influences the activity of gene promoters as altering DNA structure changes the proximity of regulatory regions and/or transcription factors[170, 171]. Enhancing DNA flexibility can also promote additional interactions between transcription factors bound on distant regulatory regions. Not only are HMGB proteins able to influence transcription factor binding through modifying chromatin structure, but they also directly bind transcription factors and can

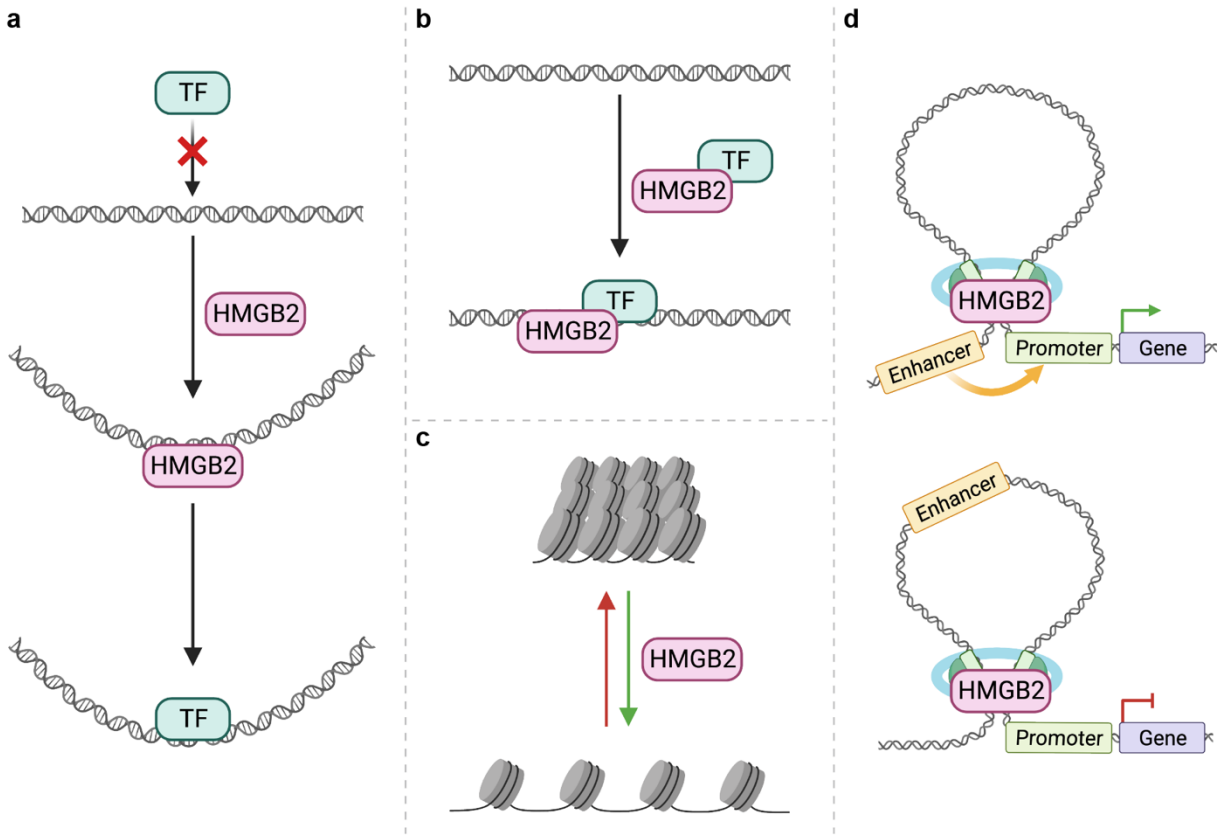

Figure 1.6 Mechanisms of gene regulation by HMGB2.
A model depicting regulatory roles of HMGB2 as an architectural factor in transcription. (**a**) HMGB2 bends DNA to enhance binding of a TF without direct interactions with HMGB2. (**b**) HMGB2 interacts with a TF and directs it to its binding site. (**c**) HMGB2 interacts with histone proteins to influence chromatin structure and accessibility. (**d**) HMGB2 enhances DNA flexibility by looping and influences the relative locations of regulatory sequences. Abbreviations: TF, transcription factor.

bring them closer to their binding sites. Other known proteins that HMGB1 and HMGB2 directly interact with include DNA repair proteins, recombination proteins, transcriptional activators/repressors, and viral proteins[162].

Since HMGB proteins act as chromatin modifiers, they are implicated in regulating various biological processes. HMGB2 is an important regulator of cellular senescence, a process where the cell cycle is stopped and which is directly influenced by alterations in chromatin structure. Through direct binding to senescence-specific genes and reorganization of the three-dimensional structure of chromatin, HMGB2 was shown to prime cells for the senescence program[172]. The role of HMGB2 in stem cells and various differentiation processes have also been characterized. In neuronal stem cells, HMGB2 expression is strongly associated with their transition from quiescence to robust proliferation[173]. HMGB2 also directly regulates hematopoietic stem cells (HSCs), which provide the long-term production of both white and red blood cells. Through binding to the promoter of latexin, a negative regulator of HSCs in mice, HMGB2 represses its transcription and thus promotes HSC number, survival, self-renewal, and proliferation[174]. Similarly, HMGB2 regulates stem cells involved in other differentiation programs, including myogenesis, spermatogenesis, and neurogenesis[175, 176, 177]. Consequently, male mice lacking HMGB2 have reduced fertility[176]. Finally, HMGB1 and HMGB2 regulate V(D)J recombination, a critical process in the development of the adaptive immune system. V(D)J recombination results in diverse antigen-binding regions of immunoglobulins and TCRs found on B cells and T cells, respectively, and is initiated by the activity of RAG1 and RAG2 proteins. By directly interacting with RAG proteins, HMGB1 and HMGB2 enhance their activity and thus V(D)J recombination both *in vitro*

and *in vivo*[178, 179, 180, 181]. Importantly, despite HMGB2's critical role in promoting this process, mice lacking HMGB2 have normal immunoglobulin serum concentrations, normal numbers of both B and T cells, and normal development and structure of the thymus, the organ responsible for producing T cells and where V(D)J recombination of TCRs occurs[176]. Therefore, HMGB1 and HMGB2 have redundant roles in both V(D)J recombination and overall lymphocyte development.

1.4.3: Expression and Localization

HMGB proteins are the second most abundant proteins in the nuclei of mammalian cells, behind histones[162, 182]. Despite being ubiquitously expressed in the nucleus, HMGB proteins can be found in the cytoplasm and/or extracellularly depending on post-translational modifications[183, 184]. In mice, HMGB1-3 are expressed early during embryogenesis, with HMGB2 and HMGB3 being redundant to HMGB1 only during this time[184]. During embryonic development, both HMGB2 and HMGB3 are downregulated, and as such, *Hmgb1*$^{-/-}$ mice die shortly after birth[161, 163, 185]. In contrast, *Hmgb2*$^{-/-}$ mice are viable. In adult mice, HMGB2 is highly expressed in the lymphoid tissues, thymus, and testes[176, 184]. Similar expression of HMGB2 in lymphoid organs is seen in humans, with biased expression in the bone marrow[186, 187]. Additionally, HMGB2 is expressed in all human and mouse immortalized cells. More recently, elevated HMGB2 expression has been characterized in various tumors, with both HMGB1 and HMGB2 expression being positively correlated with head and neck squamous cell carcinoma (HNSCC)[188], breast cancer[189, 190], colorectal cancer[191], gastric cancer[192], ovarian cancer[193], and lung cancer[194].

In summary, HMGB proteins are critical regulators of global chromatin architecture, influencing transcription, replication, and DNA repair. However, there has been much less characterization of the expression and function of HMGB2 compared to HMGB1. Therefore, future studies are required to delineate the relationships between HMGB2 binding and chromatin architecture, transcription factor localization, gene expression, and function.

CHAPTER 2

HMGB2 regulates the differentiation and function of memory CD8$^+$ T cells

Emily N. Neubert[1,2], Julia M. DeRogatis[1], Sloan A. Lewis[1,3], Karla M. Viramontes[1], Pedro Ortega[4,5], Monique L. Henriquez[1], Rémi Buisson[2,4,5], Ilhem Messaoudi[6], and Roberto Tinoco[1,2*]

[1]Department of Molecular Biology and Biochemistry, School of Biological Sciences, University of California Irvine, Irvine, CA 92697, USA
[2]Center for Virus Research, University of California Irvine, Irvine, CA 92697, USA
[3]La Jolla Institute for Immunology, La Jolla, CA 92037, USA
[4]Department of Biological Chemistry, School of Medicine, University of California, Irvine, Irvine, CA 92697, USA
[5]Center for Epigenetics and Metabolism, Chao Family Comprehensive Cancer Center, University of California Irvine, Irvine, CA 92697, USA
[6]Microbiology, Immunology, and Molecular Genetics, University of Kentucky, Lexington, KY, 40536, USA

In revision in *Nature Communications*. Neubert EN, DeRogatis JM, Lewis SA, Viramontes KM, Ortega P, et al. HMGB2 Regulates the Differentiation and Stemness of Exhausted CD8$^+$ T Cells During Chronic Viral Infection and Cancer. *Nature Communications*. 2023.

ABSTRACT

$CD8^+$ T cells are critical for mounting adaptive immune responses against pathogenic infections and cancers. During acute viral infections, cytotoxic effector $CD8^+$ T cells are able to clear pathogens, with a small proportion differentiating into memory $CD8^+$ T cells, which are essential for protective immunity to reinfections. However, the mechanisms underlying memory T cell differentiation and function are not fully known. Here we report HMGB2 expression is essential for memory precursor effector T cell (MPEC) survival, central memory T cell (Tcm) formation, and memory recall responses to secondary infections. ATAC-sequencing analysis showed HMGB2 as a cell-intrinsic epigenetic regulator of memory T cell function and survival. Despite *Hmgb2*$^{-/-}$ $CD8^+$ T cells expressing TCF-1, this master regulator was unable to sustain Tcm differentiation, survival, and recall capacity after acute viral infection. Furthermore, HMGB2 is not required for functional effector $CD8^+$ T cell differentiation. Our findings show that HMGB2 is a key regulator of memory $CD8^+$ T cells and may have implications for secondary infections.

INTRODUCTION

$CD8^+$ T cells are essential for mounting protective immune responses against pathogens. In response to acute viral infections, naïve $CD8^+$ T cells are activated and differentiate into a pool of cytotoxic effector $CD8^+$ T cells[195]. These fully differentiated effector T cells are essential for mounting protective immune responses against the pathogen and for clearing the infection. After clearance, a fraction of these antigen-specific effector T cells survive and differentiate into memory $CD8^+$ T cells[196]. Memory T cells are unique in that they are antigen-specific, can self-renew, and provide long-term immunity. Compared to naïve T cells, memory T cells can respond more quickly and with greater magnitude. The development of a functional memory T cell response is critical for rapid and efficient immune responses to subsequent infections. Furthermore, this efficient, long-term host protection conferred by memory T cells underlies the basis for vaccination[197].

Memory T cells are derived from memory precursor effector T cells (MPEC), a subset of effector T cells distinguished by high CD127 expression and low levels of KLRG-1, which arise during the peak of acute viral infections[21]. This pool of effector T cells also contain a population of KLRG-$1^{hi}CD127^{lo}$ short-lived effector T cells (SLEC) which have terminal effector functions and do not survive long-term after viral clearance[198]. The memory T cell pool can be further separated into central memory (Tcm), effector memory (Tem) and terminal-Tem (t-Tem) T cell populations, each with unique functions and localization[199]. The Tcm population is important for memory T cell function because it is responsible for providing recall responses to subsequent infections and its capacity to self-renew allows for the maintenance of a stable memory T cell pool long-term[2, 26, 200].

This memory T cell-mediated recall response is faster and higher in magnitude compared to the primary effector T cell response, conferring enhanced protection upon re-encountering the same antigen.

Given the heterogeneity within the effector and memory T cell pools, it has become evident that $CD8^+$ T cell differentiation during acute infections is dictated by a diverse and dynamic network of transcriptional regulators. Several transcription factors have been linked to effector T cell formation, including T-bet, Blimp-1, ZEB2, STAT4, and ID2[8, 201, 202, 203, 204, 205, 206]. For effective differentiation of memory T cells following acute infection, the transcription factors EOMES, BCL-6, FOXO1, STAT3, ID3 and TCF-1 are required[11, 43, 45, 47, 55, 207, 208, 209]. Recently, TCF-1 has been identified as the critical transcription factor for the longevity and recall capacity of Tcm cells. Specifically, TCF-1 creates a transcriptional program in memory T cells that supports the rapid proliferation and response of Tcm cells to secondary pathogen challenge[60, 133]. Despite numerous studies identifying fundamental transcription factors for memory T cell differentiation, the complete regulatory network remains unknown.

HMGB2 is a DNA-binding protein that belongs to the HMG transcription factor family. It is a chromatin modifier that regulates gene transcription and transcription factor binding[159, 210, 211]. HMGB2 also has known roles in regulating the formation and function of stem cells in various differentiation programs, including myogenesis, spermatogenesis, and neurogenesis[175, 176, 177]. Previous RNA-sequencing analyses have found increased *Hmgb2* expression in murine effector $CD8^+$ T cells during acute lymphocytic choriomeningitis virus (LCMV) infection[212], although its role in $CD8^+$ T cells has not been examined. Here, we investigated the role of HMGB2 in regulating effector and memory T

cell differentiation and function during acute LCMV infection. Using *Hmgb2*$^{-/-}$ virus-specific CD8^{+} T cells, we found that HMGB2 deficiency did not impact effector T cell formation or function but resulted in decreased memory T cell differentiation and maintenance. More specifically, *Hmgb2*$^{-/-}$ MPECs had increased apoptosis and the differentiation of *Hmgb2*$^{-/-}$ Tcm cells was decreased. Furthermore, *Hmgb2*$^{-/-}$ memory T cells had impaired recall capacity to secondary viral challenge. We found a distinct epigenetic signature in HMGB2-deficient CD8^{+} T cells compared to WT CD8^{+} T cells during acute infection, indicating HMGB2 supports memory T cell-specific transcriptional programming. In summary, we found that HMGB2 plays a critical role in the formation, maintenance, and function of memory CD8^{+} T cells following acute viral infection. We speculate HMGB2 may be exploited as a potential therapeutic target, through which we may leverage the memory T cell population and contribute to vaccine and immunotherapy development.

MATERIALS AND METHODS

Mice

All experimental animal procedures were approved by the Institutional Animal Care and Use Committee of University of California, Irvine (AUP-21-124) and complied with all relevant ethical regulations for animal testing and research. C57BL/6J and B6.SJL-*Ptpr*^{a} *Pepc*^{b}/BoyJ mice were purchased from the Jackson Laboratory, then bred in SPF facilities. P14 mice were obtained from The Scripps Research Institute (originally from Dr. Charles D. Surh). These mice were bred to Ly5.1 (B6.SJL-*Ptprc*^{a} *Pepc*^{b}/BoyJ) mice and to *Hmgb2*$^{-/-}$ mice, which were generously provided by Dr. Marco Bianchi (San Raffaele Scientific Institute, Milan, Italy). Male and female mice ≥ 6 weeks of age were used in experiments. Mouse selection for experiments was not formally randomized or blinded.

Virus Infection

LCMV Armstrong (Arm) was propagated in baby-hamster kidney cells and titrated on Vero African-green-monkey kidney cells. Frozen stocks were diluted in Vero cell media and $2x10^5$ plaque-forming units (PFUs) of LCMV Arm were injected intraperitoneally (i.p.).

T cell Adoptive Transfer

Bulk CD8$^+$ T cells were enriched from spleens and lymph nodes (LNs) of WT (*Hmgb2*$^{+/+}$) or *Hmgb2*$^{-/-}$ P14 transgenic mice by column-free magnetic negative selection. Single cell suspensions from pooled spleen and LNs were incubated with biotinylated antibodies against CD4 (GK1.5), B220 (RA3-6B2), CD19 (6D5), CD24 (M1/69), CD11b (M1/70), and

CD11c (N418). Non-$CD8^+$ cells were removed by mixing labeled cell suspension with Streptavidin RapidSpheres (Stemcell technologies) at room temperature (RT) for 5min, followed by two-5min incubations in an EasyEights™ EasySep™ Magnet (Stemcell technologies). The unbound $CD8^+$ T cells were washed in sterile PBS (1x) with FBS (2%), and purity was determined on a flow cytometer. For single-transfer studies, WT and *Hmgb2*$^{-/-}$ P14 T cells were transferred into separate new WT hosts of the opposite congenic marker ($1x10^3$ i.v.). For co-transfer studies, WT and *Hmgb2*$^{-/-}$ P14 T cells were mixed at a 1:1 ratio ($1x10^3$ i.v. per cell-type for virus studies) and injected into new WT recipient mice i.v. Within 18-24hr post-transfer, recipient mice were inoculated with LCMV Arm ($2x10^5$, i.p.). For re-challenge experiments, live (PI^-) WT and *Hmgb2*$^{-/-}$ P14 T cells were sorted at >95% purity from spleens and LNs at 30dpi or 68dpi using a BD FACSAria sorter. Cell numbers were normalized and transferred into new hosts ($2x10^3$ i.v. per cell-type) that were subsequently infected with LCMV Arm ($2x10^5$ PFU, i.p.).

Flow Cytometry

For cell surface staining, $2x10^6$ cells were incubated with antibodies in staining buffer (PBS, 2% FBS and 0.01% NaN_3) at 4°C. For intracellular cytokine staining, cells were resuspended in complete RPMI-1640 (containing 10 mM HEPES, 1% nonessential amino acids and L-glutamine, 1 mM sodium pyruvate, 10% heat inactivated FBS and antibiotics) supplemented with 50 U/mL IL-2 (NCI) and 1 mg/mL brefeldin A (BFA, Sigma), and then incubated with 2mg/mL LCMV GP_{33-41} peptide (AnaSpec) at 37°C for 4h. Cells were then fixed and permeabilized using a Cytofix/Cytoperm Kit (BD Biosciences) before staining. For intranuclear transcription factor staining, cells were fixed and permeabilized using a

Foxp3/transcription factor fixation/permeabilization kit (Fisher). Antibodies are listed in Star Methods. Surface stains were performed at a 1:200 dilution, while intracellular and intranuclear stains performed at a 1:100 dilution. Caspase3 staining was done using CaspGLOW Fluorescein Active Caspase-3 staining kit (ThermoFisher) following manufacturer's instructions. All data were collected on a Novocyte3000 (Agilent) and analyzed using FlowJo Software (Tree Star).

Imaging Flow Cytometry

For imaging flow cytometry, negative selection was performed (above) to isolate $CD8^+$ T cells and cells were stained as described previously. Zombie staining was done using Zombie Aqua™ Fixable Viability Kit (BioLegend) as outlined by manufacturer's instructions. 7-ADD (Fisher) was used to stain nuclei per manufacturer's instructions. Cells were resuspended at $2x10^7$ cells/mL and run on an Amnis ImageStream X Mark II imaging flow cytometer (EMD Millipore) and analyzed using IDEAS software (EMD Millipore).

***In Vivo* Proliferation**

Mice were injected i.p. with 2mg BrdU (Sigma-Aldrich) 16h before removing spleens at 8dpi to measure proliferation. Cells were stained intracellularly using FITC BrdU Flow kit (BD Biosciences) following the manufacturer's instructions. Cells were acquired with a Novocyte3000 flow cytometer.

Comet Assay

Co-transferred live (PI^-) WT and *Hmgb2*$^{-/-}$ P14 T cells were sorted at >95% purity from spleens and LNs of LCMV Arm infected mice at 8dpi using a BD FACSAria sorter. U2OS cells were cultured in DMEM supplemented with 10% fetal bovine serum, 1% L-Glutamine, and 1% penicillin/streptomycin. Single-cell alkaline gel electrophoresis was performed with comet assay Kit (Abcam) following manufacturer's instructions. Images were captured using a Leica DMi8 THUNDER microscope. Comet olive tail moments of 100 cells were analyzed using CometScore software version 2.0.0.38.

Western Blot

Co-transferred live (PI^-) WT and *Hmgb2*$^{-/-}$ P14 T cells were sorted at >95% purity from spleens and LNs of LCMV Arm infected mice at 8dpi using a BD FACSAria sorter. Cells were lysed and blots were stained for Phospho-H2AX (Ser139) (1:1000) and Histone H3 (1:140000).

Bulk RNA-Seq RNA Isolation and Library Preparation

For 8dpi studies, WT and *Hmgb2*$^{-/-}$ P14 T cells were transferred into five separate mice each before infection with LCMV Arm. On 8dpi, spleens and LNs were pooled based on infection type and P14 genotype. Live (PI^-) WT and *Hmgb2*$^{-/-}$ P14 were sorted at >95% purity (8dpi:~$1x10^6$ per condition) and resuspended in RLT Buffer and BME before storage at -80°C. Each experiment was performed three times to represent three biological replicates. Total RNA was monitored for quality control using the Agilent Bioanalyzer Nano RNA chip and Nanodrop absorbance ratios for 260/280nm and 260/230nm. Library construction was performed according to the Illumina TruSeq mRNA

stranded protocol. The input quantity for total RNA within the recommended range and mRNA was enriched using oligo dT magnetic beads. The enriched mRNA was chemically fragmented. First strand synthesis used random primers and reverse transcriptase to make cDNA. After second strand synthesis the ds cDNA was cleaned using AMPure XP beads and the cDNA was end repaired and then the 3' ends were adenylated. Illumina barcoded adapters were ligated on the ends and the adapter ligated fragments were enriched by nine cycles of PCR. The resulting libraries were validated by qPCR and sized by Agilent Bioanalyzer DNA high sensitivity chip. The concentrations for the libraries were normalized and then multiplexed together. The multiplexed libraries were sequenced using paired end 100 cycles chemistry on the NovaSeq 6000.

Bulk RNA-Seq Data Analysis

Post-processing of the run to generate FASTQ files was performed at the Institute for Genomics and Bioinformatics (UCI IGB). *PcaHubert* was used to identify any outlier samples, which were removed from further analysis[213]. The quality of the sequencing was first assessed using the *fastQC* tool (v0.11.9). Raw reads were then quality trimmed and filtered by a length of 20 bases using *trimmomatic* (v0.39). Trimmed reads were analyzed with the mouse Grcm38 reference genome using pseudo aligner Salmon (v1.2.1) and resulting quantification files were imported using R package *tximport* to get TPM values for all annotated mouse genes. Differential analysis was done using R package *DESeq2* (v1.22.2) with an FDR cut off of 0.05. PCA was done using R packages *DESeq2* and *pheatmap*. For downstream analysis, genes with adjusted p-value ≤ 0.1 and $|\log_2 FC| \geq$

0.5 were included. Gene ontology functional enrichment of gene expression changes in WT and *Hmgb2*$^{-/-}$ P14 T cells were performed using Metascape (http://metascape.org).

ATAC-Seq Library Preparation

WT and *Hmgb2*$^{-/-}$ P14 T cells were co-transferred at 1:1 into 10 mice before infection with LCMV Arm. On 8dpi, spleens and LNs were pooled (samples are pooled from 10mice/group). Live (PI^{-}) WT and *Hmgb2*$^{-/-}$ P14 were sorted at >95% purity ($2x10^5$ WT, $2x10^5$ *Hmgb2*$^{-/-}$). Each experiment was performed three times to represent three biological replicates. Following the Omni-ATAC protocol, samples were lysed in lysis buffer (10mM Tris-HCl (pH 7.4), 10mM NaCl, 3mM $MgCl_2$, 10% Np-40, 10% Tween, and 1% Digitonin) on ice for 3 minutes[214]. Immediately following lysis, nuclei were spun at 500g for 10min at 4°C to remove supernatant. Nuclei were then incubated with Tn5 transposase for 30min at 37°C. Tagmented DNA was purified using AMPure XP beads and PCR was performed to amplify the library under the following conditions: 72°C for 5min; 98°C for 30s; 5 cycles of 98°C for 10s, 63°C for 30s, and 72°C for 1min; hold at 4°C. Libraries were then purified with warm AMPure XP beads and quantified on a Bioanalyzer. Libraries were multiplexed and sequenced to a depth of 50million 100bp paired reads on a NextSeq.

ATAC-Seq Data Analysis

Paired ended reads from sequencing were QC analyzed with fastqQC (v.11.9) and aligned to mouse mm10 reference genome using bowtie2 (v2.4.1). Mitochondrial reads and reads mapped to dark list (ENCODE Stanford version) were excluded from the

downstream analysis. Duplicated reads were removed using Picard tools (v2.27.1). A union peak list was created by merging processed reads from all samples and then calling peaks using MACS2 (v2.7.1) (-q 0.01 --keep-dup all -f BAMPE). The number of reads in each peak were then counted using featureCounts (Rsubread v2.6.4) to create a counts matrix. Normalization of counts matrix was performed using DESeq2 (v1.32.0). Differentially expressed peaks were determined using edgeR (v3.34.1) with an FDR cut-off of 0.05 and a $|\log_{10}FC|$ cut-off of ≥ 0.3. Peaks were annotated using ChIPSeeker (v1.34.0). Functional enrichment of promoter regions was performed using Metascape (http://metascape.org).

Quantification and Statistical Analysis

Flow cytometry data were analyzed with FlowJo software (TreeStar). Bulk RNA-seq and ATAC-seq figures were prepared using RStudio software. Graphs were prepared with GraphPad Prism software. GraphPad Prism was used for statistical analysis to compare outcomes using a two-tailed unpaired Student's *t*-test, Mann Whitney or paired Student's *t*-test where indicated; significance was set to $p \leq 0.05$ and represented as *$p \leq 0.05$, **$p \leq 0.01$, ***$p \leq 0.001$, and ****$p \leq 0.0001$. Error bars show SEM.

Data and code availability

The authors declare that all supporting data are available within the Article and its Supplementary Information files. 3'-scRNA-seq and ATAC-seq data sets will be deposited in the Gene Expression Omnibus (GEO) database.

RESULTS

HMGB2 expression is upregulated and sustained in virus-specific CD8$^+$ T cells

Despite general characterization of HMGB2 expression in lymphoid tissues, the expression of HMGB2 in T cells had not been characterized. Therefore, we evaluated HMGB2 protein expression in naïve, effector, memory, and exhausted virus-specific CD8$^+$ T cells. We infected wild-type (WT) mice with either LCMV Armstrong (Arm) or Clone 13 (Cl13) to induce an acute or chronic viral infection, respectively, and measured HMGB2 levels in MHC class I tetramer$^+$ virus-specific CD8$^+$ T cells. We detected HMGB2 expression in naïve CD8$^+$ T cells that was upregulated in $GP_{33\text{-}41}{}^+$ CD8$^+$ effector and memory T cells (**Fig. 2.1a**). We observed upregulation of HMGB2 in early exhausted T cells (8dpi Cl13) that was sustained in late exhausted T cells (30dpi Cl13) (**Fig. 2.1a**). Furthermore, late exhausted $GP_{33\text{-}41}{}^+$ T cells had significantly increased HMGB2 expression compared to naïve and memory T cells (**Fig. 2.1a**). We next evaluated HMGB2 levels in $GP_{276\text{-}286}{}^+$ CD8$^+$ T cells, and again observed increased levels in effector, memory, and exhausted T cells compared to naïve, with sustained HMGB2 expression in late exhausted CD8$^+$ T cells (**Fig. 2.1b**). Lastly, we evaluated HMGB2 localization in $GP_{33\text{-}41}{}^+$ CD8$^+$ T cells using imaging flow cytometry. We observed nuclear localization of HMGB2, as shown by HMGB2 and nuclear 7-AAD colocalization staining (**Fig. 2.1c**). These findings showed nuclear localization of HMGB2 in virus-specific CD8$^+$ T cells, with increased expression in effector, memory, and exhausted CD8$^+$ T cells that is sustained during chronic viral infection.

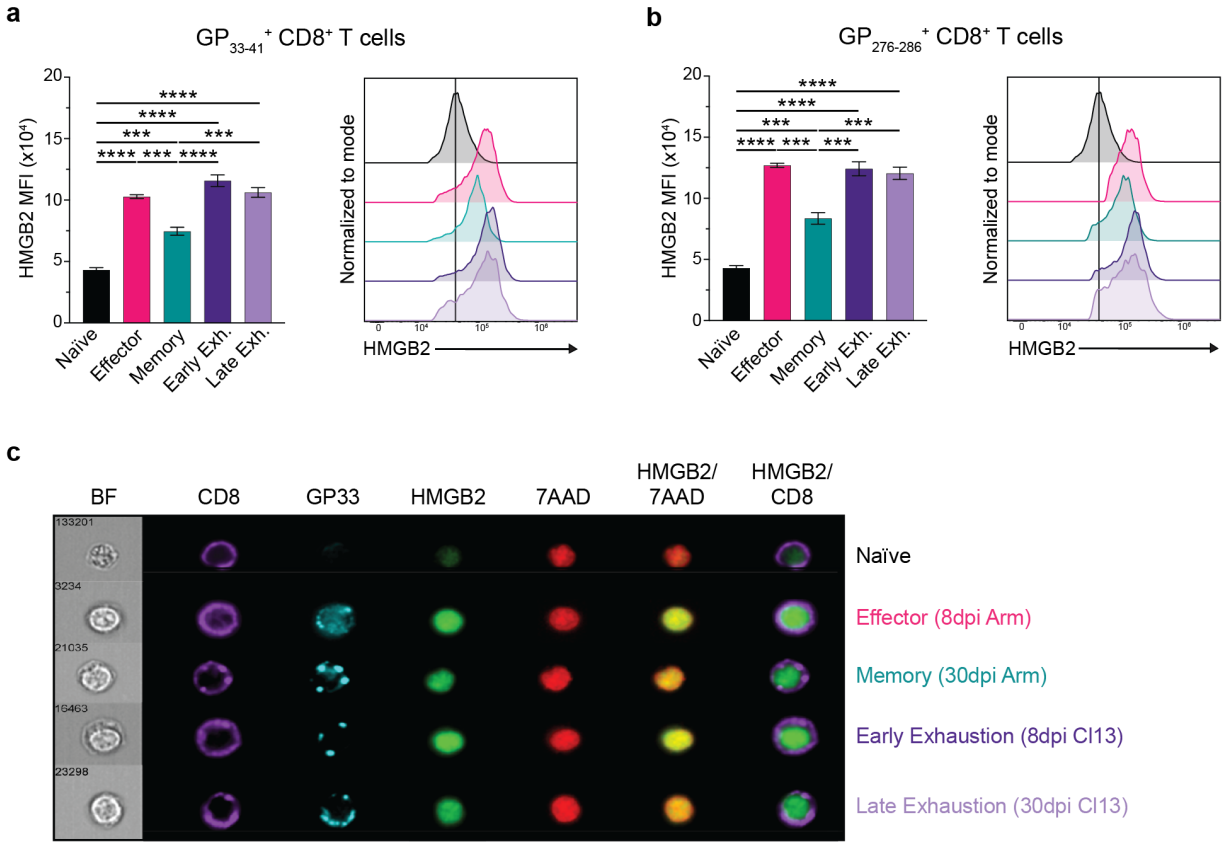

Figure 2.1 HMGB2 expression in murine virus-specific CD8⁺ T cells.
Expression levels of HMGB2 in GP_{33-41}^{+} $CD8^{+}$ T cells (**a**) and $GP_{276-286}^{+}$ $CD8^{+}$ T cells (**b**) assessed by flow cytometry in spleen with *n* = 4 mice. Naïve, uninfected; Effector, 8dpi LCMV Arm; Memory, 30dpi LCMV Arm; Early Exhaustion, 8dpi LCMV Cl13; Late Exhaustion, 30dpi LCMV Cl13; MFI, mean fluorescence intensity. Data is mean ± s.e.m and representative of two independent experiments with ≥ 4 mice per group. (**c**) Representative Imagestream analysis of GP_{33-41}^{+} $CD8^{+}$ T cells, magnification, 60x. Data are representative of two independent experiments with ≥ 4 mice per group. **p≤ 0.01, ***p ≤ 0.001, ****p ≤ 0.0001, one-way ANOVA (a-b).

Hmgb2$^{-/-}$ CD8^{+} T cells differentiate into effector and memory T cells during acute viral infection

Considering the expression of HMGB2 was increased in effector and memory CD8^{+} T cells, we next determined the cell-intrinsic role of HMGB2 in virus-specific T cells during acute LCMV infection. Small numbers (1x10^{3} cells) of congenically marked WT or *Hmgb2*$^{-/-}$ P14 CD8^{+} T cells, which are TCR transgenic T cells specific for the GP_{33-41} peptide of LCMV, were adoptively transferred into separate congenically mismatched WT mice, which were then infected with LCMV Arm (**Fig. 2.2a**). A gating strategy for this approach is shown (**Fig. S2.1a**). We observed similar expansion, contraction, and memory CD8^{+} T cell formation of both WT and *Hmgb2*$^{-/-}$ P14 T cells throughout acute infection (**Fig. 2.2b**). Furthermore, similar frequencies and numbers of WT and *Hmgb2*$^{-/-}$ P14 T cells were found in spleens at 68dpi (**Fig. 2.2c**). We next evaluated functionality of WT and *Hmgb2*$^{-/-}$ P14 T cells by *ex vivo* GP_{33-41} peptide stimulation and observed similar frequencies of GranzymeB^{+} cells at 8dpi and IFN-γ^{+} and IFN-γ^{+}TNF-α^{+} cells at 68dpi (**Fig. 2.2d, e**). To investigate T cell responses within the same host, we next co-transferred small numbers (1x10^{3} each) of congenically marked WT and *Hmgb2*$^{-/-}$ P14 T cells at a 1:1 ratio into congenically mismatched WT mice, followed by Arm infection (**Fig. 2.2f**). Despite injection at a 1:1 ratio, we observed slightly decreased frequencies of *Hmgb2*$^{-/-}$ P14 T cells compared to WT (**Fig. 2.2g**). We also observed significantly decreased numbers of splenic *Hmgb2*$^{-/-}$ P14 T cells compared to WT at both 8 and 30dpi (**Fig. 2.2h**). These findings showed *Hmgb2*$^{-/-}$ CD8^{+} T cells expand after acute LCMV infection, and

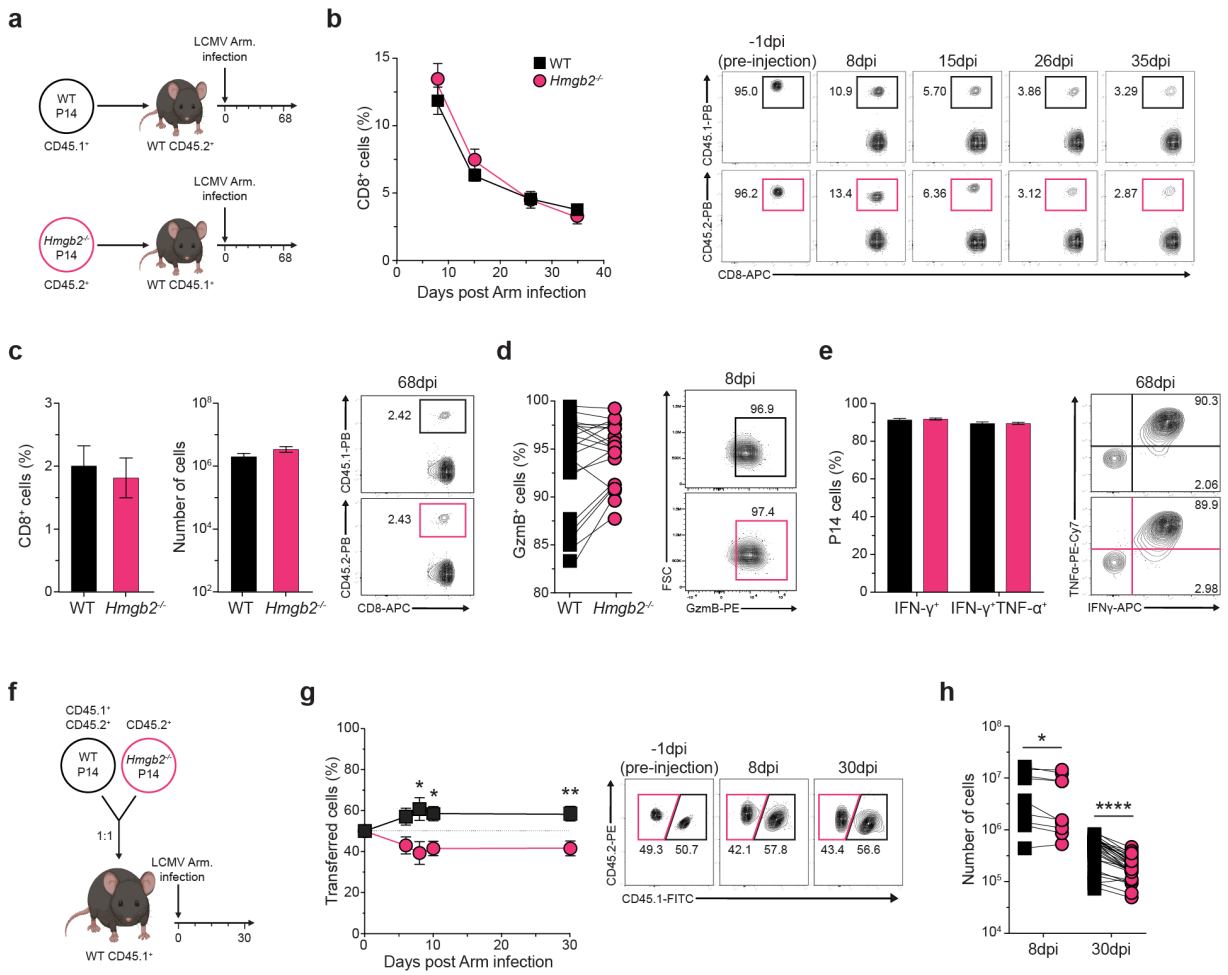

Figure 2.2 Cell-intrinsic kinetics of WT and *Hmgb2*$^{-/-}$ P14 T cells during Arm infection.

(**a**) Experimental scheme for **b-c, e**. WT and *Hmgb2*$^{-/-}$ P14 CD8^{+} T cells were transferred separately into naïve mice and infected with LCMV Arm. Blood taken at 8, 15, 26, and 35dpi. Spleens isolated at 68dpi. (**b**) Frequency of WT and *Hmgb2*$^{-/-}$ P14 T cells of total CD8^{+} population. (**c**) Splenic WT and *Hmgb2*$^{-/-}$ P14 T cell frequencies and numbers at 68dpi. (**d**) Frequencies of GranzymeB^{+} WT and *Hmgb2*$^{-/-}$ P14 T cells at 8dpi LCMV Arm in the blood. (**e**) Cytokine production by splenic WT and *Hmgb2*$^{-/-}$ P14 T cells at 68dpi. (**f**) Experimental scheme for **g-h**. WT and *Hmgb2*$^{-/-}$ P14 T cells were co-transferred at 1:1 into WT mice and infected with LCMV Arm. Frequencies (**g**) and numbers (**h**) of splenic WT and *Hmgb2*$^{-/-}$ P14 T cells at indicated timepoints post infection. Data are representative of three independent experiments with ≥ 5 mice per group. Data is mean ± s.e.m. *p ≤ 0.05, **p ≤ 0.01, ****p ≤ 0.0001, two-tailed unpaired Student's *t*-test (b-c, e), paired Student's *t*-test (d, g-h).

although present at slightly lower frequencies than WT, survive to seed the memory T cell pool.

HMGB2 regulates memory CD8$^+$ T cell differentiation after acute infection

We next evaluated the differentiation of *Hmgb2*$^{-/-}$ P14 T cells by examining KLRG-1 and CD127 expression to delineate KLRG1^{hi}CD127^{lo} short-lived effector (SLEC) and KLRG1^{lo}CD127^{hi} memory precursor effector cells (MPEC). At 8dpi, we observed decreased SLECs in *Hmgb2*$^{-/-}$ P14 T cells (**Fig. 2.3a**) and by 46dpi, we found significantly decreased frequencies of SLECs and increased frequencies of MPECs in *Hmgb2*$^{-/-}$ P14 T cells (**Fig. 2.3b**). Since we found more *Hmgb2*$^{-/-}$ MPECs compared to WT but significantly less overall *Hmgb2*$^{-/-}$ memory T cell numbers (**Fig. 2.2h**), we investigated apoptosis within this population. We found *Hmgb2*$^{-/-}$ MPECs had significantly higher frequencies of total apoptotic cells by active Caspase3 and propidium iodide (PI) staining at both 8dpi and 46dpi (**Fig. 2.3c, d**).

To further characterize the differentiation of memory *Hmgb2*$^{-/-}$ P14 T cells, we examined effector memory (Tem), central memory (Tcm) and terminal-Tem (t-Tem) T cell populations based on CD62L vs CD127 expression[199]. *Hmgb2*$^{-/-}$ P14 T cells had significantly lower frequencies of both Tcm and t-Tem cells, and increased frequencies of Tem cells compared to WT at 46dpi (**Fig. 2.3e**)**.** Finally, to confirm the loss of *Hmgb2*$^{-/-}$ P14 T cells was not due to compromised development of naïve CD8$^+$ T cells, we characterized naïve WT and *Hmgb2*$^{-/-}$ P14 T cells from spleens and lymph nodes of uninfected mice. We found no differences in expression of naïve T cell markers (CD127, CD62L, CCR7) or in frequencies of naïve vs activated T cells in lymph nodes (**Fig. S2.2a, b**) and spleens (**Fig. S2.2c, d**). We also found no differences in numbers of CD8$^+$ T cells

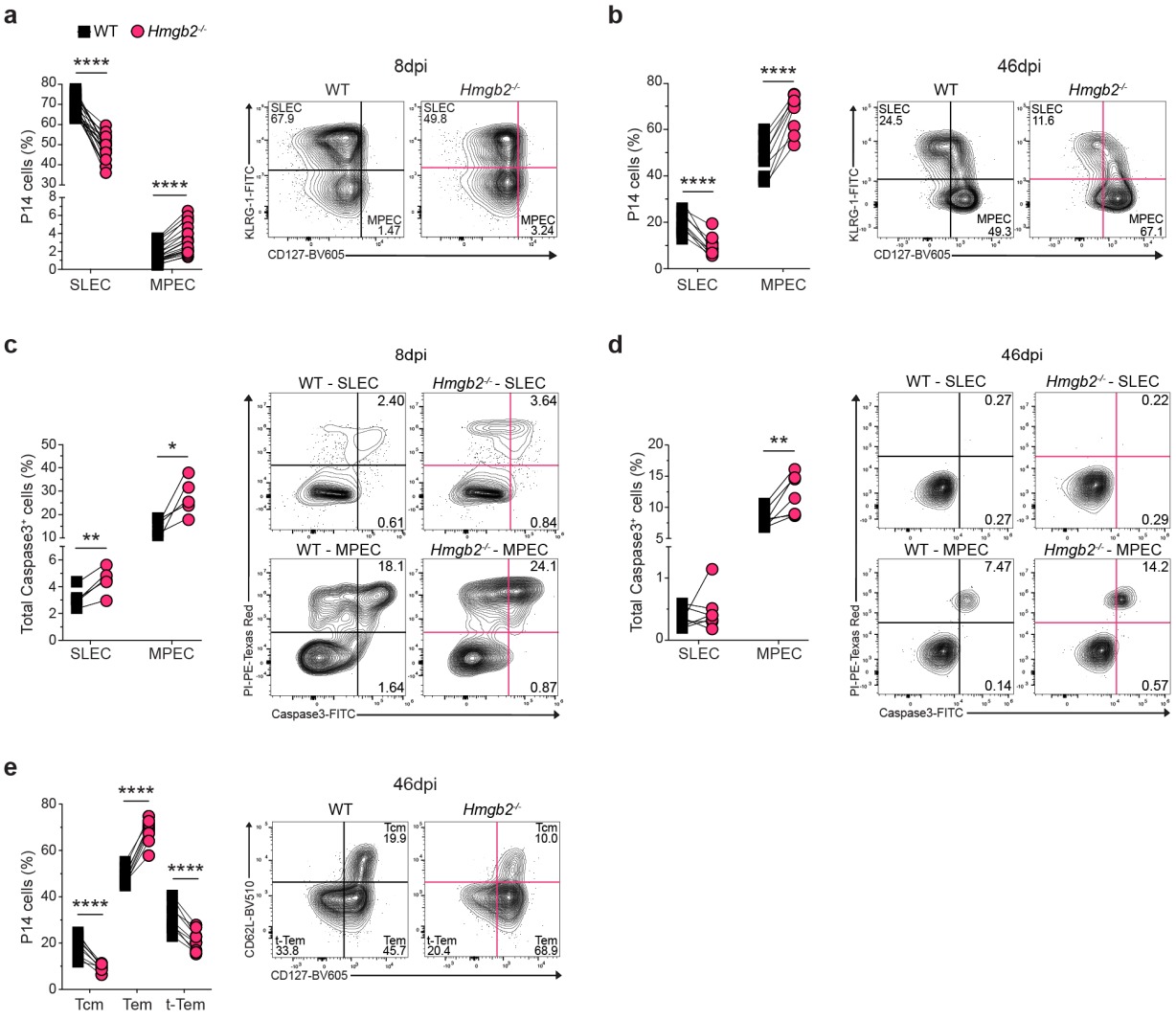

Figure 2.3 *Hmgb2*$^{-/-}$ CD8^{+} T cells have decreased central memory differentiation after Arm infection.

Frequencies of splenic WT and *Hmgb2*$^{-/-}$ P14 short-lived effector (SLEC) and memory precursor effector (MPEC) T cells in the blood at 8dpi (**a**) and 46dpi (**b**) Arm. Frequency of total Caspase3^{+} splenic WT and *Hmgb2*$^{-/-}$ SLEC and MPEC P14 T cells at 8dpi (**c**) and 46dpi (**d**) Arm. (**e**) Frequencies of WT and *Hmgb2*$^{-/-}$ P14 central memory (Tcm), effector memory (Tem) and terminal Tem (t-Tem) T cells at 46dpi Arm in the spleen. Data are representative of three independent experiments with ≥ 5 mice per group. Data is mean ± s.e.m. *p ≤ 0.05, **p ≤ 0.01, ****p ≤ 0.0001, paired Student's *t*-test.

between WT and *Hmgb2*$^{-/-}$ mice (**Fig. S2.2e**). Together, these findings showed that HMGB2 regulated the survival and differentiation of memory CD8^{+} T cells during acute viral infection.

Hmgb2$^{-/-}$ CD8^{+} T cells have decreased survival during acute viral infection

Since we found *Hmgb2*$^{-/-}$ CD8^{+} T cells were significantly decreased during acute viral infection, we next assessed whether there were differences in their proliferation and/or survival. We co-transferred WT and *Hmgb2*$^{-/-}$ P14 T cells at a 1:1 ratio into WT mice, followed by Arm infection. We first evaluated proliferation by *in vivo* BrdU incorporation and observed slightly decreased frequencies of BrdU^{+} *Hmgb2*$^{-/-}$ P14 T cells compared to WT at 8dpi Arm (**Fig. 2.4a**). Next, we evaluated survival by active Caspase3 and PI staining and observed increased frequencies of total Caspase3^{+} apoptotic *Hmgb2*$^{-/-}$ P14 T cells compared to WT at 8dpi Arm (**Fig. 2.4b**). We also found increased frequencies of total Caspase3^{+} apoptotic *Hmgb2*$^{-/-}$ P14 T cells at 46dpi Arm (**Fig. 2.4c**). We next asked whether the increased apoptosis of *Hmgb2*$^{-/-}$ P14 T cells was due to differences in DNA repair compared to WT cells. Using a comet assay to measure DNA damage[215], we found no significant differences between WT and *Hmgb2*$^{-/-}$ P14 T cells during Arm infection (**Fig. 2.4d**). We also looked at phosphorylated-H2AX (Ser139), a marker of DNA damage[216], and again found no differences between WT and *Hmgb2*$^{-/-}$ P14 T cells during Arm infection (**Fig. 2.4e**). These findings showed *Hmgb2*$^{-/-}$ CD8^{+} T cells had decreased proliferation and survival compared to WT during acute viral infection and did not show signs of DNA damage by 8dpi.

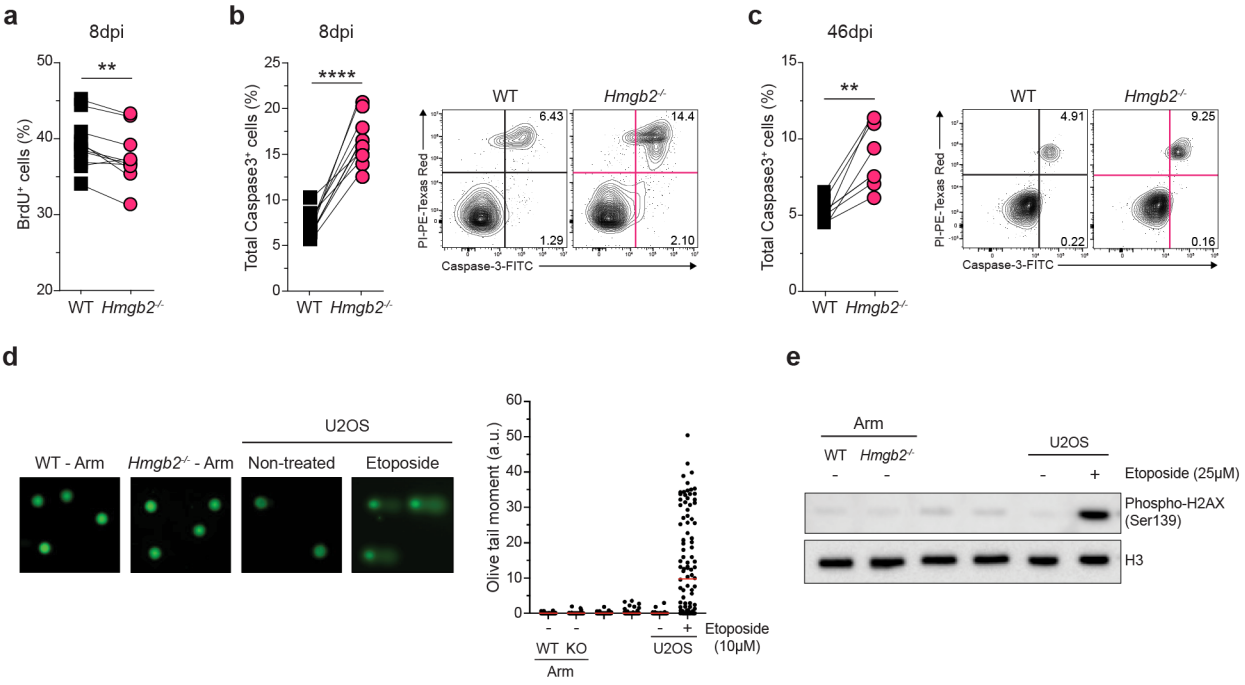

Figure 2.4 *Hmgb2*$^{-/-}$ CD8^{+} T cells have decreased proliferation and increased cell death.

WT and *Hmgb2*$^{-/-}$ P14 T cells were co-transferred at 1:1 into WT mice, followed by LCMV Arm infection. (**a**) BrdU uptake of splenic WT and *Hmgb2*$^{-/-}$ P14 T cells at 8dpi. Caspase3 and PI staining of P14 T cells at 8dpi (**b**) and 46dpi (**c**) in the spleen. (**d**) Alkaline comet assay of splenic WT and *Hmgb2*$^{-/-}$ P14 T cells isolated on 8 days post Arm infection (pooled samples from 10mice/group). Representative fluorescent comet images of cells stained with Vista Green DNA dye. U2OS human cells treated with etoposide (10μM for 30min), a topoisomerase II inhibitor used to generate DNA double-strand breaks in cells, served as controls for comet tail formation. (**e**) p-H2AX (Ser139) protein expression by western blot in purified splenic WT and *Hmgb2*$^{-/-}$ P14 T cells isolated on 8 days Arm infection (pooled samples from 10mice/group). U2OS human cells untreated or treated with 25μM etoposide for 60min served as negative and positive controls, respectively. Data are representative of three independent experiments with ≥ 5 mice per group. Data is mean ± s.e.m. **p ≤ 0.01, ****p ≤ 0.0001, paired Student's *t*-test.

HMGB2 regulates the chromatin accessibility of memory genes during Arm infection

Since we found a role for HMGB2 in memory $CD8^+$ T cells, and HMGB2 is a chromatin modifier, we next investigated whether HMGB2 regulated the transcriptional landscape of virus-specific T cells. We performed RNA-sequencing of sorted WT and *Hmgb2*$^{-/-}$ P14 T cells from Arm infected mice at 8dpi. Overall, we observed relatively few differentially expressed genes (DEG) between WT and *Hmgb2*$^{-/-}$ P14 T cells during Arm infection. During Arm infection, analysis of DEG between WT and *Hmgb2*$^{-/-}$ P14 T cells showed a total of 125, with 38 upregulated and 87 downregulated genes in *Hmgb2*$^{-/-}$ P14 T cells (**Fig. S2.3a, b**).

Since HMGB2 has a well-characterized role in chromatin remodeling, we next asked whether HMGB2 regulates the epigenetic program of virus-specific T cells during acute viral infection. We sorted WT and *Hmgb2*$^{-/-}$ P14 T cells from mice at 8dpi Arm and used ATAC-seq to identify significant changes in chromatin accessibility in the absence of HMGB2. PCA of the ATAC-seq profiles segregated WT and *Hmgb2*$^{-/-}$ P14 T cells across PC1 (90% variance), indicating that *Hmgb2* has a significant effect on chromatin accessibility (**Fig. 2.5a**). We found 5,610 differentially accessible regions (DAR), with most having decreased accessibility in *Hmgb2*$^{-/-}$ P14 T cells compared with WT (**Fig. 2.5b**). Genomic annotation showed about 17.7% of these accessibility changes were at promoters (≤1kb) or transcription start sites (TSS) (**Fig. 2.5b**). The genes in close proximity to loci with reduced accessibility in *Hmgb2*$^{-/-}$ P14 T cells were associated with memory T cells and stem-like function, including *Eomes, Foxo1, Bach2, Runx3,* and *Bcl6* (**Fig. 2.5c, d**)[217]. In contrast, loci with increased accessibility were near genes associated

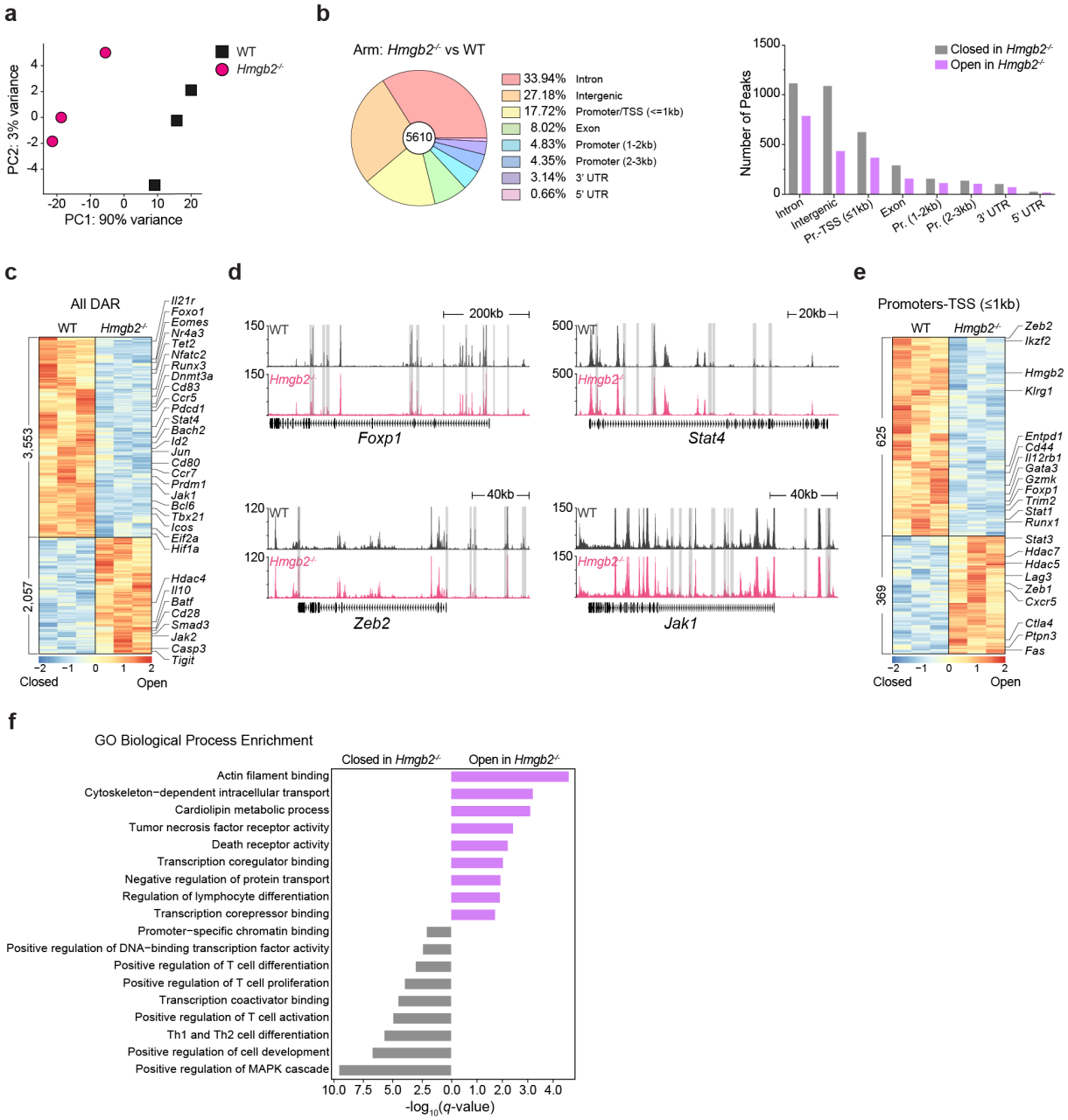

Figure 2.5 Epigenetic programming of memory T cell signature genes by HMGB2.

ATAC-seq analysis of WT and *Hmgb2*$^{-/-}$ P14 T cells at 8dpi LCMV Arm. (**a**) Principal component analysis (PCA) of all samples by global chromatin accessibility profile. (**b**) Location of significantly differentially accessible ATAC-seq peaks (FDR ≤ 0.05, $|\log_{10}FC| \geq 0.3$). (**c**) Heatmap of all significantly differentially accessible loci (DAR). Numbers on left denote number of DAR. Each column represents a biological replicate of n = 10 mice pooled. (**d**) ATAC-seq tracks of genes associated with effector and memory T cells. DAR are highlighted with grey bars. (**e**) Heatmap of DAR within promoters-TSS (≤1kb). Each column represents a biological replicate of n = 10 mice pooled. (**f**) Gene ontology (GO) biological process enrichment from Metascape of DAR within promoters-TSS (≤1kb) from **e**.

with effector T cells and apoptosis, including *Batf, Jak2,* and *Casp3* (**Fig. 2.5c, d**)[217]. We observed a similar trend when looking at promoters-TSS (≤1kb) containing DAR. Promoters of genes associated with memory T cells had reduced accessibility in *Hmgb2*$^{-/-}$ P14 T cells (*Foxp1, Runx1, Stat1*)[217, 218, 219], while promoters of terminal effector T cell genes were more accessible (*Stat3, Ctla4*, *Lag3)* (**Fig. 2.5e**)[1].

To further characterize genes associated with DAR at promoters-TSS (≤1kb), we performed pathway enrichment. Genes with increased accessibility at promoters in *Hmgb2*$^{-/-}$ P14 T cells showed significant enrichment for GO terms associated with (i) tumor necrosis factor receptor activity; (ii) cardiolipin metabolic process; and (iii) transcription corepressor binding (**Fig. 2.5f**). Conversely, genes with less accessible promoter regions in *Hmgb2*$^{-/-}$ P14 T cells had significant enrichment of GO terms associated with (i) positive regulator of T cell activation; (ii) Transcription coactivator binding; and (iii) positive regulation of DNA-binding transcription factor activity (**Fig. 2.5f**). Our data suggests a significant role for HMGB2 in CD8^{+} T cell chromatin accessibility, and more specifically, the opening of genomic regions associated with memory T cells and the closing of genomic regions associated with terminal cell differentiation. Together, these data contribute to our understanding of the mechanisms by which HMGB2 regulates the development of memory CD8^{+} T cells.

Hmgb2$^{-/-}$ memory CD8^{+} T cells are defective in their recall to secondary infection

We found that *Hmgb2*$^{-/-}$ P14 T cells survived to form memory T cells but were deficient in Tcm formation and had decreased accessibility of genes associated with memory T cells. Since Tcm cells can self-renew to maintain the memory T cell pool and mediate memory T cell recall responses[60, 199], we next assessed whether HMGB2 played

a role in the functionality of memory $CD8^+$ T cells. Small numbers ($1x10^3$ cells/each) of WT and *Hmgb2*$^{-/-}$ P14 T cells were adoptively co-transferred at a 1:1 ratio into WT mice and subsequently infected with LCMV Arm (**Fig. 2.6a**). At 30dpi, memory P14 T cells were sorted from spleens and co-transferred ($2x10^3$ cells/each) at a 1:1 ratio into naïve WT mice, which were then infected with LCMV Arm (**Fig. 2.6a**). WT P14 T cells robustly re-expanded with secondary challenge, while *Hmgb2*$^{-/-}$ P14 T cell frequencies were significantly decreased in the blood (**Fig. 2.6b**). Furthermore, we observed decreased frequencies and numbers of *Hmgb2*$^{-/-}$ P14 T cells in spleens at 20dpi (**Fig. 2.6c, d**). Similar results were seen when memory WT and *Hmgb2*$^{-/-}$ P14 T cells were transferred separately into WT hosts and infected with LCMV Arm (**Fig. 2.6e**). Since TCF-1 is required to generate $CD8^+$ memory T cell recall responses[60], we next investigated the expression of TCF-1 in *Hmgb2*$^{-/-}$ P14 memory T cells prior to secondary infection. We found similar TCF-1^+ frequencies between WT and *Hmgb2*$^{-/-}$ P14 T cells both during and after acute Arm infection (**Fig. 2.6f**). These findings showed that HMGB2 expression was required for the re-expansion of memory $CD8^+$ T cells during secondary viral infection.

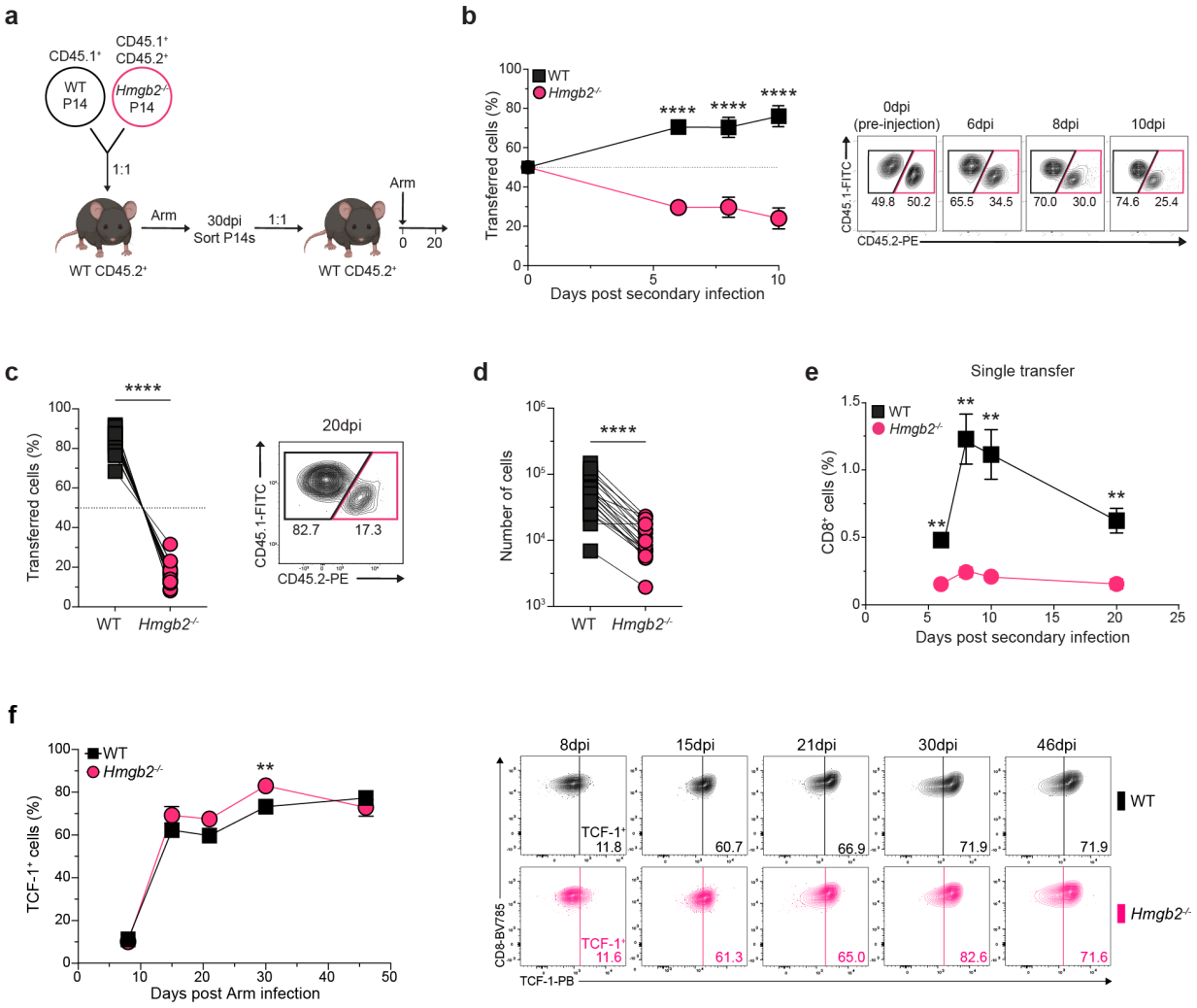

Figure 2.6 Memory *Hmgb2*$^{-/-}$ CD8^{+} T cells are defective in their recall capacity. (**a**) Experimental scheme for **b-d**. WT and *Hmgb2*$^{-/-}$ P14 T cells were co-transferred into WT mice at 1:1, followed by LCMV Arm infection. At 30dpi, memory WT and *Hmgb2*$^{-/-}$ P14 T cells were sorted and normalized to 1:1 before co-transferred into new naïve mice, followed by Arm infection (secondary infection). (**b**) Frequency of WT and *Hmgb2*$^{-/-}$ P14 T cells in blood during secondary Arm infection. Frequency (**c**) and number (**d**) of splenic WT and *Hmgb2*$^{-/-}$ P14 T cells at 20dpi secondary Arm. (**e**) WT and *Hmgb2*$^{-/-}$ P14 T cells were transferred separately into WT hosts and sorted at 68dpi Arm before adoptive transfer into separate naïve mice, followed by Arm infection (secondary infection). Frequency of WT and *Hmgb2*$^{-/-}$ P14 T cells in the blood during secondary Arm infection. (**f**) TCF-1 expression in co-transferred WT and *Hmgb2*$^{-/-}$ P14 T cells during LCMV Arm infection in the blood. Data is mean ± s.e.m. **p ≤ 0.01, ****p ≤ 0.0001, paired Student's *t*-test (b-d, f), two-tailed unpaired Student's *t*-test (e).

SUPPLEMENTARY FIGURES

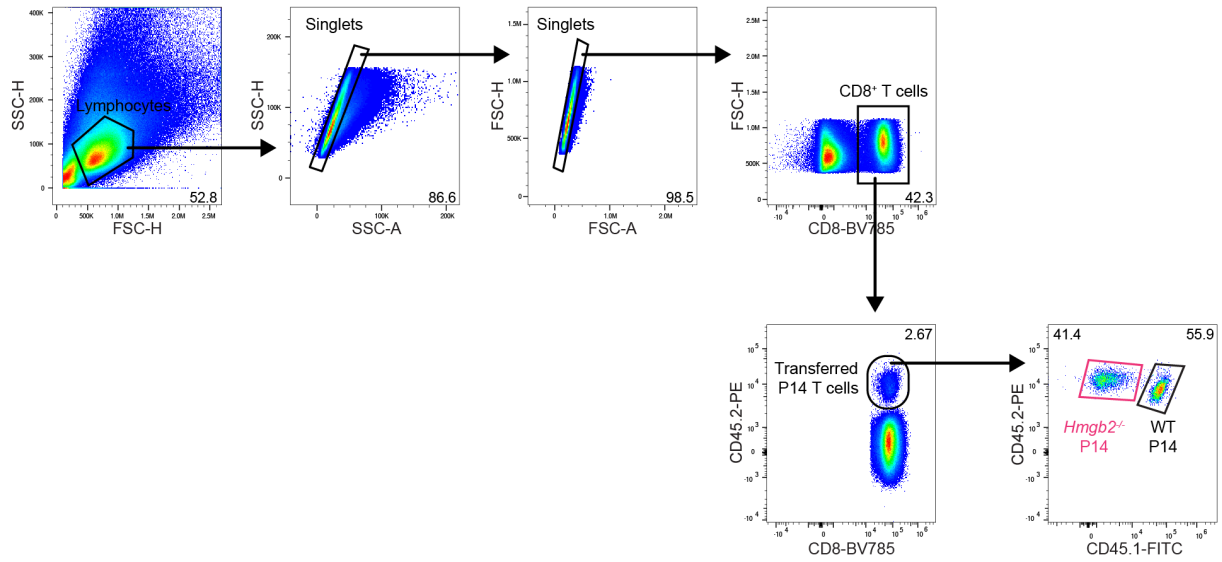

Supplementary Figure 2.1 Gating strategy.
Gating strategy used in co-adoptive transfer experiments.

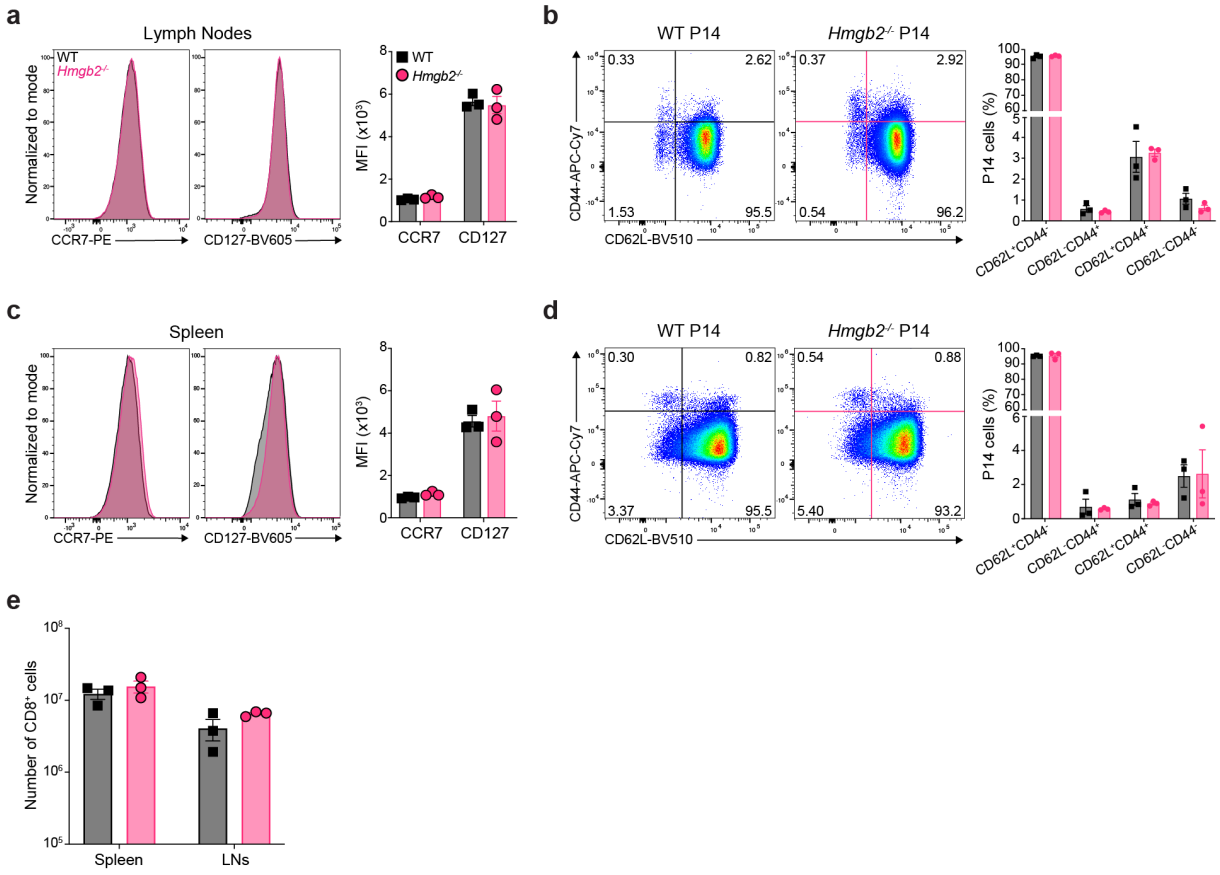

Supplementary Figure 2.2 HMGB2 expression is dispensable for naïve CD8⁺ T cell development.

CCR7/CD127 (**a**) and CD44/CD62L (**b**) protein expression of naïve WT and *Hmgb2*$^{-/-}$ P14 T cells isolated from lymph nodes of uninfected mice. CCR7/CD127 (**c**) and CD44/CD62L (**d**) protein expression of naïve WT and *Hmgb2*$^{-/-}$ P14 T cells isolated from spleens of uninfected mice. (**e**) Number of naïve WT and *Hmgb2*$^{-/-}$ CD8⁺ T cells. Each symbol represents an individual mouse. Data are representative of two independent experiments with ≥ 5 mice per group. Data is mean ± s.e.m. Two-sided Student's *t*-test.

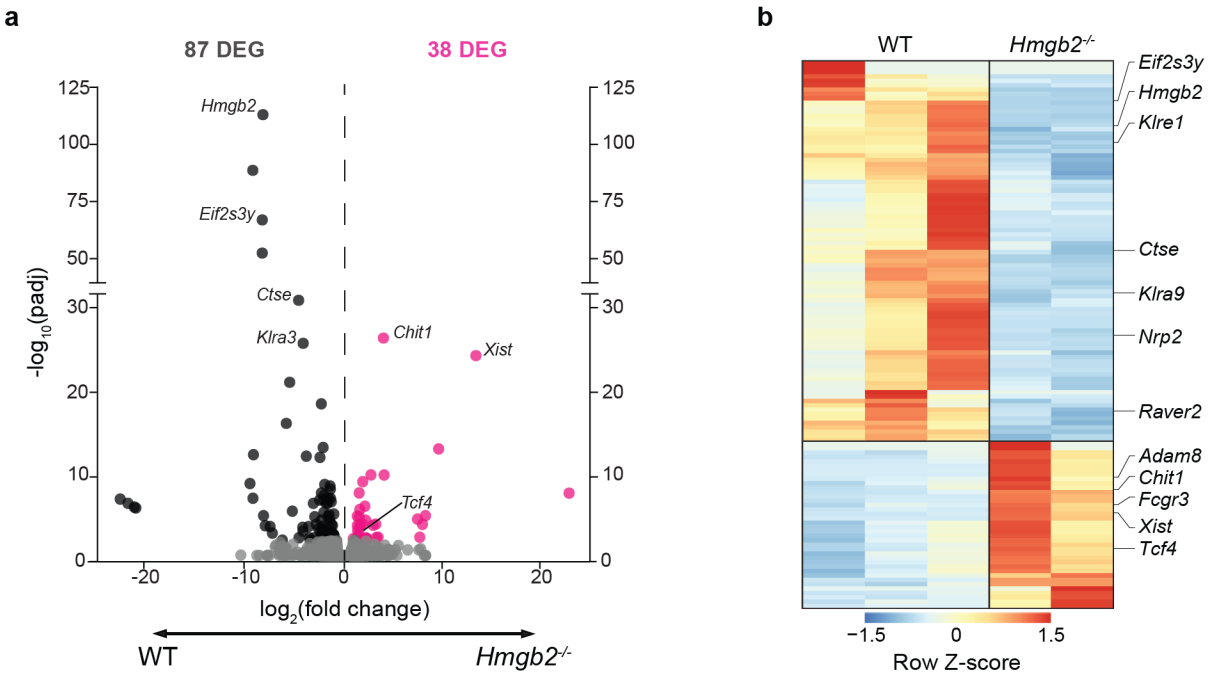

Supplementary Figure 2.3 Transcriptomics of WT and *Hmgb2*$^{-/-}$ CD8^{+} T cells after acute viral infection.

(**a**) Volcano plot highlighting differentially expressed genes (DEG) between WT and *Hmgb2*$^{-/-}$ P14 T cells at 8dpi LCMV Arm infection from Fig. 4a. Significant DEG (padj ≤ 0.1) are colored (pink = upregulated in *Hmgb2*$^{-/-}$ P14 T cells; black = upregulated in WT P14 T cells). (**b**) Heatmap of average normalized expression of significant DEG. Each column represents one independent experiment with *n* = 5 mice.

DISCUSSION

Our findings showed a cell-intrinsic role for HMGB2 in the differentiation and stemness of memory $CD8^+$ T cells during acute viral infection. In effector $CD8^+$ T cells, the expression of *Hmgb2* was dispensable for their formation and function during acute LCMV infection. However, we found a critical role for HMGB2 in memory T cells (Tmem), as shown by decreases in *Hmgb2*$^{-/-}$ memory precursor effector T cell (MPEC) survival, central memory T cell (Tcm) differentiation, and recall responses to secondary infections. Despite *Hmgb2*$^{-/-}$ memory $CD8^+$ T cells expressing TCF-1, this critical transcriptional regulator of memory T cell stemness was insufficient to induce the re-expansion of *Hmgb2*$^{-/-}$ T cells during secondary infection. Epigenetic analysis showed *Hmgb2*$^{-/-}$ T cells during acute viral infection had decreased accessibility of memory-specific gene signatures, while those associated with terminal effector function were increased.

After clearance of acute viral infections, MPECs give rise to $CD8^+$ Tmem cells, which can self-renew, persist long term, and provide protection upon secondary infection[1, 21, 56, 220]. Interestingly, we found HMGB2 negatively regulated MPEC differentiation, but was critical for their survival. Within the Tmem compartment, there is heterogeneity that vastly impacts the quantity and quality of T cell responses. We observed a cell-intrinsic role for HMGB2 in regulating Tmem subset formation, as there was a defect in the differentiation of *Hmgb2*$^{-/-}$ Tcm cells. These cells are important for Tmem responses as they contribute to their proliferation, longevity, multipotency, and recall potential[26, 200]. We correspondingly found diminished maintenance and recall capacity of *Hmgb2*$^{-/-}$ Tmem cells. Additionally, although *Hmgb2*$^{-/-}$ Tmem cells had high expression of the transcription factor TCF-1, a critical regulator for Tmem transcriptional programs and Tcm-mediated

recall responses[55, 56, 60], they were still unable to persist and respond to secondary infection. Together, this suggests a cell-intrinsic role for HMGB2 in supporting memory T cell function by regulating both MPEC survival and Tcm subset formation. We also propose HMGB2 as a critical partner of TCF-1 in promoting memory T cell transcriptional programs and recall responses.

The epigenetic state of memory T cells is critical for their durability and recall capacity upon secondary infections. Recently, studies have shown Tcm cells have decreased methylation of promoters for effector and survival genes, including *Ifng*, *Gzmb*, *Prf1, Bcl2* and *Il7r*, which support their rapid expansion upon secondary challenge[48, 49, 50, 51]. Additionally, the TCF-1 regulated transcriptional profile of memory T cells directly supports the bioenergetic and proliferative needs of Tcm cells during recall[60]. However, there is still a need to fully characterize the epigenetic and transcriptional regulators of memory T cells as their re-expansion capacity and long-term survival are critical for secondary immune responses and the efficacy of vaccinations. HMGB2 is a known chromatin modifier that regulates cellular stemness, but its role in the epigenetic program of memory T cells is not known. Here, we found that HMGB2 regulated 5,610 genomic regions in effector T cells during the contraction phase of acute viral infection. HMGB2 directly supported the accessibility of memory associated genes while suppressing the accessibility of genes associated with short-lived effector T cells (SLEC). The role of HMGB2 in maintaining the accessibly of genes important for memory T cell responses and self-renewal was critical for the re-expansion of these cells upon secondary challenge, as demonstrated by the inability of *Hmgb2*$^{-/-}$ memory T cells to mount a response to secondary LCMV infection. The ability to preserve memory T cells and

enhance their recall capacity is a key objective of various immunotherapies and vaccines. Therefore, modulating HMGB2 in T cells during acute viral infections may enhance memory survival and secondary responses to increase clinical efficacy. Together, our findings showed HMGB2 regulates the differentiation, survival, and recall capacity of memory T cells, and may help predict vaccine efficacy.

In summary, we show that *Hmgb2* expression is required for the differentiation and survival of memory T cells during acute viral infection. *Hmgb2*$^{-/-}$ CD8^{+} memory T cells developed, but they were defective in their formation of Tcm cells and recall capacity. We found HMGB2 positively regulates the epigenetic program of memory cells, promoting their differentiation, maintenance, and function. We found a previously unidentified role for HMGB2 in the differentiation and survival of functional memory T cells, with vast implications for secondary reinfections and vaccinations. This new understanding of HMGB2's role in memory T cell stemness and function is a novel contribution to TCF-1 mediated regulation of secondary recall responses and shows that HMGB2 is an indispensable partner of TCF-1 in the formation and maintenance of memory T cells.

ACKNOWLEDGMENTS

We would like to thank all the current and former members in the Tinoco Laboratory (Twitter: @Tinoco_Lab) for all their constructive comments and advice during this project. We would like to thank Dr. Jennifer Atwood at the UCI Institute for Immunology Flow Core, a shared resource of the Cancer Center Support Grant (CA-62203) at the University of California, Irvine, for assistance with FACS. We would like to thank Dr. Jie Wu and Dr. Melanie Oakes at the UCI Genomics High Throughput Facility (UCI GHTF) for setup and analysis of RNA-sequencing and setup of ATAC-sequencing data. The UCI GHTF is another shared resource of the Cancer Center Support Grant (CA-62203) at the University of California, Irvine, and NIH shared instrumentation grants 1S10RR025496-01, 1S10OD010794-01, and 1S10OD021718-01. This work was supported by the National Institutes of Health (R01 AI137239 to R.T. and R37 CA252081 to R.B.) Department of Defense (CA171198 to R.T.), The Melanoma Research Alliance (571135 to R.T.), The ACS (to R.T.), T32 virus-host interactions: a multi-scale training program (T32AI007319 to E.N.N.), T32 training grant in Cancer Biology and Therapeutics (T32 CA009054 to J.M.D.), NIH IMDS training grant (GM055246 to K.V.M.), and an EMBO postdoctoral fellowship (P.O.).

CHAPTER 3

HMGB2 regulates the differentiation and stemness of exhausted CD8$^+$ T cells during chronic viral infection and cancer

Emily N. Neubert[1,2], Julia M. DeRogatis[1], Sloan A. Lewis[1,3], Karla M. Viramontes[1], Pedro Ortega[4,5], Monique L. Henriquez[1], Rémi Buisson[2,4,5], Ilhem Messaoudi[6], and Roberto Tinoco[1,2*]

[1]Department of Molecular Biology and Biochemistry, School of Biological Sciences, University of California Irvine, Irvine, CA 92697, USA
[2]Center for Virus Research, University of California Irvine, Irvine, CA 92697, USA
[3]La Jolla Institute for Immunology, La Jolla, CA 92037, USA
[4]Department of Biological Chemistry, School of Medicine, University of California, Irvine, Irvine, CA 92697, USA
[5]Center for Epigenetics and Metabolism, Chao Family Comprehensive Cancer Center, University of California Irvine, Irvine, CA 92697, USA
[6]Microbiology, Immunology, and Molecular Genetics, University of Kentucky, Lexington, KY, 40536, USA

In revision in *Nature Communications*. Neubert EN, DeRogatis JM, Lewis SA, Viramontes KM, Ortega P, et al. HMGB2 Regulates the Differentiation and Stemness of Exhausted CD8$^+$ T Cells During Chronic Viral Infection and Cancer. *Nature Communications*. 2023.

ABSTRACT

Chronic infections and cancers evade the host immune system through mechanisms that induce T cell exhaustion. The heterogeneity within the exhausted $CD8^+$ T cell pool has revealed the importance of stem-like progenitor (Tpex) and terminal (Tex) exhausted T cells, although the mechanisms underlying their development are not fully known. Here we report HMGB2 expression is upregulated and sustained in exhausted $CD8^+$ T cells, and HMGB2 expression is critical for their differentiation. Through epigenetic and transcriptional programming, we identify HMGB2 as a cell-intrinsic regulator of the differentiation and maintenance of Tpex cells during chronic viral infection and in tumors. Despite *Hmgb2*$^{-/-}$ $CD8^+$ T cells expressing TCF-1 and TOX, these master regulators were unable to sustain Tpex differentiation and long-term survival during persistent antigen. Our findings show that HMGB2 is a key regulator of exhausted $CD8^+$ T cells and may be an important molecular target for future T cell-based immunotherapies.

INTRODUCTION

During chronic viral infections there is a dynamic interplay between host and pathogen, where multiple cellular and molecular mechanisms inhibit the immune response and facilitate viral persistence. A key mechanism is the differentiation of exhausted T cells, which are dysfunctional and fail to clear the virus. Despite being less functional than effector $CD8^+$ T cells, exhausted T cells still provide some protection to the host[106, 221], which is highlighted in simian immunodeficiency virus studies showing host progression to AIDS-like disease and death when T cells are depleted[74]. Chronic antigen stimulation results in responding T cell dysfunction and heterogeneity, with altered transcription, epigenome, and metabolism unique to exhausted T cells[18, 116, 138, 222, 223]. Two key exhausted T cell subsets, defined by phenotype and transcription factor expression, are progenitor exhausted (Tpex) and terminal exhausted (Tex) T cells[100, 102, 111]. Tpex cells are long-lived, self-renew, and give rise to Tex cells[100]. They also express the key transcription factors TCF-1, BCL-6, and BACH2[224]. In contrast, terminal Tex cells express high TOX, BLIMP-1, and TIM-3, have increased effector functions, and undergo higher rates of apoptosis[224]. Despite detailed characterization of these two main subsets, their differentiation mechanisms have not been fully described.

Understanding exhausted T cell heterogeneity has important clinical implications for immune checkpoint blockade (ICB) therapy against chronic viral infections and cancer[145]. Studies have shown anti-PD-1/anti-PD-L1 blockade reinvigorates the Tpex population, which proliferates and further increases numbers of the more cytotoxic Tex cells[135]. Emerging evidence also suggests Tpex cell frequencies may predict patient responsiveness to ICB therapy[102, 111, 225] and ability to control HIV viremia[226]. Importantly,

exhausted T cells undergo unique epigenetic changes during differentiation, including permanent marks which sustain their exhausted state[227]. Therefore, although exhausted T cells can be re-invigorated with ICB therapy, they revert to their exhausted phenotype and thereby provide only temporary clinical response in some patients[120, 121, 44, 142, 143, 228]. Identifying mechanisms of exhausted T cell differentiation and the associated epigenetic changes remains of high clinical interest as these cells may need to be reprogrammed transcriptionally and/or epigenetically to improve immunotherapy efficacy.

HMGB2 is a member of the high-mobility group box (HMGB) family, which are relatively abundant and highly conserved DNA-binding proteins that modify chromatin structure and regulate gene transcription and transcription factor binding[159, 210, 211]. HMGB2 has known roles in regulating stem cells during various differentiation programs, including myogenesis, spermatogenesis, and neurogenesis[175, 176, 177]. In mice, *Hmgb2* is expressed early in embryogenesis, but is limited to lymphoid organs and testes in adults[159]. Despite its characterization in numerous cell types, the role of HMGB2 in $CD8^+$ T cells has not been investigated. Previous RNA-sequencing analyses found increased *Hmgb2* expression in murine exhausted $CD8^+$ T cells during lymphocytic choriomeningitis virus (LCMV) infection[212] and increased *HMGB2* expression in $CD8^+$ T cells from cancer patients[229, 230, 231, 232]. Given HMGB2's role in both modulating chromatin architecture and regulating stem cells, along with its high gene expression in $CD8^+$ T cells, we investigated the function of HMGB2 in exhausted $CD8^+$ T cells.

We found a cell-intrinsic role for HMGB2 in the differentiation and stemness of exhausted $CD8^+$ T cells. Exhausted $CD8^+$ T cells had high HMGB2 expression that was sustained with persistent antigen. In response to chronic viral infection, *Hmgb2*$^{-/-}$ $CD8^+$ T

cells showed decreased Tpex differentiation. Even though *Hmgb2*$^{-/-}$ CD8^{+} T cells expressed both TCF-1 and TOX, these transcription factors were unable to support the differentiation and maintenance Tpex and Tex cells. Mechanistically, HMGB2 regulated Tpex-specific transcriptional programming through increasing chromatin accessibility of Tpex genes, while decreasing accessibility of regions specific for terminal Tex cells during chronic infection. Our findings show a previously unknown role for HMGB2 as an essential regulator of exhausted CD8^{+} T cell differentiation, that protects these cells from a terminal fate.

MATERIALS AND METHODS

Mice

All experimental animal procedures were approved by the Institutional Animal Care and Use Committee of University of California, Irvine (AUP-21-124) and complied with all relevant ethical regulations for animal testing and research. C57BL/6J and B6.SJL-*Ptpr*^{a} *Pepc*^{b}/BoyJ mice were purchased from the Jackson Laboratory, then bred in SPF facilities. P14 mice were obtained from The Scripps Research Institute (originally from Dr. Charles D. Surh). These mice were bred to Ly5.1 (B6.SJL-*Ptprc*^{a} *Pepc*^{b}/BoyJ) mice and to *Hmgb2*$^{-/-}$ mice, which were generously provided by Dr. Marco Bianchi (San Raffaele Scientific Institute, Milan, Italy). Male and female mice ≥ 6 weeks of age were used in experiments. Mouse selection for experiments was not formally randomized or blinded.

Virus Infection and Titers

LCMV Clone 13 (Cl13) was propagated in baby-hamster kidney cells and titrated on Vero African-green-monkey kidney cells. Frozen stocks were diluted in Vero cell media and $2x10^{6}$ PFUs of LCMV Cl13 were injected intravenously (i.v.). Virus titers were determined from serial dilutions of either sera or tissues taken from mice using a plaque assay.

T cell Adoptive Transfer

Bulk CD8^{+} T cells were enriched from spleens and lymph nodes (LNs) of WT (*Hmgb2*$^{+/+}$) or *Hmgb2*$^{-/-}$ P14 transgenic mice by column-free magnetic negative selection. Single cell suspensions from pooled spleen and LNs were incubated with biotinylated antibodies

against CD4 (GK1.5), B220 (RA3-6B2), CD19 (6D5), CD24 (M1/69), CD11b (M1/70), and CD11c (N418). Non-$CD8^+$ cells were removed by mixing labeled cell suspension with Streptavidin RapidSpheres (Stemcell technologies) at room temperature (RT) for 5min, followed by two-5min incubations in an EasyEights™ EasySep™ Magnet (Stemcell technologies). The unbound $CD8^+$ T cells were washed in sterile PBS (1x) with FBS (2%), and purity was determined on a flow cytometer. For single-transfer studies, WT and *Hmgb2*$^{-/-}$ P14 T cells were transferred into separate new WT hosts of the opposite congenic marker ($1x10^3$ i.v. for virus studies, $1x10^6$ for tumor survival studies). For co-transfer studies, WT and *Hmgb2*$^{-/-}$ P14 T cells were mixed at a 1:1 ratio ($1x10^3$ i.v. per cell-type for virus studies, $1x10^6$ i.v. per cell-type for tumor studies) and injected into new WT recipient mice i.v. Within 18-24hr post-transfer, recipient mice were inoculated with LCMV Cl13 ($2x10^6$ PFU, i.v.) or B16-GP_{33-41} tumor cells ($1x10^6$, s.c.). For re-challenge experiments, live (PI^-) WT and *Hmgb2*$^{-/-}$ P14 T cells were sorted at >95% purity from spleens and LNs at 30dpi or 68dpi using a BD FACSAria sorter. Cell numbers were normalized and transferred into new hosts ($2x10^3$ i.v. per cell-type) that were subsequently infected with LCMV Arm ($2x10^5$ PFU, i.p.).

B16-GP_{33-41} Tumor Model and Digestion

B16-GP_{33-41} melanoma cells were kindly provided by Dr. Ananda Goldrath. All cell lines maintained in Iscove's Modified Dulbecco's medium supplemented with 10% fetal bovine serum (FBS) and antibiotics. All cell lines were free of mycoplasma. For co-transfer and survival tumor experiments, mice were injected subcutaneously (s.c.) with $1x10^6$ tumor cells. Tumor size was measured by caliper daily for calculation of B16-GP_{33-41} tumor

volume and tumors of <1800mm^3 were designated as surviving per IACUC protocol. Tumors were weighed at time of excision before being minced and digested in gentleMACS™ C Tubes for 40min at 37°C using the gentleMACS™ Dissociator (Miltenyi Biotec). Digests were then passed through a 70-μm cell strainer to generate a single-cell suspension. The cells were then stained for flow cytometry.

Flow Cytometry

For cell surface staining, 2x10^6 cells were incubated with antibodies in staining buffer (PBS, 2% FBS and 0.01% NaN_3) at 4°C . For tetramer surface staining, 2x10^6 cells were stained with conjugated H-2D^b-GP$_{33–41}$, H-2D^b-GP$_{276-286}$, or H-2D^b-NP$_{396–404}$ tetramers (NIH core facility) for 1h and 15min at RT in staining buffer. For intracellular cytokine staining, cells were resuspended in complete RPMI-1640 (containing 10 mM HEPES, 1% nonessential amino acids and L-glutamine, 1 mM sodium pyruvate, 10% heat inactivated FBS and antibiotics) supplemented with 50 U/mL IL-2 (NCI) and 1 mg/mL brefeldin A (BFA, Sigma), and then incubated with 2mg/mL LCMV GP$_{33-41}$ peptide (AnaSpec) at 37°C for 4h. Cells were then fixed and permeabilized using a Cytofix/Cytoperm Kit (BD Biosciences) before staining. For intranuclear transcription factor staining, cells were fixed and permeabilized using a Foxp3/transcription factor fixation/permeabilization kit (Fisher). Antibodies are listed in Star Methods. Surface stains were performed at a 1:200 dilution, while intracellular and intranuclear stains performed at a 1:100 dilution. Caspase3 staining was done using CaspGLOW Fluorescein Active Caspase-3 staining kit (ThermoFisher) following manufacturer's instructions. All data were collected on a Novocyte3000 (Agilent) and analyzed using FlowJo Software (Tree Star).

In Vivo Proliferation

Mice were injected i.p. with 2mg BrdU (Sigma-Aldrich) 16h before removing spleens at 8dpi to measure proliferation. Cells were stained intracellularly using FITC BrdU Flow kit (BD Biosciences) following the manufacturer's instructions. Cells were acquired with a Novocyte3000 flow cytometer.

Comet Assay

Co-transferred live (PI^-) WT and *Hmgb2*$^{-/-}$ P14 T cells were sorted at >95% purity from spleens and LNs of LCMV Cl13 infected mice at 8dpi using a BD FACSAria sorter. U2OS cells were cultured in DMEM supplemented with 10% fetal bovine serum, 1% L-Glutamine, and 1% penicillin/streptomycin. Single-cell alkaline gel electrophoresis was performed with comet assay Kit (Abcam) following manufacturer's instructions. Images were captured using a Leica DMi8 THUNDER microscope. Comet olive tail moments of 100 cells were analyzed using CometScore software version 2.0.0.38.

Western Blot

Co-transferred live (PI^-) WT and *Hmgb2*$^{-/-}$ P14 T cells were sorted at >95% purity from spleens and LNs of LCMV Cl13 infected mice at 8dpi using a BD FACSAria sorter. Cells were lysed and blots were stained for Phospho-H2AX (Ser139) (1:1000) and Histone H3 (1:140000).

Bulk RNA-Seq RNA Isolation and Library Preparation

For 8dpi studies, WT and *Hmgb2*$^{-/-}$ P14 T cells were transferred into five separate mice each before infection with LCMV Cl13. For 20dpi studies, WT and *Hmgb2*$^{-/-}$ P14 T cells were co-transferred at 1:1 into 10 mice before infection with LCMV Cl13. On 8dpi or 20dpi, spleens and LNs were pooled based on infection type and P14 genotype. Live (PI^{-}) WT and *Hmgb2*$^{-/-}$ P14 were sorted at >95% purity (8dpi:~1x10^{6} per condition; 20dpi: ~300k WT, ~100k *Hmgb2*$^{-/-}$) and resuspended in RLT Buffer and BME before storage at -80°C. Each experiment was performed three times to represent three biological replicates. Total RNA was monitored for quality control using the Agilent Bioanalyzer Nano RNA chip and Nanodrop absorbance ratios for 260/280nm and 260/230nm. Library construction was performed according to the Illumina TruSeq mRNA stranded protocol. The input quantity for total RNA within the recommended range and mRNA was enriched using oligo dT magnetic beads. The enriched mRNA was chemically fragmented. First strand synthesis used random primers and reverse transcriptase to make cDNA. After second strand synthesis the ds cDNA was cleaned using AMPure XP beads and the cDNA was end repaired and then the 3' ends were adenylated. Illumina barcoded adapters were ligated on the ends and the adapter ligated fragments were enriched by nine cycles of PCR. The resulting libraries were validated by qPCR and sized by Agilent Bioanalyzer DNA high sensitivity chip. The concentrations for the libraries were normalized and then multiplexed together. The multiplexed libraries were sequenced using paired end 100 cycles chemistry on the NovaSeq 6000.

Bulk RNA-Seq Data Analysis

Post-processing of the run to generate FASTQ files was performed at the Institute for Genomics and Bioinformatics (UCI IGB). *PcaHubert* was used to identify any outlier samples, which were removed from further analysis[213]. The quality of the sequencing was first assessed using the *fastQC* tool (v0.11.9). Raw reads were then quality trimmed and filtered by a length of 20 bases using *trimmomatic* (v0.39). Trimmed reads were analyzed with the mouse Grcm38 reference genome using pseudo aligner Salmon (v1.2.1) and resulting quantification files were imported using R package *tximport* to get TPM values for all annotated mouse genes. Differential analysis was done using R package *DESeq2* (v1.22.2) with an FDR cut off of 0.05. PCA was done using R packages *DESeq2* and *pheatmap*. For downstream analysis, genes with adjusted p-value ≤ 0.1 and $|\log_2 FC| \geq 0.5$ were included. Gene ontology functional enrichment of gene expression changes in WT and *Hmgb2*$^{-/-}$ P14 T cells were performed using Metascape (http://metascape.org).

ATAC-Seq Library Preparation

WT and *Hmgb2*$^{-/-}$ P14 T cells were co-transferred at 1:1 into 10 mice before infection with LCMV Cl13. On 8dpi, spleens and LNs were pooled (samples are pooled from 10mice/group). Live (PI^-) WT and *Hmgb2*$^{-/-}$ P14 were sorted at >95% purity ($2x10^5$ WT, $2x10^5$ *Hmgb2*$^{-/-}$). Each experiment was performed three times to represent three biological replicates. Following the Omni-ATAC protocol, samples were lysed in lysis buffer (10mM Tris-HCl (pH 7.4), 10mM NaCl, 3mM $MgCl_2$, 10% Np-40, 10% Tween, and 1% Digitonin) on ice for 3 minutes[214]. Immediately following lysis, nuclei were spun at 500g for 10min at 4°C to remove supernatant. Nuclei were then incubated with Tn5 transposase for 30min at 37°C. Tagmented DNA was purified using AMPure XP beads

and PCR was performed to amplify the library under the following conditions: 72°C for 5min; 98°C for 30s; 5 cycles of 98°C for 10s, 63°C for 30s, and 72°C for 1min; hold at 4°C. Libraries were then purified with warm AMPure XP beads and quantified on a Bioanalyzer. Libraries were multiplexed and sequenced to a depth of 50million 100bp paired reads on a NextSeq.

ATAC-Seq Data Analysis

Paired ended reads from sequencing were QC analyzed with fastqQC (v.11.9) and aligned to mouse mm10 reference genome using bowtie2 (v2.4.1). Mitochondrial reads and reads mapped to dark list (ENCODE Stanford version) were excluded from the downstream analysis. Duplicated reads were removed using Picard tools (v2.27.1). A union peak list was created by merging processed reads from all samples and then calling peaks using MACS2 (v2.7.1) (-q 0.01 --keep-dup all -f BAMPE). The number of reads in each peak were then counted using featureCounts (Rsubread v2.6.4) to create a counts matrix. Normalization of counts matrix was performed using DESeq2 (v1.32.0). Differentially expressed peaks were determined using edgeR (v3.34.1) with an FDR cut-off of 0.05 and a $|\log_{10}FC|$ cut-off of ≥ 0.3. Peaks were annotated using ChIPSeeker (v1.34.0). Functional enrichment of promoter regions was performed using Metascape (http://metascape.org).

Quantification and Statistical Analysis

Flow cytometry data were analyzed with FlowJo software (TreeStar). Bulk RNA-seq and ATAC-seq figures were prepared using RStudio software. Graphs were prepared with

GraphPad Prism software. GraphPad Prism was used for statistical analysis to compare outcomes using a two-tailed unpaired Student's *t*-test, Mann Whitney or paired Student's *t*-test where indicated; significance was set to $p \leq 0.05$ and represented as $*p \leq 0.05$, $**p \leq 0.01$, $***p \leq 0.001$, and $****p \leq 0.0001$. Error bars show SEM.

Data and code availability

The authors declare that all supporting data are available within the Article and its Supplementary Information files. 3'-scRNA-seq and ATAC-seq data sets will be deposited in the Gene Expression Omnibus (GEO) database.

RESULTS

Cell-intrinsic HMGB2 expression is essential for long-term maintenance of exhausted CD8$^+$ T cells

Since HMGB2 expression was increased and sustained in exhausted CD8$^+$ T cells, we next determined the cell-intrinsic role of HMGB2 in virus-specific T cells during chronic LCMV infection. Small numbers (1x10^3 cells) of congenically marked WT or *Hmgb2*$^{-/-}$ P14 T cells were adoptively transferred into congenically mismatched WT mice and infected with LCMV Cl13 (**Fig. 3.1a**). We observed similar expansion of both WT and *Hmgb2*$^{-/-}$ P14 T cells at 8dpi, but *Hmgb2*$^{-/-}$ P14 T cells had an accelerated decline and were present at significantly lower frequencies compared to WT by 15dpi (**Fig. 3.1b**). Furthermore, we observed significantly decreased frequencies and numbers of *Hmgb2*$^{-/-}$ P14 T cells in spleens at 68dpi (**Fig. 3.1c**). We next evaluated the functionality of WT and *Hmgb2*$^{-/-}$ P14 T cells and observed similar frequencies of GranzymeB$^+$ cells at 8dpi and IFN-γ^+ and IFN-γ^+TNF-α^+ cells at 68dpi (**Fig. 3.1d, e**). To investigate cell-intrinsic HMGB2 function during chronic infection, we co-transferred WT and *Hmgb2*$^{-/-}$ P14 T cells at a 1:1 ratio into WT mice and then infected with Cl13 (**Fig. 3.1f**). Despite starting at a 1:1 ratio, we observed a significant decrease in frequencies of *Hmgb2*$^{-/-}$ P14 T cells compared to WT cells as early as 8dpi (**Fig. 3.1g**). Additionally, we observed significantly decreased numbers of *Hmgb2*$^{-/-}$ P14 T cells compared to WT at 8 and 30dpi (**Fig. 3.1h**). We next evaluated co-inhibitory receptor expression and found that *Hmgb2*$^{-/-}$ CD8$^+$ T cells were increased in PD-1$^+$TIM-3$^+$ cells throughout Cl13 infection (**Fig. S3.1a**). Furthermore, we observed higher PD-1 expression in *Hmgb2*$^{-/-}$ P14 T cells at 26 and 35dpi (**Fig. S3.1b**). Since it has been established TOX is required for the generation of exhausted T cells during Cl13

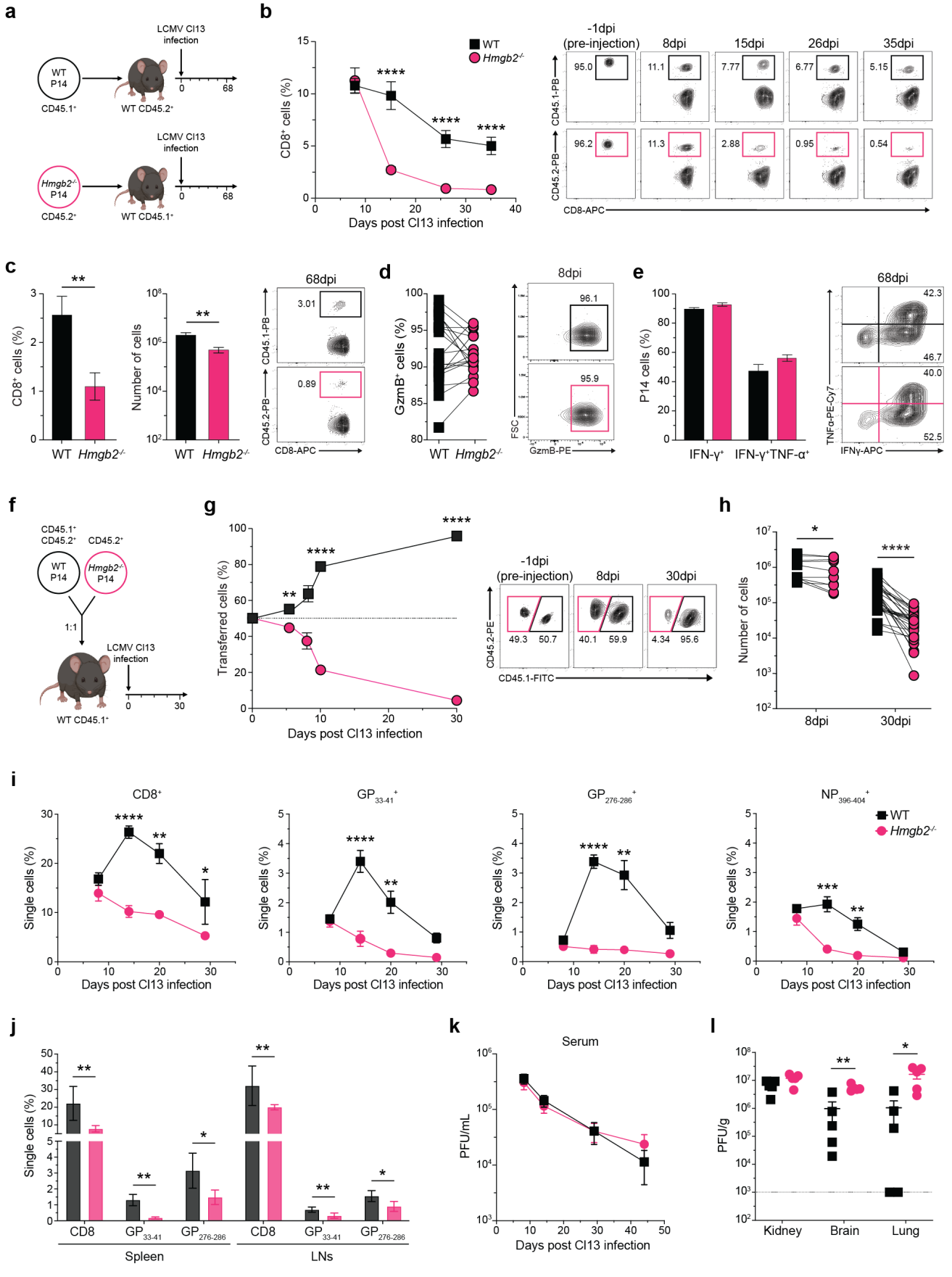
a
LCMV Cl13 infection
WT P14
CD45.1+
WT CD45.2+
0
68
Hmgb2-/- P14
CD45.2+
WT CD45.1+
b
WT
Hmgb2-/-
CD8+ cells (%)
Days post Cl13 infection
-1dpi (pre-injection)
8dpi
15dpi
26dpi
35dpi
CD45.1-PB
CD45.2-PB
CD8-APC
95.0
11.1
7.77
6.77
5.15
96.2
11.3
2.88
0.95
0.54
c
CD8+ cells (%)
Number of cells
WT
Hmgb2-/-
68dpi
3.01
0.89
d
GzmB+ cells (%)
8dpi
96.1
95.9
FSC
GzmB-PE
e
P14 cells (%)
IFN-γ+
IFN-γ+TNF-α+
68dpi
42.3
46.7
40.0
52.5
TNFα-PE-Cy7
IFNγ-APC
f
CD45.1+ CD45.2+
CD45.2+
WT P14
Hmgb2-/- P14
1:1
LCMV Cl13 infection
WT CD45.1+
g
Transferred cells (%)
Days post Cl13 infection
-1dpi (pre-injection)
8dpi
30dpi
CD45.2-PE
CD45.1-FITC
49.3
50.7
40.1
59.9
4.34
95.6
h
Number of cells
8dpi
30dpi
i
CD8+
GP33-41+
GP276-286+
NP396-404+
WT
Hmgb2-/-
Single cells (%)
Days post Cl13 infection
j
Single cells (%)
CD8
GP33-41
GP276-286
Spleen
LNs
k
Serum
PFU/mL
Days post Cl13 infection
l
PFU/g
Kidney
Brain
Lung

Figure 3.1 Cell-intrinsic kinetics of WT and *Hmgb2*$^{-/-}$ P14 T cells during Cl13 infection.

(**a**) Experimental scheme for **b-c, e**. WT and *Hmgb2*$^{-/-}$ P14 CD8^{+} T cells were transferred separately into naïve mice and infected with LCMV Cl13. Blood taken at 8, 15, 26, and 35dpi. Spleens isolated at 68dpi. (**b**) Frequency of WT and *Hmgb2*$^{-/-}$ P14 T cells of total CD8^{+} population. (**c**) Splenic WT and *Hmgb2*$^{-/-}$ P14 T cell frequencies and numbers at 68dpi Cl13. (**d**) Frequencies of GranzymeB^{+} WT and *Hmgb2*$^{-/-}$ P14 T cells at 8dpi LCMV Cl13 infection in the blood (**e**) Cytokine production by splenic WT and *Hmgb2*$^{-/-}$ P14 T cells at 68dpi Cl13. (**f**) Experimental scheme for **g-h**. WT and *Hmgb2*$^{-/-}$ P14 T cells were co-transferred at 1:1 into WT mice and infected with Cl13. Frequencies (**g**) and numbers (**h**) of splenic WT and *Hmgb2*$^{-/-}$ P14 T cells at indicated timepoints post infection. Data are representative of three independent experiments with ≥ 5 mice per group. (**i**) Frequencies of total CD8^{+}, $GP_{33\text{-}41}{}^{+}$, $GP_{276\text{-}286}{}^{+}$, and $NP_{396\text{-}404}{}^{+}$ T cells during Cl13 infection in the blood of WT and *Hmgb2*$^{-/-}$ mice. (**j**) Frequencies of total CD8^{+}, $GP_{33\text{-}41}{}^{+}$, $GP_{276\text{-}286}{}^{+}$, and $NP_{396\text{-}404}{}^{+}$ T cells during Cl13 infection in the spleen and lymph nodes (LNs) of WT and *Hmgb2*$^{-/-}$ mice at 44dpi. (**k**) Virus titers in serum at 44dpi by plaque forming units (PFU) and expressed as PFU/mL. (**l**) Virus titers in the kidney, brain, and lung, expressed as PFU/g. Limits of detection are indicated by dashed lines. Data are representative of three independent experiments with ≥ 5 mice per group (a-h) or two independent experiments with ≥ 3 mice per group (i-l). Data is mean ± s.e.m. *p ≤ 0.05, **p ≤ 0.01, ***p ≤ 0.001, ****p ≤ 0.0001, two-tailed unpaired Student's *t*-test (b-c, e, i-l), paired Student's *t*-test (d, g-h).

infection[126, 127, 136], we next asked if the loss of exhausted *Hmgb2*$^{-/-}$ P14 T cells was due to decreased TOX expression compared to WT. Significantly, we found *Hmgb2*$^{-/-}$ P14 T cells had both similar and increased frequencies of TOX^{+} cells compared to WT, but had impaired generation of exhausted T cells (**Fig. S3.1c**).

Since we saw diminished maintenance of exhausted *Hmgb2*$^{-/-}$ P14 T cells, we wanted to investigate the impact of HMGB2 deletion on other virus-specific T cell clones by infecting WT and *Hmgb2*$^{-/-}$ mice with Cl13. By 8dpi there was similar expansion of CD8^{+}, GP$_{33-41}$$^{+}$, GP$_{276-286}$$^{+}$, and NP$_{396-404}$$^{+}$ T cells in both WT and *Hmgb2*$^{-/-}$ mice, but by 14dpi and onwards there were significantly less virus-specific CD8^{+} T cells in *Hmgb2*$^{-/-}$ mice (**Fig. 3.1i**). At 44dpi, there were significantly decreased frequencies of CD8^{+}, GP$_{33-41}$$^{+}$, and GP$_{276-286}$$^{+}$ T cells in spleens and lymph nodes of *Hmgb2*$^{-/-}$ mice compared to WT (**Fig. 3.1j**). Throughout the course of infection there were no differences serum viral titers, but we observed significantly increased viral titers in the brains and lungs of *Hmgb2*$^{-/-}$ mice at 44dpi (**Fig. 3.1k, l**). Together, these findings showed HMGB2 was essential for the formation and long-term maintenance of exhausted CD8^{+} T cells during chronic viral infection.

HMGB2 regulates the transcriptional signature of progenitor exhausted CD8^{+} T cells

Since we found roles for HMGB2 in exhausted CD8^{+} T cells, and HMGB2 is a chromatin modifier, we next investigated whether HMGB2 regulated the transcriptional landscape of virus-specific T cells. We performed RNA-sequencing of sorted WT and *Hmgb2*$^{-/-}$ P14 T cells from Cl13 infected mice at 8dpi. Principal component analysis (PCA) showed the type of infection accounted for transcriptional differences across PC1 (47%

variance), while *Hmgb2* expression accounted for transcriptional changes across PC2 (30% variance) (**Fig. 3.2a**). Overall, we observed 350 differentially expressed genes (DEG) between WT and *Hmgb2*$^{-/-}$ P14 T cells at 8dpi Cl13, with 119 upregulated and 231 downregulated genes in *Hmgb2*$^{-/-}$ P14 T cells (**Fig. 3.2b**). In WT P14 T cells, we observed increased expression of genes promoting stem-like progenitor exhausted T cell (Tpex) differentiation (*Eomes*, *Bcl6*, *Id3*, *Bach2*), whereas *Hmgb2*$^{-/-}$ P14 T cells had increased expression of genes associated with terminal exhausted T cells (Tex) (*Casp3*, *Tigit*, *Tox*, *Ctla4*, *Ifng*) (**Fig. 3.2b**)[92]. To identify the biological significance of these DEG during Cl13 infection, we performed gene ontology (GO) analysis. We found WT P14 T cells were enriched for pathways associated with (i) leukocyte differentiation; (ii) regulation of cellular respiration and oxidative phosphorylation; and (iii) transferase activity (**Fig. 3.2c**). In contrast, *Hmgb2*$^{-/-}$ P14 T cells were enriched for pathways associated with (i) negative regulation of T cell activation; (ii) immune receptor activity; and (iii) apoptosis (**Fig. 3.2c**). These findings showed *Hmgb2*$^{-/-}$ CD8^{+} T cells are enriched for gene signatures and pathways of terminal exhaustion during chronic viral infection.

HMGB2 is required for expression of Tpex genes, including genes regulated by TCF-1

To further investigate the transcriptional changes driven by HMGB2 in CD8^{+} T cells during chronic infection, we performed RNA-sequencing on WT and *Hmgb2*$^{-/-}$ P14 T cells sorted from Cl13 infected mice at 20dpi. PCA showed clear separation of WT and *Hmgb2*$^{-/-}$ P14 T cells, with *Hmgb2* expression accounting for the transcriptional differences across PC1 (77% variance) (**Fig. 3.2d**). There were 679 DEG, with 494 upregulated and 185 downregulated in *Hmgb2*$^{-/-}$ P14 T cells (**Fig. 3.2e**). Similar to 8dpi Cl13, we observed

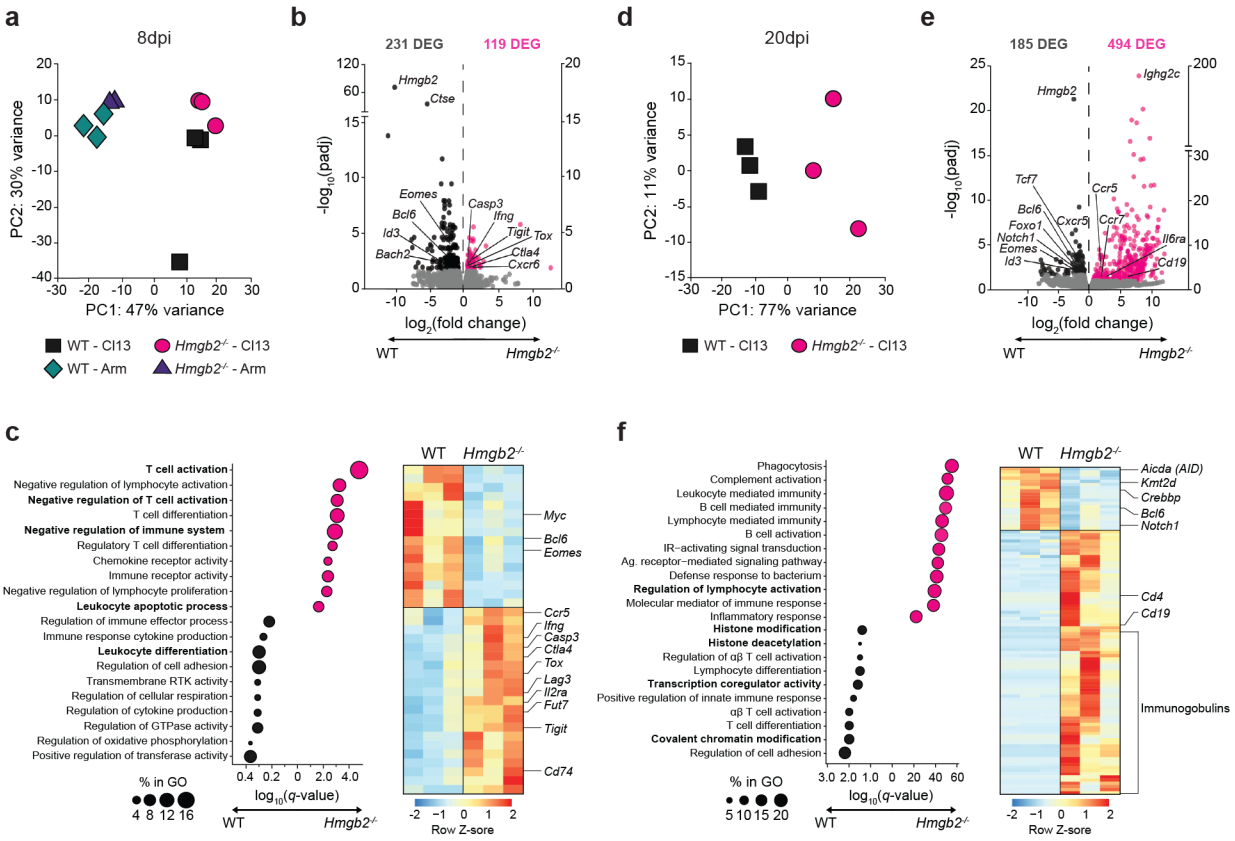

Figure 3.2 *Hmgb2*$^{-/-}$ CD8^{+} T cells have decreased expression of Tpex signature genes.

Bulk RNA-seq analysis of WT and *Hmgb2*$^{-/-}$ P14 T cells during LCMV Arm and Cl13 infection. (**a**) Principal component analysis (PCA) of WT and *Hmgb2*$^{-/-}$ P14 T cells at 8 days post either Arm or Cl13 infection. (**b**) Volcano plot highlighting differentially expressed genes (DEG) between WT and *Hmgb2*$^{-/-}$ P14 T cells at 8dpi Cl13. Significant DEG (padj ≤ 0.1, $|\log_2 FC| \geq 0.5$) are colored (pink = upregulated in *Hmgb2*$^{-/-}$ P14 T cells; black = upregulated in WT P14 T cells). (**c**) Left: Gene ontology (GO) biological process enrichment from Metascape of significant DEG from **b**. X-axis represents $\log_{10}(q\text{-value})$ and size of dot represents proportion of the total DEG enriched to that given pathway. Right: Heatmap of average normalized expression of genes associated with bolded pathways. Each column represents one independent experiment with $n = 5$ mice. (**d**) PCA of co-transferred WT and *Hmgb2*$^{-/-}$ P14 T cells at 20dpi Cl13. (**e**) Volcano plot highlighting DEG between WT and *Hmgb2*$^{-/-}$ P14 T cells at 20dpi Cl13. Significant DEG (padj ≤ 0.1, $|\log_2 FC| \geq 0.5$) are colored (pink = upregulated in *Hmgb2*$^{-/-}$ P14 T cells; black = upregulated in WT P14 T cells). (**f**) Left: GO biological process enrichment from Metascape of DEG from **e**. X-axis represents $\log_{10}(q\text{-value})$ and size of dot represents proportion of the total DEG enriched to that given pathway. Right: Heatmap of average normalized expression of genes associated with bolded pathways. Each column represents one independent experiment with $n = 10$ mice.

increased expression of Tpex associated genes in WT P14 T cells (*Tcf7*, *Cxcr5*, *Bcl6*, *Foxo1*, *Eomes*, *Id3*) compared to *Hmgb2*$^{-/-}$ P14 T cells (**Fig. 3.2e**)[92]. *Hmgb2*$^{-/-}$ P14 T cells expressed a dysregulated gene expression program, including non-CD8^{+} T cell lineage associated genes (*Ighg2c, Cd19*) (**Fig. 3.2e**). GO term analysis showed WT P14 T cells were enriched for pathways associated with (i) histone modification; (ii) histone deacetylation; (iii) lymphocyte differentiation; (iv) transcription coregulator activity; and (v) covalent chromatin modification (**Fig. 3.2f**). In contrast, *Hmgb2*$^{-/-}$ P14 T cells were enriched for pathways associated with (i) phagocytosis; (ii) complement activation; (iii) B cell activation; (iv) regulation of lymphocyte activation; and (v) inflammatory responses (**Fig. 3.2f**).

Since HMGB proteins are also known to modulate transcription factor binding, we next used Ingenuity Pathway Analysis (IPA)[233] to investigate any transcriptional regulators modified by HMGB2 that may be responsible for the DEG between WT and *Hmgb2*$^{-/-}$ P14 T cells at 20dpi Cl13. Upstream causal network analysis identified TCF-1 as a possible master regulator of the 20dpi Cl13 DEG, with the TCF-1 regulator network predicated to be significantly inhibited in exhausted *Hmgb2*$^{-/-}$ P14 T cells (activation *z*-score = -3.236, network bias-corrected *p*-value = 0.00001) (**Fig. S3.2a**). Of the 679 DEG regulated by HMGB2 at 20dpi Cl13, 117 are downstream targets of TCF-1, including *Bcl6*, *Eomes*, *Id3*, *Foxo1*, *Notch1*, and *Tcf7* (**Fig. S3.2a**). This suggests that HMGB2 in CD8^{+} T cells regulates the Tpex transcription program during Cl13 infection, and may do so through modifying the TCF-1 transcriptional network.

***Hmgb2*$^{-/-}$ CD8^{+} T cells have decreased survival during chronic viral infection**

Since we found *Hmgb2*$^{-/-}$ CD8^{+} T cells were significantly decreased during chronic viral infection, we next assessed whether there were differences in their proliferation and/or survival. We co-transferred WT and *Hmgb2*$^{-/-}$ P14 T cells at a 1:1 ratio into WT mice, followed by Cl13 infection. We first evaluated proliferation by *in vivo* BrdU incorporation and observed slightly decreased frequencies of BrdU^{+} *Hmgb2*$^{-/-}$ P14 T cells compared to WT at 8dpi Cl13 (**Fig. 3.3a**). Next, we evaluated survival by active Caspase3 and PI staining and observed increased frequencies of total Caspase3^{+} apoptotic *Hmgb2*$^{-/-}$ P14 T cells compared to WT at 8dpi Cl13 (**Fig. 3.3b**)**.** However, we found no differences between WT and *Hmgb2*$^{-/-}$ total Caspase3^{+} apoptotic P14 T cells at 46dpi Cl13 (**Fig. 3.3c**)**.** We next asked whether the increased apoptosis of *Hmgb2*$^{-/-}$ P14 T cells was due to differences in DNA repair compared to WT cells. Using a comet assay to measure DNA damage[215], we found no significant differences between WT and *Hmgb2*$^{-/-}$ P14 T cells during Cl13 infection (**Fig. 3.3d**). We also looked at phosphorylated-H2AX (Ser139), a marker of DNA damage[216], and again found no differences between WT and *Hmgb2*$^{-/-}$ P14 T cells during Cl13 infection (**Fig. 3.3e**). These findings showed *Hmgb2*$^{-/-}$ CD8^{+} T cells had decreased proliferation and survival compared to WT during chronic viral infection and did not show signs of DNA damage by 8dpi.

HMGB2 is essential for the differentiation of progenitor exhausted T cells during chronic viral infection

Recent findings have shown heterogeneity within the exhausted CD8^{+} T cell population, including the identification of Tpex and Tex cells. Since our sequencing data showed decreased expression of Tpex signature genes in *Hmgb2*$^{-/-}$ P14 T cells compared to WT (*Tcf7, Eomes, Bcl6, Id3*), we wanted to determine changes in Tpex differentiation

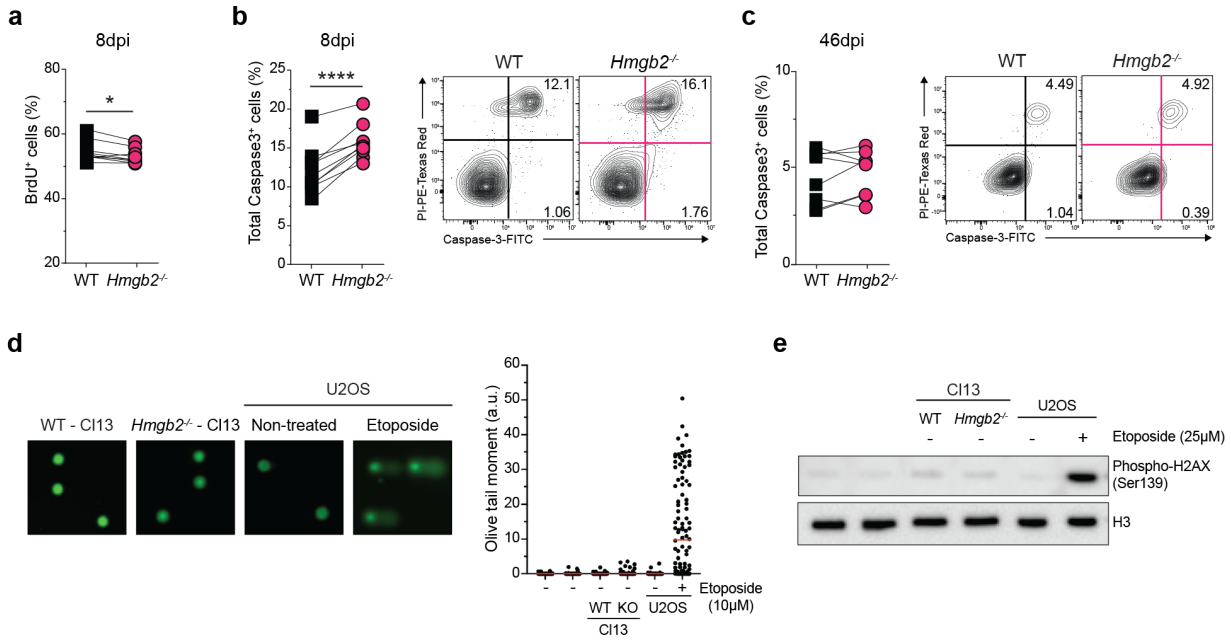

Figure 3.3 Exhausted *Hmgb2*$^{-/-}$ CD8^{+} T cells have decreased proliferation and increased cell death.

WT and *Hmgb2*$^{-/-}$ P14 T cells were co-transferred at 1:1 into WT mice, followed by LCMV Cl13 infection. (**a**) BrdU uptake of splenic WT and *Hmgb2*$^{-/-}$ P14 T cells at 8dpi. Caspase3 and PI staining of P14 T cells at 8dpi (**b**) and 46dpi (**c**) in the spleen. (**d**) Alkaline comet assay of splenic WT and *Hmgb2*$^{-/-}$ P14 T cells isolated on 8 days post Cl13 infection (pooled samples from 10mice/group). Representative fluorescent comet images of cells stained with Vista Green DNA dye. U2OS human cells treated with etoposide (10μM for 30min), a topoisomerase II inhibitor used to generate DNA double-strand breaks in cells, served as controls for comet tail formation. (**e**) p-H2AX (Ser139) protein expression by western blot in purified splenic WT and *Hmgb2*$^{-/-}$ P14 T cells isolated on 8 days post Cl13 infection (pooled samples from 10mice/group). U2OS human cells untreated or treated with 25μM etoposide for 60min served as negative and positive controls, respectively. Data are representative of three independent experiments with ≥ 5 mice per group. Data is mean ± s.e.m. *p ≤ 0.05, ****p ≤ 0.0001, paired Student's *t*-test.

between WT and *Hmgb2*$^{-/-}$ P14 T cells. At 8dpi Cl13, we stained adoptively co-transferred P14 T cells with Slamf6 and TIM-3 to identify Tpex (Slamf6^{hi}TIM-3^{lo}) and Tex (Slamf6^{lo}TIM-3^{hi}) cells. We found that *Hmgb2*$^{-/-}$ P14 T cells had significantly diminished Tpex cell frequencies compared to WT (**Fig. 3.4a**). Consistent with the loss of the Tpex subset, *Hmgb2*$^{-/-}$ P14 T cells were enriched for Tex-phenotype cells (**Fig. 3.4a**). Furthermore, we observed a significant decrease in the number of *Hmgb2*$^{-/-}$ Tpex cells at both 8 and 46dpi, while the numbers of Tex cells were similar (**Fig. 3.4a, b**). We also found significantly decreased CXCR5^{+} *Hmgb2*$^{-/-}$ P14 T cells compared to WT, which is an additional surface marker of the Tpex population (**Fig. 3.4c**)**.** Since we found decreased *Tcf7* expression in *Hmgb2*$^{-/-}$ P14 T cells and TCF-1 (*Tcf7*) is a key transcription factor driving Tpex cell differentiation, we investigated if the loss of *Hmgb2*$^{-/-}$ Tpex cells was due to decreased TCF-1 expression compared to WT. Surprisingly, WT and *Hmgb2*$^{-/-}$ P14 T cells had similar frequencies of TCF-1^{+} cells during Cl13 infection (**Fig. 3.4d**). In *Hmgb2*$^{-/-}$ mice, we also found similar and even higher frequencies of TCF-1^{+} cells in *Hmgb2*$^{-/-}$ CD8^{+}, GP_{33-41}^{+}, $GP_{276-286}^{+}$, and $NP_{396-404}^{+}$ T cells compared to WT mice during Cl13 infection (**Fig. S3.3a**)**.**

Given the substantial loss of *Hmgb2*$^{-/-}$ Tpex cells and the overall increased cell death of exhausted *Hmgb2*$^{-/-}$ P14 T cells, we next investigated if *Hmgb2*$^{-/-}$ Tpex cells were preferentially dying. At 8dpi Cl13, we found no differences in Tpex cell death between WT and *Hmgb2*$^{-/-}$ P14 T cells (**Fig. 3.4e**) but found a significant increase in apoptosis of *Hmgb2*$^{-/-}$ Tpex cells compared to WT at 46dpi (**Fig. 3.4f**).

Lastly, since we found HMGB2 played a critical role in the formation of Tpex cells, we wanted to evaluate the regulation of HMGB2 in this exhausted subset. Within WT P14

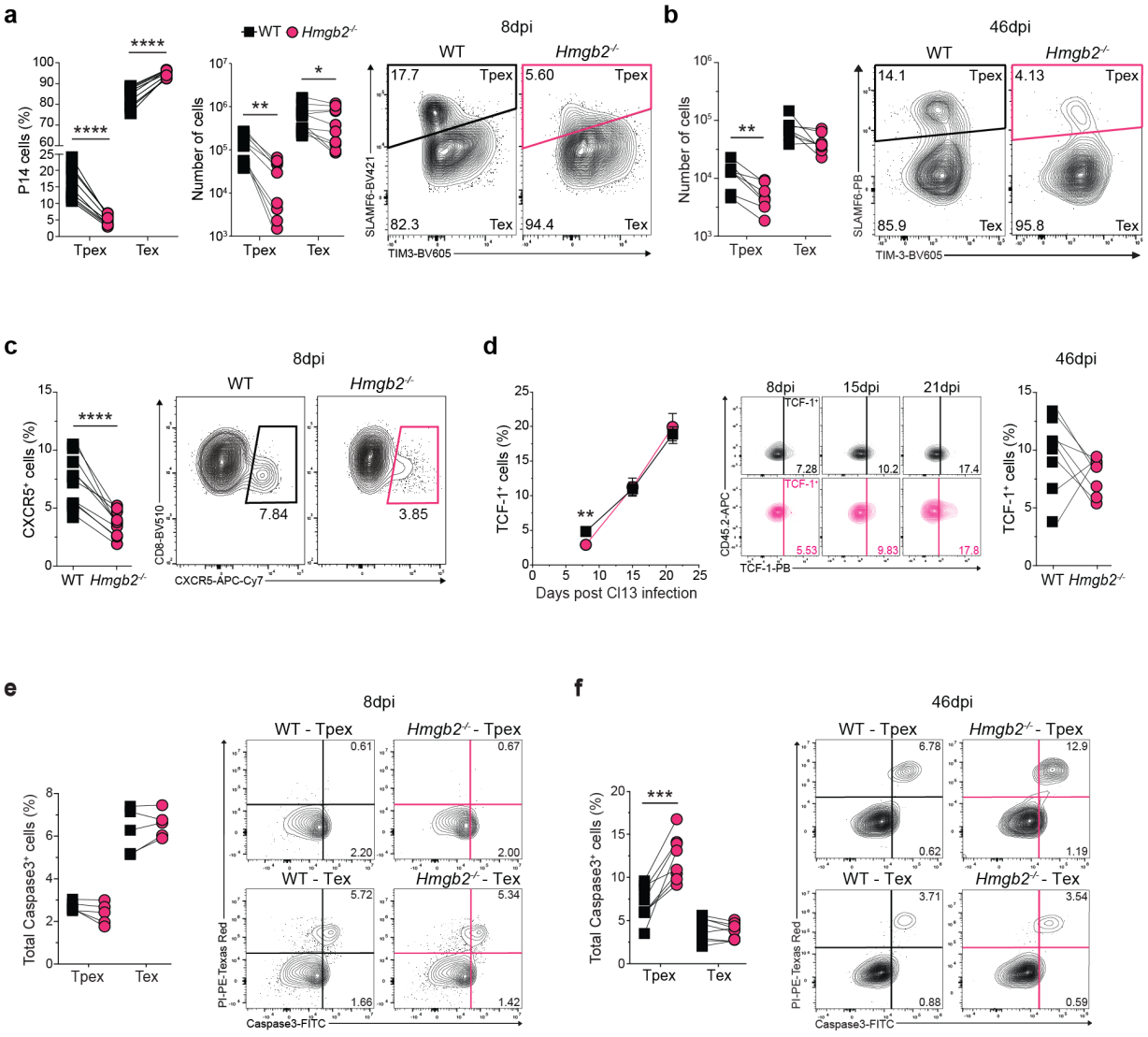

Figure 3.4 *Hmgb2*$^{-/-}$ CD8^{+} T cells have decreased progenitor exhausted T cell differentiation.

WT and *Hmgb2*$^{-/-}$ P14 T cells were co-transferred at 1:1 into WT mice, followed by LCMV Cl13 infection. (**a**) Frequencies and numbers of splenic progenitor exhausted (Tpex) and terminal exhausted (Tex) T cells at 8dpi Cl13. (**b**) Number of splenic WT and *Hmgb2*$^{-/-}$ P14 progenitor exhausted (Tpex) and terminal exhausted (Tex) T cells at 46dpi Cl13. (**c**) Frequencies of CXCR5^{+} P14 T cells at 8dpi Cl13 in the spleen. (**d**) TCF-1 expression during LCMV Cl13 infection in the blood (8-21dpi) and spleen (46dpi). Frequency of total Caspase3^{+} splenic WT and *Hmgb2*$^{-/-}$ Tpex and Tex cells at 8dpi (**e**) and 46dpi (**f**) Cl13. Data are representative of three independent experiments with ≥ 5 mice per group. Data is mean ± s.e.m. *p ≤ 0.05, **p ≤ 0.01, ***p ≤ 0.001, ****p ≤ 0.0001, paired Student's *t*-test.

T cells, we found the highest expression of HMGB2 in the Tpex subset compared to the Tex (**Fig. S3.3b**). We also found the highest frequencies of Tpex cells within the WT P14 HMGB2^{+} population compared to the WT P14 HMGB2^{-} population (**Fig. S3.3c**). Together, these findings showed that HMGB2 is a critical regulator of the differentiation and preservation of Tpex cells, which self-renew and maintain the exhausted T cell pool during Cl13 infection.

***Hmgb2*$^{-/-}$ exhausted CD8^{+} T cells are decreased after secondary acute LCMV challenge**

We observed significantly decreased frequencies of *Hmgb2*$^{-/-}$ Tpex cells during Cl13 infection, and since these cells drive the limited reinvigoration of exhausted T cells after secondary infections[100, 224], we next examined whether exhausted *Hmgb2*$^{-/-}$ CD8^{+} T cells could respond to Arm infection. Small numbers (1x10^{3} cells/each) of WT and *Hmgb2*$^{-/-}$ P14 T cells were adoptively co-transferred at a 1:1 ratio into WT mice and infected with Cl13 (**Fig. 3.5a**). At 30dpi, exhausted P14 T cells were sorted from spleens and co-transferred (2x10^{3} cells/each) at a 1:1 ratio into new WT mice, which were then infected with LCMV Arm (**Fig. 3.5a**). Exhausted WT P14 T cells re-expanded with secondary challenge, while *Hmgb2*$^{-/-}$ P14 T cells failed to expand and were at significantly decreased frequencies in the blood (**Fig. 3.5b**). Furthermore, we observed significantly decreased frequencies and numbers of *Hmgb2*$^{-/-}$ P14 T cells in spleens at 20dpi (**Fig. 3.5c, d**). Similar results were seen when exhausted WT and *Hmgb2*$^{-/-}$ P14 T cells were transferred separately into WT hosts and re-challenged with LCMV Arm (**Fig. 3.5e**). These findings showed HMGB2 expression is essential for the re-expansion of exhausted CD8^{+} T cells after a secondary viral challenge.

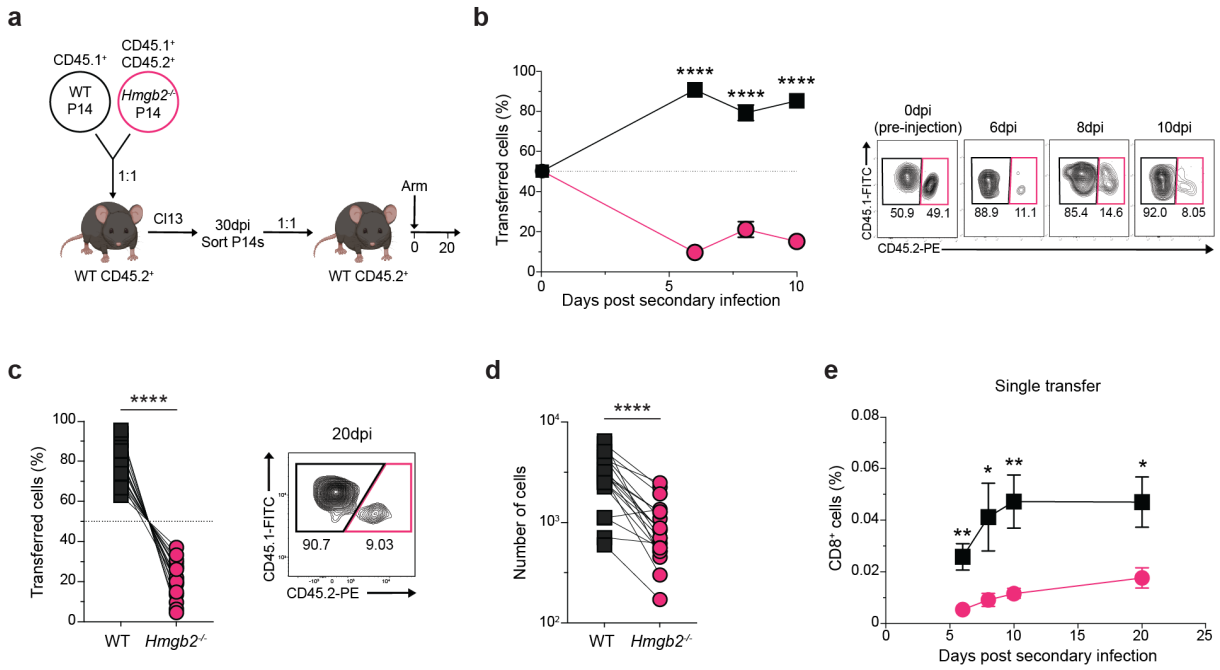

Figure 3.5 Exhausted *Hmgb2*$^{-/-}$ CD8^{+} T cells are defective in their recall capacity. (**a**) Experimental scheme for **b-d**. WT and *Hmgb2*$^{-/-}$ P14 T cells were co-transferred into WT mice at 1:1, followed by LCMV Cl13 infection. At 30dpi, exhausted WT and *Hmgb2*$^{-/-}$ P14 T cells were sorted and normalized to 1:1 before co-transferred into new naïve mice, followed by Arm infection (secondary infection). (**b**) Frequency of WT and *Hmgb2*$^{-/-}$ P14 T cells in blood during secondary Arm infection. Frequency (**c**) and number (**d**) of splenic WT and *Hmgb2*$^{-/-}$ P14 T cells at 20dpi secondary Arm. (**e**) WT and *Hmgb2*$^{-/-}$ P14 T cells were transferred separately into WT hosts and sorted at 68dpi Cl13 before adoptive transfer into separate naïve mice, followed by Arm infection (secondary infection). Frequency of WT and *Hmgb2*$^{-/-}$ P14 T cells in the blood during secondary Arm infection. Data are representative of three independent experiments with ≥ 10 mice per group. Data is mean ± s.e.m. *p ≤ 0.05, **p ≤ 0.01, ****p ≤ 0.0001, paired Student's *t*-test (b-d), two-tailed unpaired Student's *t*-test (e).

HMGB2 regulates the chromatin accessibility of Tpex and Tex genes during Cl13 infection

Since HMGB2 has a well-characterized role in chromatin remodeling, we next asked whether HMGB2 regulates the epigenetic program of exhausted T cells. We sorted WT and *Hmgb2*$^{-/-}$ P14 T cells from mice at 8dpi Cl13 and used ATAC-seq to identify significant changes in chromatin accessibility in the absence of HMGB2. PCA of the ATAC-seq profiles segregated WT and *Hmgb2*$^{-/-}$ P14 T cells across PC1 (91% variance), indicating that *Hmgb2* has a significant effect on chromatin accessibility (**Fig. 3.6a**). We found 6,542 differentially accessible regions (DAR), with most having decreased accessibility in *Hmgb2*$^{-/-}$ P14 T cells compared with WT (**Fig. 3.6b**). Genomic annotation showed about 17.5% of these accessibility changes were at promoters (≤1kb) or transcription start sites (TSS) (**Fig. 3.6b**). The genes in close proximity to loci with reduced accessibility in *Hmgb2*$^{-/-}$ P14 T cells were associated with Tpex cells, including *Batf, Foxo1, Id3, Ikzf2, Slamf6, Sell* and *Bach2* (**Fig. 3.6c**)[92]. Notably, we also observed decreased accessibility near the pro-survival gene *Bcl2*, which is required for Tpex cell survival (**Fig. 3.6c**)[234]. This is consistent with the decreased numbers and increased cell death of *Hmgb2*$^{-/-}$ Tpex cells observed during Cl13 infection. In contrast, loci with increased accessibility in *Hmgb2*$^{-/-}$ P14 T cells were near genes associated with apoptosis and terminal Tex cells, including *Tigit, Klrg1, Ccr5, Casp3, Ifng, Ctla4, Tbx21, Prf1, Adam8, Lgals3,* and *Gzmb* (**Fig. 3.6c, d**)[92]. We observed a similar trend when looking at promoters-TSS (≤1kb) containing DAR. Promoters of genes associated with Tpex cells had reduced accessibility in *Hmgb2*$^{-/-}$ P14 T cells (*Tcf7, Cxcr5, Ccr7, Gata3, Bcl6, Il7r,*

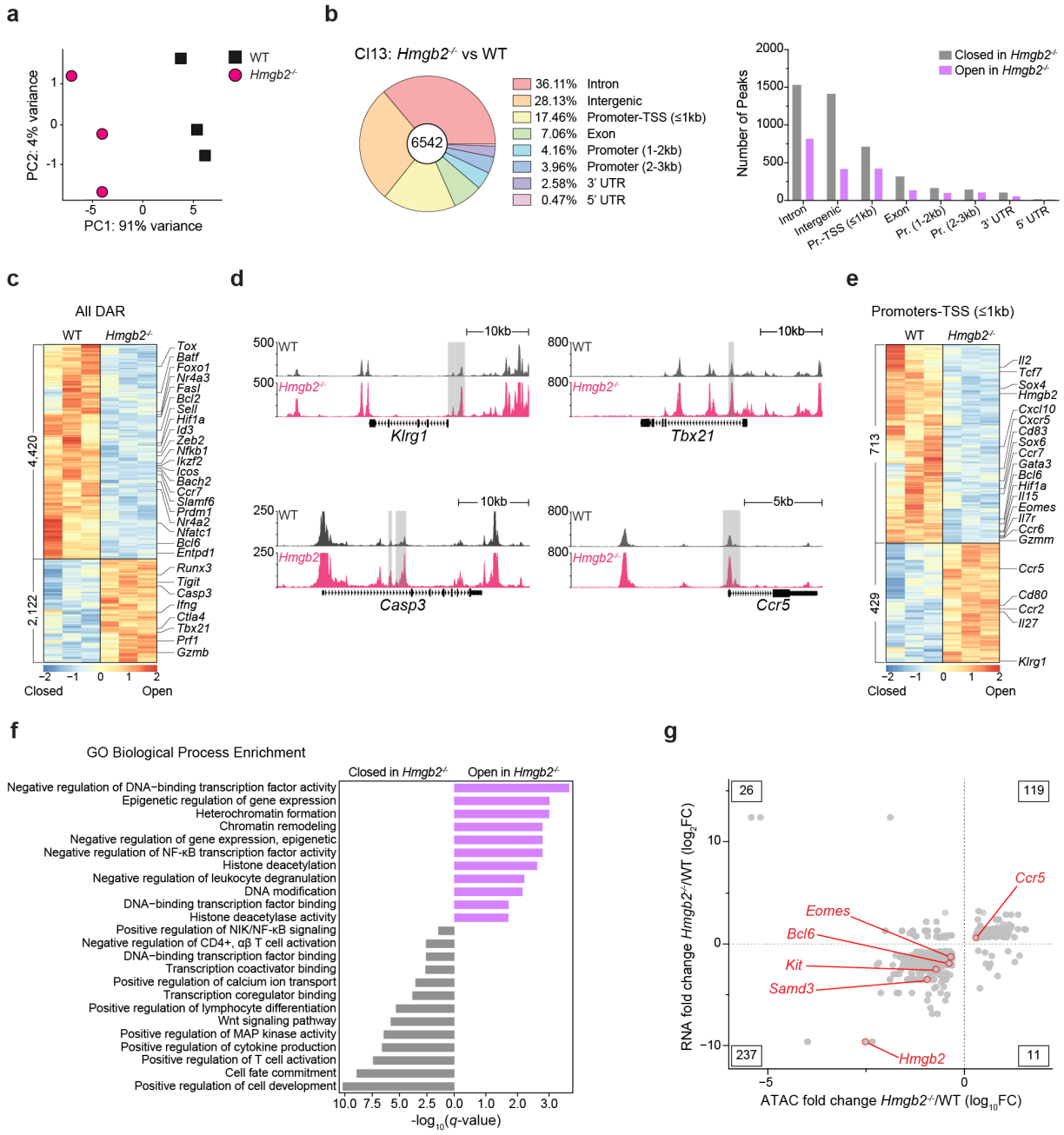

Fig. 3.6 Epigenetic programming of exhausted T cells by HMGB2.
ATAC-seq analysis of WT and *Hmgb2*$^{-/-}$ P14 T cells at 8dpi LCMV Cl13. (**a**) Principal component analysis (PCA) of all samples by global chromatin accessibility profile. (**b**) Location of significantly differentially accessible ATAC-seq peaks (FDR ≤ 0.05, $|\log_{10}FC| \geq 0.3$). (**c**) Heatmap of all significantly differentially accessible loci (DAR). Numbers on left denote number of DAR. Each column represents a biological replicate of n = 10 mice pooled. (**d**) ATAC-seq tracks of genes associated with effector and terminal exhausted T cells. DAR are highlighted with grey bars. (**e**) Heatmap of DAR within promoters-TSS (≤1kb). Each column represents a biological replicate of n = 10 mice pooled. (**f**) Gene ontology (GO) biological process enrichment from Metascape of DAR within promoters-TSS (≤1kb) from **e**. (**g**) Fold change in ATAC accessibility versus RNA expression. Key genes with DAR in promoters-TSS (≤1kb) are highlighted in red. Inset, table enumerating number of ATAC peak-gene pairs in each quadrant.

Bcl2a1c, Eomes), while promoters of terminal Tex genes were more accessible (*Klrg1*, *Ccr5)* (**Fig. 3.6e**)[95, 107, 111, 131].

To further characterize genes associated with DAR at promoters-TSS (≤1kb), we performed pathway enrichment. Genes with increased accessibility at promoters in *Hmgb2*$^{-/-}$ P14 T cells showed significant enrichment for GO terms associated with (i) negative regulation of DNA-binding transcription factor activity; (ii) heterochromatin formation; and (iii) negative regulation of gene expression (**Fig. 3.6f**). Conversely, genes with less accessible promoter regions in *Hmgb2*$^{-/-}$ P14 T cells had significant enrichment of GO terms associated with (i) positive regulation of cell development; (ii) positive regulation of T cell activation; and (iii) transcription coregulator/coactivator binding (**Fig. 3.6f**). To assess the correlation between chromatin accessibility and gene transcription, we compared these DAR with our 8dpi Cl13 DEG (**Fig. 3.2a, b**). Overall, the epigenetic changes induced by HMGB2 corresponded to functionally relevant events, with the majority of DEG having accompanying changes in chromatin accessibility (119 upregulated DEG with increased accessibility, 237 downregulated DEG with decreased accessibility) (**Fig. 3.6g**). For instance, the promoters-TSS (≤1kb) for *Eomes, Bcl6 and Samd3* were less accessible with lower RNA expression in *Hmgb2*$^{-/-}$ P14 T cells, while the *Ccr5* promoter was more accessible with increased RNA expression in *Hmgb2*$^{-/-}$ P14 T cells (**Fig. 3.6g**). Our data suggests a significant role for HMGB2 in CD8^{+} T cell chromatin accessibility, and more specifically, the opening of genomic regions associated with progenitor cells and the closing of genomic regions associated with terminal cell differentiation. Together, these data contribute to our understanding of the mechanisms by which HMGB2 regulates the development of exhausted CD8^{+} T cells.

Cell-intrinsic HMGB2 expression in CD8$^+$ T cells is required for anti-tumor responses

Since persistent antigen presentation in tumors also drives differentiation of exhausted CD8$^+$ T cells, we next asked whether HMGB2 regulated tumor-specific CD8$^+$ T cells. We co-transferred congenically marked (1x10^6 cells/each) WT and *Hmgb2*$^{-/-}$ P14 T cells at a 1:1 ratio into WT mice and subcutaneously injected B16-GP$_{33-41}$ melanoma cells (1x10^6 cells) a day later. B16-GP$_{33-41}$ melanoma cells are highly aggressive and express the LCMV GP$_{33-41}$ epitope, which is recognized by P14 T cells. We observed significantly decreased frequencies of *Hmgb2*$^{-/-}$ P14 T cells compared to WT in the tumor and tumor draining lymph nodes (TdLNs) at day 18 post melanoma cell injection (**Fig. 3.7a**). The numbers of *Hmgb2*$^{-/-}$ P14 T cells were also significantly decreased in the tumor and TdLNs (**Fig. 3.7b**). We next evaluated the frequencies of Tpex and Tex cells by measuring TCF-1 and TIM-3 expression of tumoral WT and *Hmgb2*$^{-/-}$ P14 T cells and found significantly less *Hmgb2*$^{-/-}$ Tpex cells compared to WT, similar to our findings during Cl13 infection (**Fig. 3.7c**). These data indicate HMGB2 expression is also required for the maintenance and differentiation of Tpex and exhausted CD8$^+$ T cells in melanoma tumors.

To assess the role of HMGB2 expression in CD8$^+$ T cells on tumor control, we adoptively transferred 1x10^6 congenically marked WT or *Hmgb2*$^{-/-}$ P14 T cells into separate, congenically mismatched WT mice. The next day, mice were given 1x10^6 B16-GP$_{33-41}$ melanoma cells s.c. We observed the highest median survival in mice given WT P14 T cells, with mice receiving *Hmgb2*$^{-/-}$ P14 T cells or no T cells having similar survival

(**Fig. 3.7d**). These findings suggest HMGB2 expression in exhausted CD8⁺ T cells is critical for anti-tumor immunity in melanoma tumors.

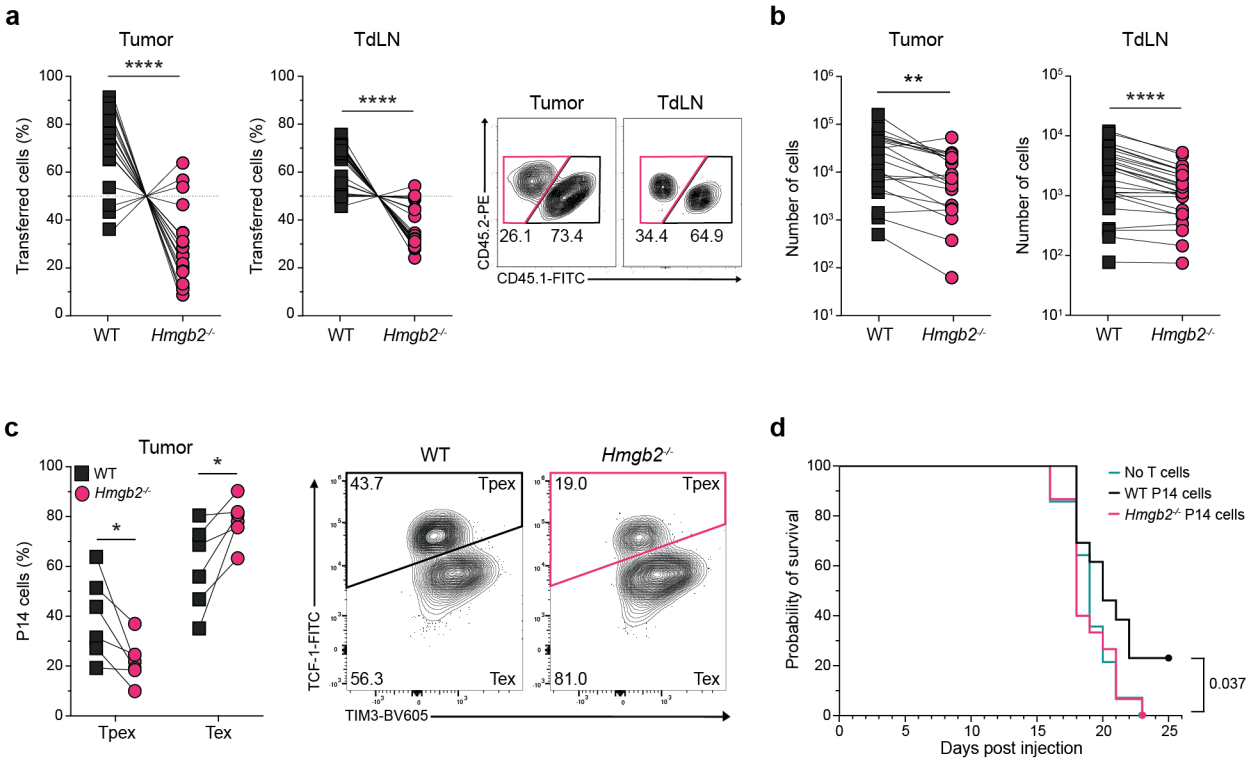

Figure 3.7 HMGB2 regulation of anti-tumor CD8⁺ T cells.
(**a**) WT and *Hmgb2*$^{-/-}$ P14 T cells were co-transferred into WT mice at 1:1 and given B16-GP$_{33-41}$ melanoma cells s.c. Tumors and tumor draining lymph nodes (TdLN) isolated at 18dpi. Frequencies (**a**) and numbers (**b**) of WT and *Hmgb2*$^{-/-}$ P14 T cells within the tumor and TdLN at 18dpi. (**c**) Frequencies of progenitor exhausted (Tpex) and terminal exhausted (Tex) T cells at 18dpi in the tumor. (**d**) Survival of mice with B16-GP$_{33-41}$ melanoma and adoptive transfer of either WT, *Hmgb2*$^{-/-}$, or no P14 T cells. Data are representative of three independent experiments with ≥ 10 mice per group (a-c) or two independent experiments combined with ≥ 13 mice per group (d). Data is mean ± s.e.m. *p ≤ 0.05, **p ≤ 0.01, ****p ≤ 0.0001, paired Student's *t*-test (a-c), log-rank (Mantel-Cox) test (d).

SUPPLEMENTARY FIGURES

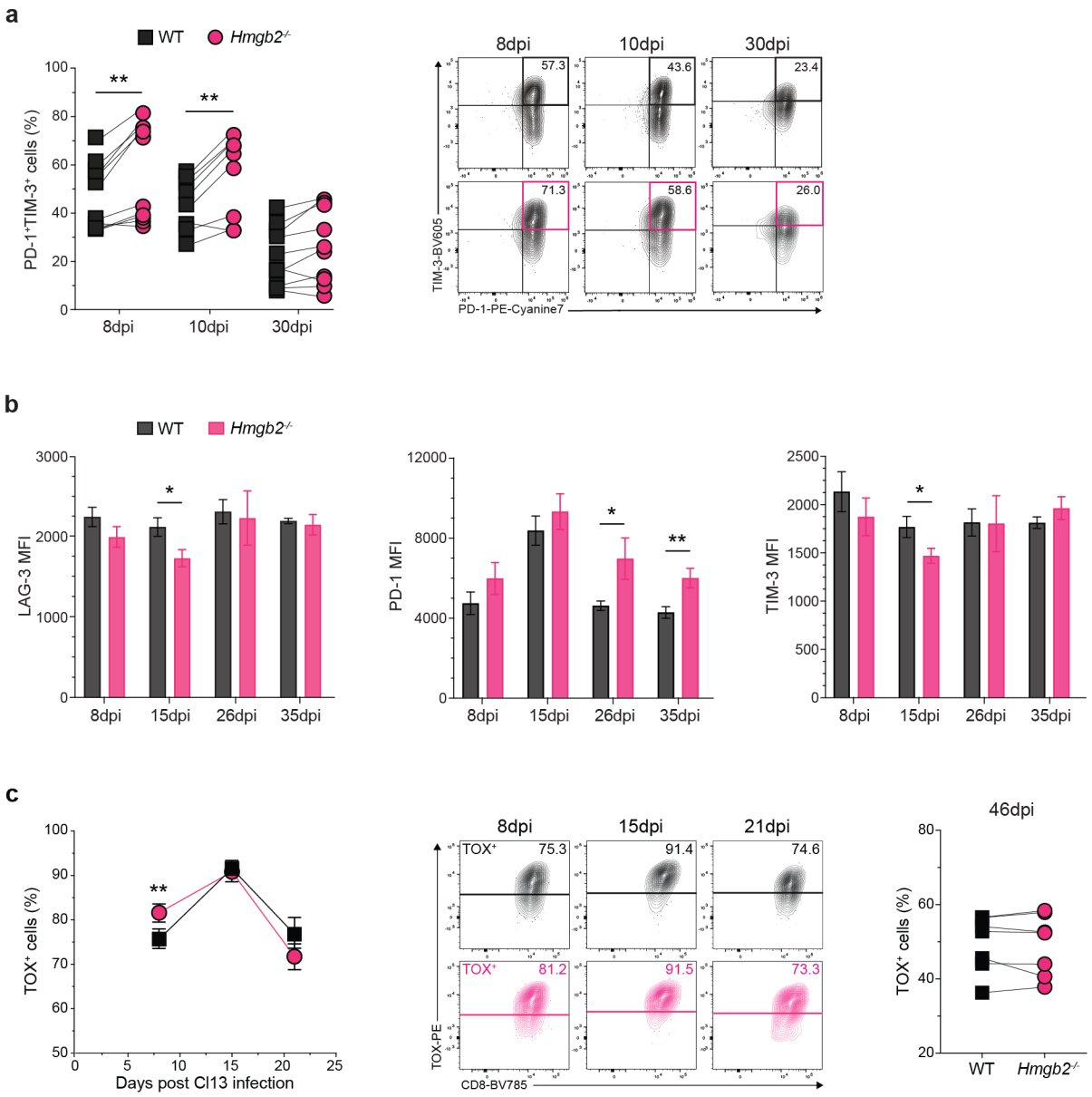

Supplementary Figure 3.1 Terminal exhaustion of *Hmgb2*$^{-/-}$ CD8^{+} T cells during chronic LCMV infection.
Inhibitory-receptor expression in WT and *Hmgb2*$^{-/-}$ P14 T cells during Cl13 infection in spleens (**a**) and blood (**b**). (**c**) TOX expression during LCMV Cl13 infection in the blood (8-21dpi) and spleen (46dpi). Each symbol represents an individual mouse. Data are representative of three independent experiments with ≥ 5 mice per group. Data is mean ± s.e.m. *p ≤ 0.05, **p ≤ 0.01, Paired Student's *t*-test (a, c), two-sided Student's *t*-test (b).

a

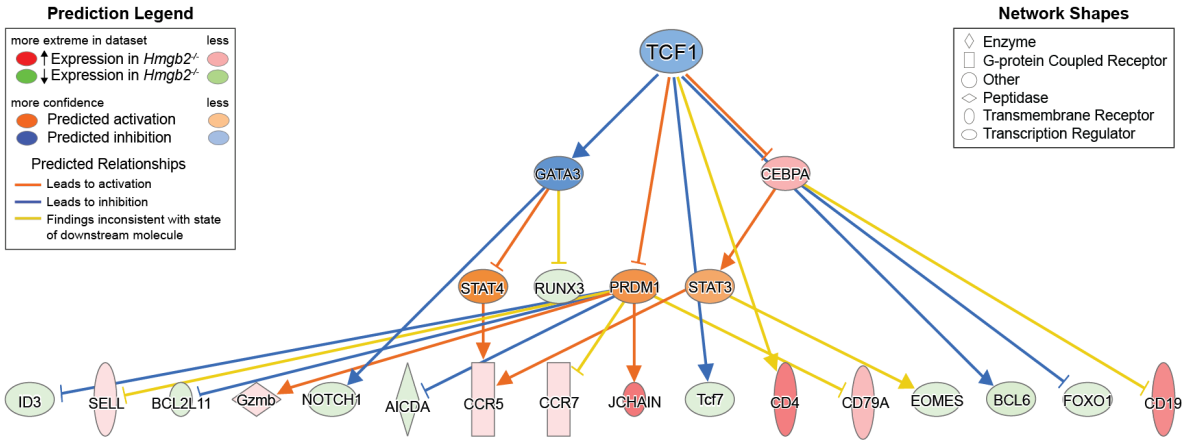

Supplementary Figure 3.2 HMGB2 regulates the TCF-1 transcriptional network in CD8⁺ T cells during Cl13 infection.

(**a**) TCF-1 causal network identified with Ingenuity Pathway Core Analysis (IPA) (activation *z*-score = -3.236, network bias-corrected *p*-value = 0.00001). Input was differentially expressed genes (DEG) (padj ≤ 0.1, $|\log_2 FC| \geq 0.5$) between WT and *Hmgb2*$^{-/-}$ P14 T cells at 20dpi Cl13.

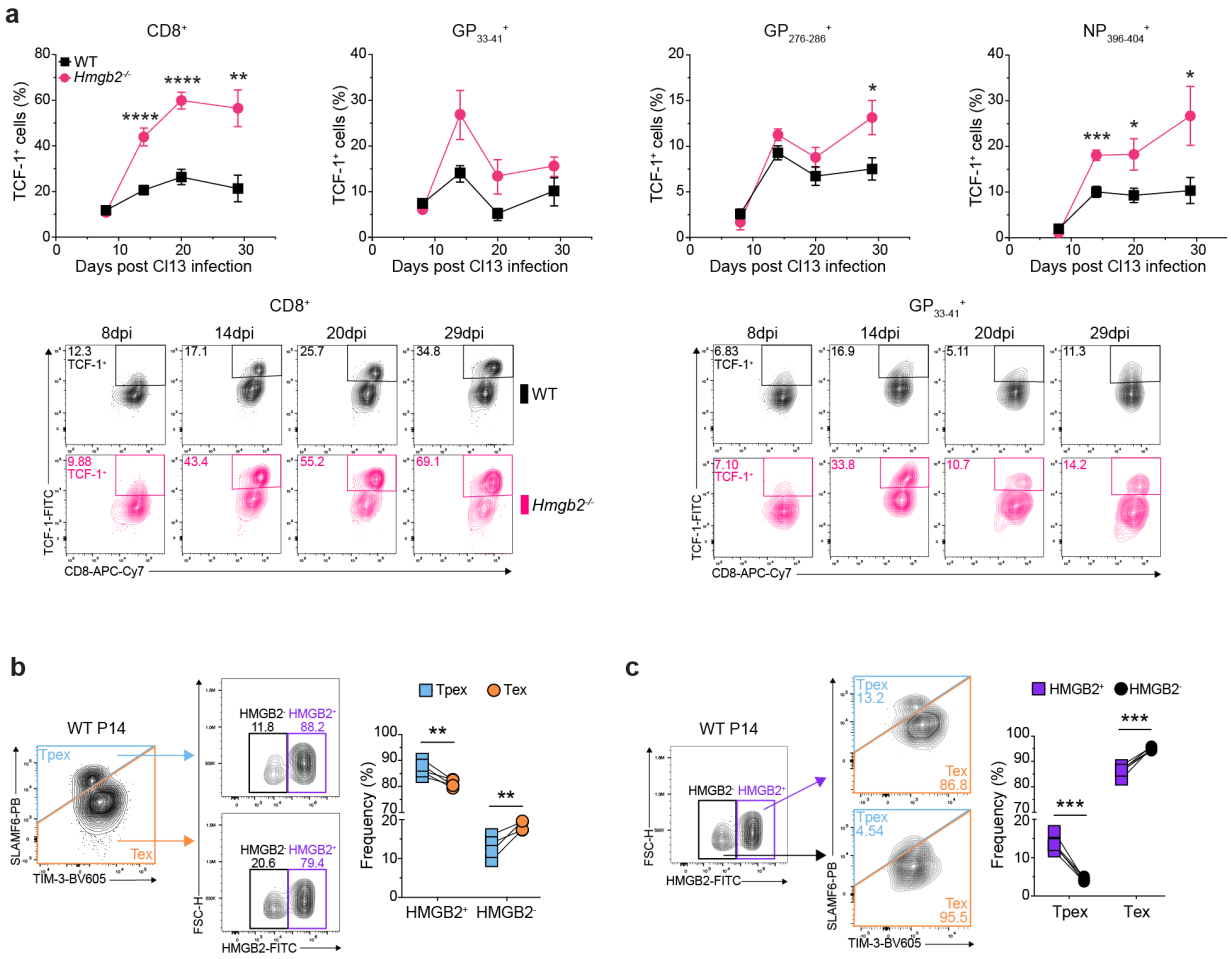

Supplementary Figure 3.3 HMGB2 regulation of Tpex cells during chronic LCMV infection.

(**a**) TCF-1 expression in WT and *Hmgb2*$^{-/-}$ mice during Cl13 infection in the blood. (**b**) Frequencies of HMGB2^{+} and HMGB2^{-} cells within Tpex and Tex WT P14 T cells isolated from spleens at 8dpi Cl13. (**c**) Frequencies of Tpex and Tex within HMGB2^{+} and HMGB2^{-} WT P14 T cells isolated from spleens at 8dpi Cl13. Each symbol represents an individual mouse. Data are representative of three independent experiments with ≥ 5 mice per group. Data is mean ± s.e.m. *p ≤ 0.05, **p ≤ 0.01, ***p ≤ 0.001, ****p ≤ 0.0001, two-sided Student's *t*-test (a), Paired Student's *t*-test (b-c),

DISCUSSION

Our findings showed a cell-intrinsic role for HMGB2 in the differentiation and stemness of exhausted $CD8^+$ T cells in viral and tumor models. We found HMGB2 expression and upregulation in exhausted $CD8^+$ T cells. In response to chronic viral infection, exhausted *Hmgb2*$^{-/-}$ $CD8^+$ T cells showed decreased progenitor exhausted T cell (Tpex) differentiation and survival, with these cells unable to persist during prolonged infection. Despite *Hmgb2*$^{-/-}$ $CD8^+$ T cells expressing TCF-1 and TOX master regulators, these transcription factors failed to induce the differentiation of Tpex and terminal exhausted T cells (Tex). Transcriptomic and chromatin accessibility analyses revealed that HMGB2 in exhausted $CD8^+$ T cells functioned to increase expression and accessibility of Tpex-specific gene signatures, while decreasing expression and accessibility of terminal Tex gene signatures.

Compared to effector and memory T cells, the regulation of exhausted $CD8^+$ T cells remains poorly understood. Persistent Cl13 infection induces NFAT and calcineurin signaling, which induces TOX expression in $CD8^+$ T cells[126, 136, 235]. We observed similar levels of TOX expressed in WT and *Hmgb2*$^{-/-}$ $CD8^+$ T cells during Cl13 infection, suggesting effective TCR, NFAT, and calcineurin signaling in *Hmgb2*$^{-/-}$ $CD8^+$ T cells. Accordingly, both WT and *Hmgb2*$^{-/-}$ P14 T cells expanded to similar numbers by 8dpi Cl13 infection, indicating that *Hmgb2*$^{-/-}$ P14 T cells were effectively primed and activated during early stages of chronic viral infection. However, despite similar phenotypes and initial responses of exhausted WT and *Hmgb2*$^{-/-}$ P14 T cells, *Hmgb2*$^{-/-}$ P14 T cells drastically declined after 8dpi Cl13 infection and did not persist. During Cl13 infection, the transcription factors TOX and TCF-1 are critical to form exhausted T cells[106, 127]. However,

the loss of exhausted *Hmgb2*$^{-/-}$ P14 T cells was not due to diminished TOX or TCF-1 expression, as both transcriptional regulators were expressed at similar levels to WT. Importantly, TOX and TCF-1 were insufficient to establish and sustain *Hmgb2*$^{-/-}$ Tex cells throughout Cl13 infection. This links HMGB2 proteins with TOX and TCF-1 regulation of exhausted T cell differentiation.

HMGB2 proteins regulate cellular stemness, as shown by defects in various differentiation programs in *Hmgb2*$^{-/-}$ mice[174, 236, 237, 238, 239]. During chronic infection, stem-like Tpex cells arise, which can self-renew and seed the Tex pool. Using transcriptomics, we found HMGB2 positively regulated the expression of Tpex cell associated genes and correspondingly, we found HMGB2 positively regulated Tpex cell frequencies, numbers, and survival. HMGB2's regulation of Tpex cell differentiation and long-term maintenance is similar to that of TCF-1, a key transcriptional regulator of Tpex-specific programming; *Tcf7*$^{-/-}$ CD8^{+} T cells fail to develop into Tpex cells and decline throughout Cl13 infection[98, 106]. However, despite the loss of *Hmgb2*$^{-/-}$ Tpex cells, *Hmgb2*$^{-/-}$ T cells had similar frequencies of TCF-1^{+} cells compared to WT. Furthermore, exhausted *Tcf7*$^{-/-}$ CD8^{+} T cells have increased expression of *Hmgb2* compared to TCF-1^{+} CD8^{+} T cells[106]. Together, these data suggest HMGB2 and TCF-1 co-regulate Tpex cell differentiation. There is significant clinical interest in understanding the differentiation of Tpex cells for immunotherapy use in cancer and chronically infected patients; Tpex cells provide the effector T cell proliferative burst after immune checkpoint blockade (ICB) and may have therapeutic predictive value in patients[240, 241, 111, 225, 226]. Although we did not evaluate the response of *Hmgb2*$^{-/-}$ Tpex cells to anti-PD-1/anti-PD-L1 blockade, we observed a defect in their reinvigoration with secondary Arm infection. Therefore, combining HMGB2

modulation with anti-PD-1/anti-PD-L1 therapy may enhance and preserve Tpex cell differentiation and increase clinical efficacy in the settings of chronic infections and cancer. Together, our findings showed HMGB2 regulates the differentiation, survival, and reinvigoration of Tpex cells, and may help predict ICB efficacy.

Exhausted T cells develop permanent epigenetic marks early in their differentiation, with additional epigenetic changes acquired at later stages of exhaustion[116, 138, 222]. Since the epigenetic program of exhausted T cells is relatively stable, ICBs can only transiently reinvigorate exhausted T cells, as they reacquire their exhausted epigenetic program over time[44, 100, 120, 142, 143]. Combining chromatin remodeling with ICBs may represent a new clinical approach to increase the reinvigoration potential of exhausted T cells. Therefore, identifying exhaustion-specific epigenetic regulators is a pressing clinical need for patients with chronic diseases. HMGB2 is a known chromatin modifier, but its role in the epigenetic programming of exhausted T cells is not known. Here, we found that HMGB2 regulated the accessibility of genomic regions in exhausted T cells, with most of these changes corresponding to functionally relevant events in gene transcription. HMGB2 directly supported the accessibility of Tpex associated genes, many of which are regulated by the transcription factor TCF-1, while decreasing the accessibility of genes associated with terminal Tex cells and apoptosis. Therefore, we hypothesize that HMGB2 supports Tpex cell differentiation by modulating the accessibility and expression of genes regulated by TCF-1 and possibly other critical transcriptional regulators. Notably, Ingenuity Pathway Analysis (IPA) identified the TCF-1 master regulatory pathway as being one of many significantly inhibited in *Hmgb2*$^{-/-}$ P14 T cells, suggesting HMGB2 is required for TCF-1

mediated transcriptional programs in exhausted T cells. HMGB2 may enhance TCF-1 binding to its targets, as it does with LEF1, a transcription factor functionally similar to TCF-1[239, 242]. Furthermore, TCF-1 and LEF1 have been shown to regulate $CD8^+$ T cell identity and function, with ablation of these transcription factors resulting in expression of non-T cell lineage genes[243]. Although exhausted *Hmgb2*$^{-/-}$ P14 T cells had high TCF-1 expression, we found similar aberrant T cell gene expression at 20dpi Cl13 (*Cd19, Cd4,* and immunoglobulins). We propose that HMGB2 and TCF-1 co-regulate exhaustion-specific transcriptional and epigenetic programs in $CD8^+$ T cells through chromatin remodeling and facilitating transcription factor binding.

In summary, we show that *Hmgb2* expression is required for the differentiation and survival of Tpex cells during chronic viral infection. During chronic Cl13 infection, *Hmgb2*$^{-/-}$ $CD8^+$ T cells initially proliferated and expanded to similar levels as WT but were severely hindered in their formation of Tpex cells, thus preventing long-term exhausted T cell responses. We found HMGB2 increased the accessibility of Tpex signature genes, positively regulating the transcriptional program, differentiation, and maintenance of Tpex cells. We also observed decreased *Hmgb2*$^{-/-}$ Tpex cells in melanoma tumors and tumor-draining lymph nodes, indicating HMGB2 sustains exhausted T cells in multiple models of persistent antigen. We found a novel and previously unidentified role for HMGB2 in the differentiation and survival of exhausted T cells, with vast implications for immunotherapies to chronic viruses and cancer. This new understanding of HMGB2's role in exhausted T cell stemness is a novel contribution to TCF-1 and TOX mediated regulation of exhaustion and shows that HMGB2 is an indispensable partner of TCF-1 and TOX in the formation and maintenance of exhausted T cells.

ACKNOWLEDGMENTS

We would like to thank all the current and former members in the Tinoco Laboratory (Twitter: @Tinoco_Lab) for all their constructive comments and advice during this project. We would like to thank Dr. Jennifer Atwood at the UCI Institute for Immunology Flow Core, a shared resource of the Cancer Center Support Grant (CA-62203) at the University of California, Irvine, for assistance with FACS. We would like to thank Dr. Jie Wu and Dr. Melanie Oakes at the UCI Genomics High Throughput Facility (UCI GHTF) for setup and analysis of RNA-sequencing and setup of ATAC-sequencing data. The UCI GHTF is another shared resource of the Cancer Center Support Grant (CA-62203) at the University of California, Irvine, and NIH shared instrumentation grants 1S10RR025496-01, 1S10OD010794-01, and 1S10OD021718-01. We would like to thank Makena Ewald for technical assistance on naïve T cell characterization experiments. This work was supported by the National Institutes of Health (R01 AI137239 to R.T. and R37 CA252081 to R.B.) Department of Defense (CA171198 to R.T.), The Melanoma Research Alliance (571135 to R.T.), The ACS (to R.T.), T32 virus-host interactions: a multi-scale training program (T32AI007319 to E.N.N.), T32 training grant in Cancer Biology and Therapeutics (T32 CA009054 to J.M.D.), NIH IMDS training grant (GM055246 to K.V.M.), and an EMBO postdoctoral fellowship (P.O.).

CHAPTER 4

Summary and Future Directions

Naïve $CD8^+$ T cells develop into effector T cells after TCR activation by cognate antigen. In acute infections, when the antigen is cleared, the majority of effector T cells die with few surviving to seed the protective memory T cell pool. However, if the antigen is not cleared, as occurs during chronic viral infections and cancers, the responding $CD8^+$ T cells adapt to persistent TCR signaling by upregulating inhibitory receptors and differentiating into dysfunctional exhausted T cells. The differentiation mechanisms of effector, memory, and exhausted $CD8^+$ T are unique to each subset, resulting in diverse functions and phenotypes that define them. These observed lineage differences are regulated at the epigenetic and transcriptional level, with unique profiles of chromatin accessibility and transcription factors. Understanding the regulatory mechanisms underlying $CD8^+$ T cell responses to both acute and chronic infections has vast clinical implications for vaccinations and immunotherapies. However, these regulatory networks are not fully defined, and it is important to characterize the proteins governing the differentiation of effector, memory, and exhausted $CD8^+$ T cells.

The goal of this dissertation is to elucidate the possible regulatory role of HMGB2 in antigen-specific $CD8^+$ T cell differentiation during both acute and chronic infections (**Fig. 4.1**). First, we used a model of acute viral infection and found HMGB2 was not required for the development of functional virus-specific effector $CD8^+$ T cells. When adoptively co-transferred or separately transferred into mice, both effector WT and *Hmgb2*$^{-/-}$ P14 T cells had similar frequencies and numbers at the peak of LCMV Arm infection (8dpi). They also had similar production of GranzymeB, IFN-γ, and TNF-α, all

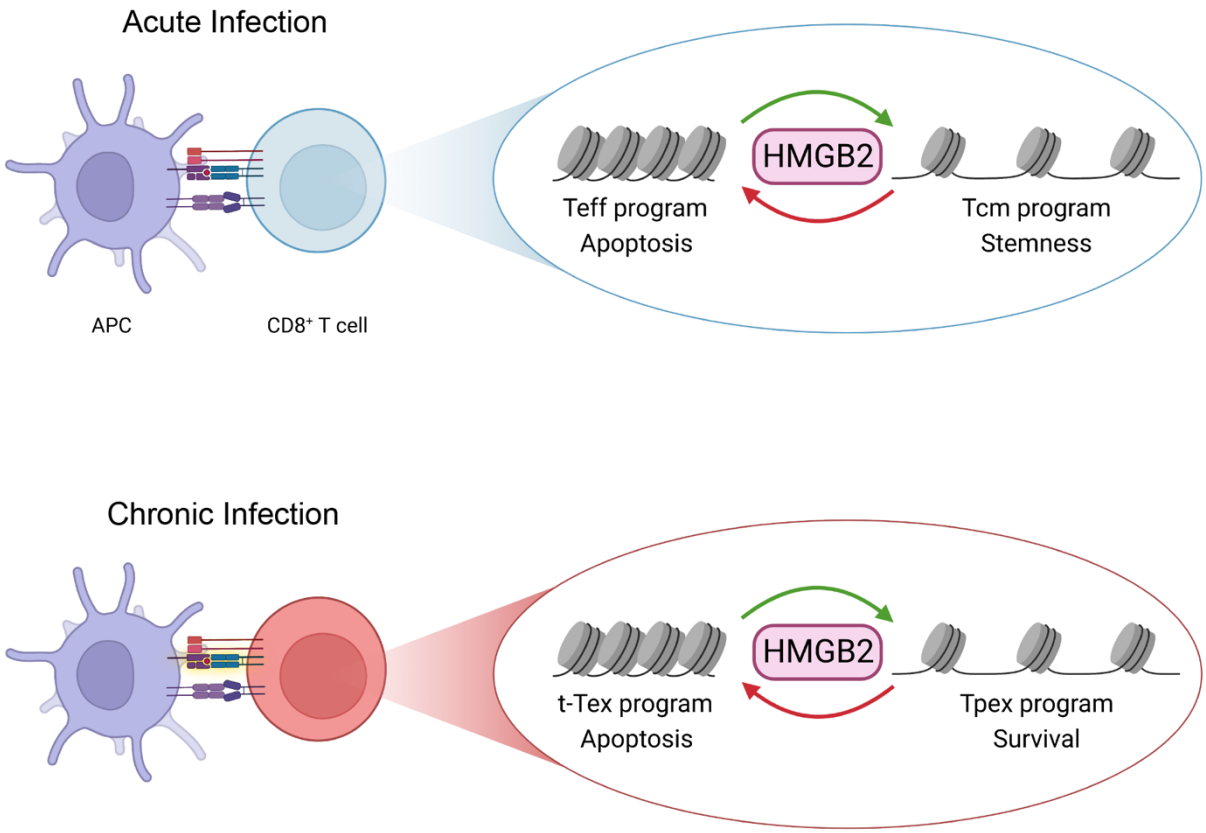

Figure 4.1 HMGB2 epigenetically regulates virus-specific CD8⁺ T cells.
Role of HMGB2 in epigenetic programming of CD8⁺ T cells during acute and chronic infections. *Top*: After activation and expansion of Teff cells during acute infection (i.e. LCMV Arm), HMGB2 epigenetically enforces the Tcm transcriptional program, promoting the expression of genes required for self-renewal, recall, and survival (*Eomes, Foxo1, Bach2, Bcl6*). HMGB2 also represses the accessibility of genes associated with Teff cells and apoptosis (*Batf, Lag3, Casp3*), further promoting Tmem differentiation. *Bottom*: During chronic infection (i.e. LCMV Cl13), HMGB2 epigenetically enforces the Tpex transcriptional program by promoting the expression of genes associated with stemness and survival (*Bcl6, Eomes, Bcl2, Foxo1, Id3, Bach2*) and repressing transcription of genes associated with terminal Tex cells and apoptosis (*Tigit, Casp3, Ctla4, Gzmb, Klrg1*). Abbreviations: APC, antigen presenting cell; Teff, effector T cell; Tcm, central memory T cell; Tpex, progenitor exhausted T cell; t-Tex, terminally exhausted T cell.

measurements of effector $CD8^+$ T cell function. However, after acute viral clearance, memory *Hmgb2*$^{-/-}$ P14 T cells were at decreased numbers and frequencies compared to WT, with deficient differentiation of central memory T cells (Tcm). Correspondingly, memory *Hmgb2*$^{-/-}$ P14 T cells could not re-expand upon secondary infection. We found HMGB2 positively regulated the expression and accessibility of memory-associated genes and decreased the accessibility of genes associated with effector T cells and apoptosis. Together, this demonstrated HMGB2 was critical for memory T cell differentiation and recall capacity (**Chapter 2**). Using models of chronic viral infection and cancer, we next found HMGB2 was critical for exhausted T cell differentiation, maintenance, and stemness. Compared to WT, *Hmgb2*$^{-/-}$ P14 T cells were at significantly lower frequencies and numbers throughout chronic LCMV infection, with decreased frequencies of progenitor exhausted T cells (Tpex). Tpex cells can self-renew and seed the more terminal exhausted (Tex) population, thereby maintaining the exhausted T cell pool during chronic infections. Notably, the loss of exhausted *Hmgb2*$^{-/-}$ P14 T cells was not due to diminished TCF-1 or TOX expression, as these master regulators were expressed at wild-type levels in *Hmgb2*$^{-/-}$ cells during Cl13 infection. A similar role for HMGB2 in the maintenance and development of Tpex cells was also seen in melanoma tumors and tumor draining lymph nodes (TdLNs) from mice. We found that HMGB2 positively regulated the accessibility and expression of Tpex associated genes, while suppressing genes associated with terminal exhaustion. Collectively, we found HMGB2 is critical for the development and maintenance of exhausted T cells through promoting the expression of genes associated with the formation of Tpex cells during chronic infections (**Chapter 3**). However, there still remains many future areas of research

regarding the role of HMGB2 in antigen-specific $CD8^+$ T cells, as well as its role in other adaptive immune responses.

The importance of HMGB2 expression in maintaining exhausted T cell responses during both chronic viral infection and cancer opens many avenues for future research. One important question that arises is how HMGB2 expression impacts overall viral and tumor control in mice. Since we found HMGB2 is critical for the formation and persistence of exhausted $CD8^+$ T cells, and these dysfunctional cells still provide some protection to chronically infected hosts, we hypothesize *Hmgb2*$^{-/-}$ exhausted T cells will be impaired in chronic viral and tumor control, resulting in increased viral loads and tumor burdens in mice. To investigate the impact of HMGB2 expression specifically in $CD8^+$ T cells on viral load, we would take a similar separate adoptive transfer approach to that outlined in Fig. 3.1a. However, the experimental setup would need to be adjusted as the original transfer of only $1x10^3$ WT or *Hmgb2*$^{-/-}$ P14 T cells is insufficient to impact LCMV Cl13 viral control[244]. In order to overcome this limitation, we would take a similar approach to that in Blattman et al. and deplete mice of $CD4^+$ T cells to prevent immunopathology and adoptively transfer $\geq 10^5$ WT or *Hmgb2*$^{-/-}$ P14 T cells[244]. Viral load in the serum of mice will be measured throughout chronic LCMV infection, with viral loads in tissues being examined at the end of the experiment, including brain, liver, kidney, and lung. To investigate whether HMGB2 expression in exhausted P14 T cells impacts tumor control, we would separately adoptively transfer $1x10^6$ WT or *Hmgb2*$^{-/-}$ P14 T cells into mice before inoculation with $1x10^6$ B16-GP_{33-41} melanoma cells, and measure tumor growth and survival. Given previous studies in the lab using B16-GP_{33-41} melanoma cells, measurements would begin at 8dpi and continue until mice reached the tumor burden

threshold of 1800mm^3. At the end of the experiment, tumors would be excised and weighed. For studies evaluating the impact of HMGB2 expression in all cell types on viral control, we would infect C57BL/6J and *Hmgb2*$^{-/-}$ mice with LCMV Cl13, similarly to the experiment outlined in Fig. 3.1i-l. Our preliminary studies show HMGB2 expression is critical for the formation and maintenance of multiple virus-specific CD8$^+$ T cell clones. We found a slight trend towards increased viral load in both the serum and kidneys of *Hmgb2*$^{-/-}$ mice, which warrants future repeats of the experiment that are carried out to later timepoints post-infection. However, we did find significantly increased viral loads in the brains and lungs of *Hmgb2*$^{-/-}$ mice. To investigate the global impact of HMGB2 expression on tumor control, C57BL/6J and *Hmgb2*$^{-/-}$ mice would be implanted with 1x10^6 B16-GP$_{33-41}$ melanoma cells subcutaneously and the tumor burden would be measured with tumor weights collected at the end. Additionally, mouse survival would be determined throughout the experiment. Together, these studies would allow us to investigate whether HMGB2 expression impacts viral and/or tumor control, and if this impact is due to HMGB2 expression in CD8$^+$ T cells alone.

Our study discovered a critical role for HMGB2 expression in the formation and maintenance of Tpex cells, which not only seed the exhausted T cell pool, but are important for patient responses to immune checkpoint blockade (ICB) therapy. With ICB therapies, including anti-PD-1/PD-L1, the Tpex population expands and is responsible for the effector T cell burst in responding patients. Therefore, an important question to ask is if HMGB2 expression is critical for T cell responses to ICB therapies (**Fig. 4.2a**). To address this, we would follow the same co-transfer experimental approach as outlined in Fig. 3.1f, but would additionally treat mice with either IgG or anti-PD-1/PD-L1. We would

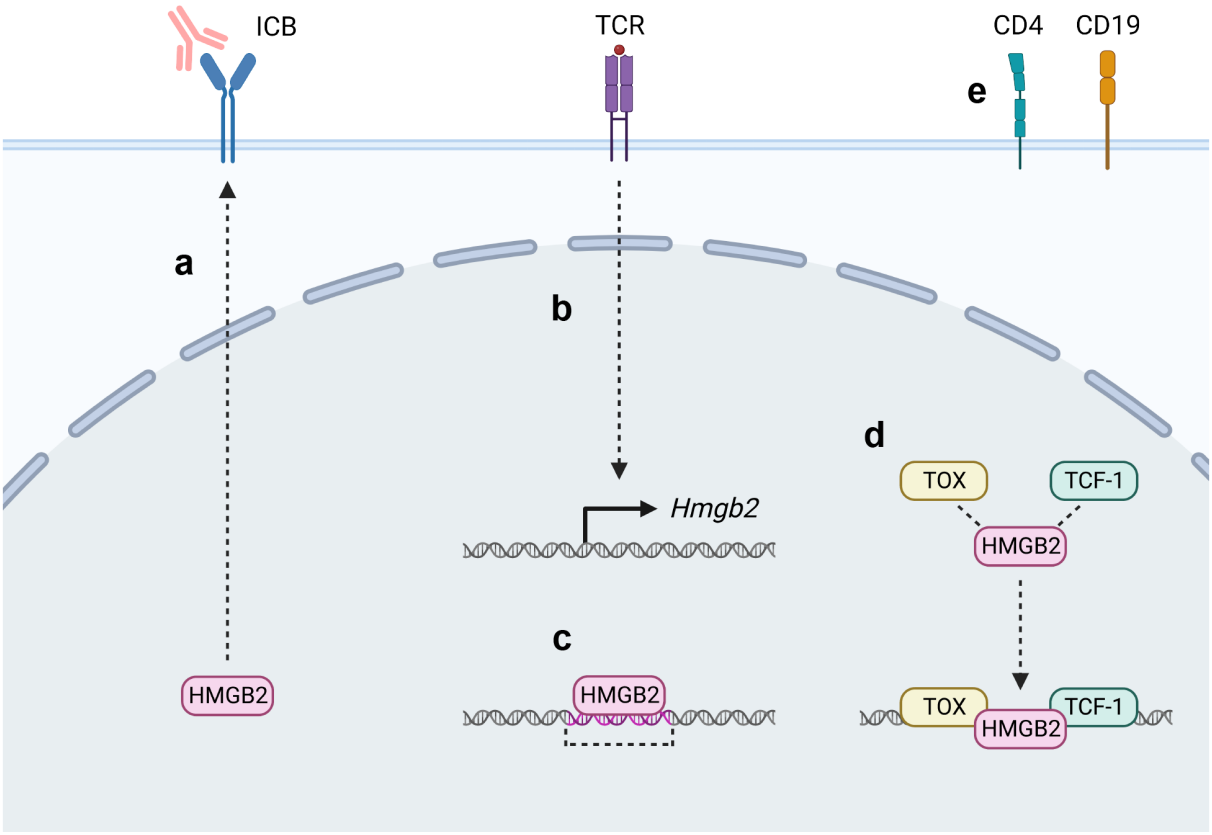

Figure 4.2 Future areas of research for HMGB2 in adaptive immune responses. (**a**) The role of HMGB2 in preserving the Tpex cell population and enhancing responses of exhausted T cells to ICB therapy in chronic viral infections and cancers remains unknown. (**b**) How HMGB2 expression is regulated in T cells and whether it is linked to TCR signaling/calcineurin/NFAT proteins is unknown. (**c**) HMGB2-specific binding sites in T cell subsets have not been characterized. (**d**) Interactions with other transcription factors and/or chromatin remodeling proteins in Teff, Tmem, and Tex cells are unknown. More specifically, possible co-regulation with TOX and/or TCF-1 requires further investigation. (**e**) The role of HMGB2 in other immune cells, including antigen-specific $CD4^+$ T cells and B cells, is unknown. Abbreviations: Tpex, progenitor exhausted T cell; Teff, effector T cell; Tcm, central memory T cell; Tex, exhausted T cell.

follow a well-documented anti-PD-1/PD-L1 treatment plan in order to best examine the responses of exhausted P14 T cells to ICB therapy[221]. Frequencies, proliferation, and effector function of adoptively transferred WT and *Hmgb2*$^{-/-}$ P14 T cells would be measured throughout Cl13 infection in order to determine whether HMGB2 expression impacted ICB-mediated T cell responses. Additionally, we would further evaluate responses of exhausted *Hmgb2*$^{-/-}$ T cells to ICB therapy by inoculating *Hmgb2*$^{-/-}$ mice with LCMV Cl13 or B16-GP$_{33-41}$ melanoma and following both T cell responses and overall viral and tumor loads with anti-PD-1/PD-L1 treatment. The above-mentioned studies could also be done using other ICB therapies, including anti-CTLA-4. If we find HMGB2 expression is indeed required for ICB responses to chronic infections, these studies would reveal HMGB2 expression as a possible predictor of ICB responsiveness.

Additionally, we want to investigate how HMGB2 overexpression in exhausted T cells would impact the stability of the Tpex population during chronic infections. We found that HMGB2 was required for both the formation and survival of Tpex cells during Cl13 infection, and thus hypothesize that overexpressing HMGB2 in exhausted T cells may help preserve this clinically relevant population. Using an optimized protocol for adoptive transfer of retrovirally transduced murine T cells[245], we would engineer P14 T cells that overexpress HMGB2 (HMGB2^{OE}) and compare their anti-viral responses *in vivo* to non-transduced WT and *Hmgb2*$^{-/-}$ P14 T cells. In addition to evaluating frequencies, numbers, inhibitory receptor expression, and effector function of exhausted HMGB2^{OE} T cells, we would also characterize the differentiation and survival of HMGB2^{OE} Tpex cells. This would provide new insight into whether HMGB2 is sufficient to drive Tpex development and persistence during chronic viral infection. Furthermore, we want to investigate the

impact of HMGB2 overexpression on tumor-specific exhausted T cells using a similar approach but with adoptive transfer of HMGB2^{OE} into mice before inoculation with B16-GP$_{33-41}$ melanoma tumors. The balance between Tpex and Tex cells in the tumor microenvironment and TdLN is a therapeutic marker of patient responses to immunotherapies[111, 246]. Therefore, using the adoptive transfer of HMGB2^{OE} P14 T cells in tumor-bearing mice allows us to investigate whether HMGB2 promotes the formation of Tpex cells, tipping the balance towards increased responsiveness to ICB therapies. We would evaluate HMGB2^{OE} Tpex and Tex cell frequencies, numbers, phenotype, and function in tumors and TdLNs compared to adoptively transferred non-transduced WT and *Hmgb2*$^{-/-}$ P14 T cells. In addition to general characterization of HMGB2^{OE} Tpex cells during chronic viral infection and cancer, we would also want to evaluate the ICB responsiveness of these cells to anti-PD-1/PD-L1 checkpoint blockade. Using the adoptive transfer approach outlined above, we would also treat Cl13 infected and tumor bearing mice that received HMGB2^{OE} P14 T cells with anti-PD-1/PD-L1 and investigate the impact of HMGB2 overexpression on Tpex cell re-expansion and effector function. Additionally, we could investigate the impact of HMGB2 overexpression on viral and tumor control, both with and without the addition of ICB therapy. Together, these overexpression studies would help provide insight into the role of HMGB2 in preserving the Tpex population and may have the potential to help improve therapeutic approaches that rely on the re-expansion and function of Tpex cells for durable patient responses.

We could also utilize HMGB2^{OE} P14 T cells to investigate how HMGB2 overexpression might impact memory T cell differentiation and recall capacity. After LCMV Arm viral clearance, we found *Hmgb2*$^{-/-}$ P14 T cells had decreased differentiation

of Tcm cells, with the majority being effector memory T cells (Tem). Tcm cells are critical for secondary immune responses to reinfections, as this population can self-renew to maintain the memory T cell pool and can re-expand to mount secondary effector T cell responses. Therefore, we want to determine if HMGB2 expression is sufficient for the formation and function of Tcm cells after acute viral infection. Using the retrovirally transduced HMGB2^{OE} P14 T cells described above, we would adoptively transfer these into mice before infection with LCMV Arm and follow effector and memory CD8^{+} T cell responses. We would focus on how the differentiation of memory T cell subsets may be impacted in HMGB2^{OE} T cells, and using a model of secondary infection similar to Fig. 2.6a, we would also investigate the recall responses, secondary effector functions, and pathogen control of HMGB2^{OE} memory T cells. These studies would be an important addition to our findings of HMGB2 as a regulator of the differentiation and self-renewal of Tcm cells. Importantly, understanding whether HMGB2 overexpression may increase frequencies and recall responses of Tcm cells could have potential impacts on approaches to vaccination and immunotherapy design.

Despite our thorough characterization of HMGB2's role in memory and exhausted CD8^{+} T cell differentiation and stemness, there are still many important unanswered questions regarding its regulation. It was previously unknown how HMGB2 expression was regulated in CD8^{+} T cells, but we found upregulation of HMGB2 with T cell activation and sustained expression with chronic infection. This suggests HMGB2 expression is induced by T cell receptor (TCR) signaling, although this dissertation did not directly investigate this possibility (**Fig. 4.2b**). One approach to elucidate the upstream regulators of HMGB2 expression in CD8^{+} T cells is to investigate if HMGB2 expression depends on

calcineurin signaling. When T cells are activated by antigen through their TCR, downstream signals result in the release of calcium (Ca^{2+}) and the activation of calcineurin, which operates through NFAT proteins to induce the expression of genes required for T cell expansion and responses[247]. We would first measure HMGB2 expression in naïve $CD8^+$ T cells after treatment with ionomycin, which induces Ca^{2+} influx and calcineurin signaling. The HMGB2 expression in these T cells would be compared to naïve $CD8^+$ T cells treated with either phorbol myristate acetate (protein kinase C activator) alone or in combination with ionomycin to comprehensively determine the role of calcineurin signaling on HMGB2 expression. Since calcineurin signaling acts primarily through NFAT proteins, we could additionally investigate the role of NFAT1 and NFAT2 in driving HMGB2 expression. We could explore this possible regulation *in vitro* using stimulated T cells retrovirally transduced with constitutively active, nucleus-restricted NFAT1 or NFAT2 and measuring their HMGB2 expression. Moreover, we could analyze HMGB2 expression in NFAT1 or NFAT2 conditional knock-out P14 T cells in LCMV Cl13 infected mice (from *Nfatc1/2*$^{flox/flox}$*Cd4*^{cre} P14 mice). Utilizing these approaches will help elucidate whether HMGB2 expression is regulated by calcineurin-mediated TCR signaling and/or NFAT proteins in $CD8^+$ T cells.

HMGB2 functions as a chromatin modifier, regulating the accessibility and transcription of various genes. However, the exact binding sites of HMGB2 in $CD8^+$ T cells are unknown (**Fig. 4.2c**). Of note, it may be difficult to identify these sites because HMGB proteins bind DNA without sequence specificity, preferentially interacting with noncanonical DNA structures. However, various studies have used omics to identify the binding sites of HMGB1 in various cell types[168]. First, we would perform chromatin

immunoprecipitation sequencing (ChIP-seq) to analyze HMGB2 interactions with DNA in naïve, effector, memory, and exhausted $CD8^+$ T cells. Of note, HMGB proteins are not compatible with standard formaldehyde fixation and thus a dual-cross-linking ChIP-seq method has been efficient in capturing HMGB proteins bound to their cognate sites[248]. ChIP-seq allows us to identify genome-wide DNA binding sites of HMGB2, which are currently unknown in all T cell subsets. To further characterize the location of HMGB2 binding sites, we would also utilize high-throughput chromosome conformation capture (Hi-C) to analyze the organization of chromatin, including the location of topologically associating domains (TADs). This technique incorporates 3-D chromatin structure with binding site locations, allowing for a more comprehensive picture of where HMGB2 binds the genome during different stages of T cell differentiation. We could also integrate the ChIP-sequencing data with our ATAC-sequencing data to visualize the proximity between HMGB2 binding sites and the changes in chromatin accessibility we discovered. These studies will also determine if HMGB2 directly regulates the accessibility of transcription factor binding sites. The binding sites of TCF-1 would be of particular interest as we hypothesize TCF-1 requires HMGB2 in exhausted $CD8^+$ T cells to regulate transcription of its target genes. In addition to modulating the accessibility of binding sites, HMGB2 could also regulate transcription factor activity through direct binding. The majority of HMGB binding partners have been identified through interactions with HMGB1, with very little known about binding partners of HMGB2 (**Fig. 4.2d**). Thus, we would perform immunoprecipitation followed by mass spectrometry to identify proteins bound to HMGB2 in $CD8^+$ T cells at homeostasis and during both acute and chronic infections. To validate some proteins of interest that interact with HMGB2, we would perform co-

immunoprecipitation. Not only would this allow us to identify any transcription factors directly bound to HMGB2, but could also inform us about possible interactions with other chromatin remodeling proteins or proteins involved with DNA replication.

Through RNA- and ATAC-sequencing, we were able to profile $CD8^+$ T cell gene expression and chromatin accessibility regulated by HMGB2. However, in the future we should expand our analysis to include additional timepoints during infection and additional bioinformatic strategies. Given the critical role for HMGB2 in memory T cell differentiation, survival, and re-expansion, we should perform both RNA- and ATAC-sequencing on memory WT and *Hmgb2*$^{-/-}$ P14 T cells (i.e. >20dpi Arm). Since we identified HMGB2 as a regulator of Tcm differentiation, we should also perform the previously mentioned analyses on sorted Tcm cells. On top of identifying global transcriptional and epigenetic changes regulated by HMGB2 in memory $CD8^+$ T cells, we would also focus on regions of chromatin required for recall upon secondary infections. Some of these regions in Tcm cells are regulated by TCF-1, and include those associated with glycolytic enzymes, cell cycle regulators, and transcriptional regulators[60]. We could then directly compare regions identified in our studies with those regulated by TCF-1 to gain a better understanding of how HMGB2 and TCF-1 may co-regulated memory T cell differentiation. This could be further investigated by comparing RNA- and ATAC-sequencing results from sorted Tcm cells that are at either resting state or had experienced *ex vivo* stimulation with GP_{33-41} peptide. Together, these genomic studies will provide us with insight into how HMGB2 may be regulating Tcm differentiation and recall capacity. We should also perform ATAC-sequencing on exhausted WT and *Hmgb2*$^{-/-}$ P14 T cells at 20dpi Cl13 to accompany our

20dpi RNA-sequencing data. This would provide us with additional mechanisms through which HMGB2 may regulate exhaustion-specific gene expression.

Although we thoroughly analyzed our RNA- and ATAC-sequencing data for this dissertation, we were limited by my expertise in comparative genomics and next-generation analyses and should perform additional bioinformatic analyses. First, we should integrate our RNA- and ATAC-sequencing data from WT and *Hmgb2*$^{-/-}$ P14 T cells at 8dpi Cl13. Through this, we would be able to visualize the overlaid RNA- and ATAC-sequencing tracks and could get a better understanding of genomic regions where accessibility and thus gene expression were regulated by HMGB2. Additionally, we should perform gene set enrichment analysis (GSEA) on our RNA- and ATAC-sequencing experiments (both 8dpi and 20dpi). This analysis would characterize the global transcriptional and epigenetic signatures of WT and *Hmgb2*$^{-/-}$ P14 T cells in terms of having weak or strong enrichments to naïve, effector, memory, and/or exhausted T cells. GSEA would further characterize the differentially expressed genes (DEG) and differentially accessible regions (DAR) we observed between samples during LCMV Arm and Cl13 infection. Although we performed Ingenuity Pathway Analysis (IPA) on our RNA-sequencing data to identify transcriptional networks regulated by HMGB2, more recently, studies are using a different platform called PageRank network analysis[249]. We would perform PageRank analysis on our transcriptional and epigenetic data to identify transcription factor networks regulated by HMGB2 expression. This analysis could corroborate our IPA findings, but could also identify new transcriptional networks. Furthermore, we should perform transcription factor binding motif analysis on our DAR to identify any binding sites within regions where accessibility is regulated by HMGB2[250].

Combining PageRank network analysis and transcription factor binding motif analysis would elucidate any transcription factors whose binding sites are regulated by HMGB2 in $CD8^+$ T cells. This would provide more insight into the mechanisms through which HMGB2 regulates memory and exhausted T cell differentiation and function.

The epigenetic stability of exhausted $CD8^+$ T cells has been well characterized and underlies the transient responses of patients to ICB therapy. In our studies, we identified numerous regions of chromatin regulated by HMGB2, but did not investigate whether HMGB2 regulates regions that are “scarred”, referring to regions where accessibility remains unchanged after chronic infection cure or ICB therapy. Identifying the epigenetic regulators of these scarred regions has clinical implications for improving and extending responses to ICB therapies. To determine scarred loci in $CD8^+$ T cells and whether these are regulated by HMGB2, we would perform a similar co-transfer experiment to that in Fig. 3.1f using Cl13 infected mice. At 30dpi, we would isolate exhausted WT and *Hmgb2*$^{-/-}$ P14 T cells and adoptively co-transfer them into infection-free recipient mice. The exhausted P14 T cells that survive in antigen free mice will be isolated at 30 days post-transfer. We would perform ATAC-sequencing on WT and *Hmgb2*$^{-/-}$ P14 T cells isolated at either 30dpi primary Cl13 infection (Tex) or at 30 days post-transfer into infection-free mice (Recovering-Tex). We would compare the epigenetic profile of *Hmgb2*$^{-/-}$ Tex and *Hmgb2*$^{-/-}$ Recovering-Tex cells to identify any scarred regions that remained unchanged despite removal of antigen. These DAR would be compared to those identified between WT Tex and WT Recovering-Tex cells to highlight any scarred regions regulated by HMGB2. This study would provide us insight into whether HMGB2 prevents and/or maintains scarred regions in exhausted T cells that may impact ICB responses. If HMGB2

or HMGB2-dependent events regulate the epigenetic inflexibility of exhausted T cells, this would suggest potential therapeutic strategies based on HMGB2 manipulation.

Finally, further questions remain regarding the role of HMGB2 in other cell types, including $CD4^+$ T cells, B cells, and human $CD8^+$ T cells (**Fig. 4.2e**). We have initiated breeding of WT and *Hmgb2*$^{-/-}$ SMARTA mice, which are TCR transgenic mice with a $CD4^+$ T cell repertoire specific for the LCMV GP_{61-80} epitope. Using these mice for adoptive $CD4^+$ T cell transfers would allow us to investigate HMGB2 expression and function in virus-specific naïve, effector, memory, and exhausted $CD4^+$ T cells. We would perform very similar experiments to those using P14 T cells outlined in this dissertation. Since HMGB2 has not been characterized in $CD4^+$ T cells, understanding its role in $CD4^+$ T cell differentiation and responses would be a major contribution to the field of T cell biology. Similarly to $CD4^+$ and $CD8^+$ T cells, B cells express HMGB2, but its role in B cell development and function has not been investigated. To characterize HMGB2 expression specifically in B cells, we would need to create *Hmgb2*$^{flox/flox}$*Cd19*^{cre} mice either through the UCI Transgenic Mouse Facility (TMF) or by breeding *Hmgb2*$^{flox/flox}$ mice with *Cd19*^{cre} mice in house using mice purchased from Shanghai Model Organisms and Jackson Laboratory, respectively. Using the Cre-lox system will allow us to study the impact of HMGB2 expression in $CD19^+$ B cells, and since this system is geminal and not inducible, B cells at all phases of development will have *Hmgb2* deletion. This model will not only elucidate the role of HMGB2 in B cell development, but also its role in anti-viral and anti-tumor B cell responses by using LCMV and B16 melanoma models.

Since the protein sequence of HMGB2 shows 98% homology between mice and humans, we are also interested in HMGB2 regulation and function in human $CD8^+$ T cells.

We would first characterize HMGB2 expression, both RNA and protein, in human $CD8^+$ T cell subsets and determine if HMGB2 expression may be linked to T cell activation similarly to the experiment outlined above. Also, we would characterize HMGB2 expression levels in $CD8^+$ T cells from chronically infected patients and could utilize preexisting data sets where patient peripheral blood monocular cells (PBMC) were isolated pre-, during, and post-chronic infection[142, 143]. This characterization of HMGB2 expression would also extend to patient tumor-specific exhausted $CD8^+$ T cells, as we discovered HMGB2 was required for maintenance of tumor-specific $CD8^+$ T cells in mice. Furthermore, we would be interested in characterizing HMGB2 expression in Tpex, Tex, and Tcm cells from patient PBMC samples.

Although we identified HMGB2 as a critical regulator of $CD8^+$ T cell differentiation, there are some limitations to our current study. First, we did not directly investigate if HMGB2 expression impacts initial trafficking or homing of adoptively transferred naïve $CD8^+$ T cells. With our single-transfer studies, we found similar expansion and proliferation of WT and *Hmgb2*$^{-/-}$ P14 T cells at 8dpi LCMV Arm and Cl13. We used this finding to explain the loss of co-transferred *Hmgb2*$^{-/-}$ P14 T cells at 8dpi LCMV Arm and Cl13 as a deficiency in their activation, not their homing. However, we should have confirmed this by evaluating the frequencies and numbers of co-transferred WT and *Hmgb2*$^{-/-}$ P14 T cells at 24- and 48hrs post-transfer. Otherwise, we cannot refute that the decreased frequencies and numbers of *Hmgb2*$^{-/-}$ P14 T cells throughout LCMV infection were because of their diminished homing and uptake after initial transfer.

TCR signal strength is a key determinant of T cell responses and depends on a variety of factors, including TCR affinity and avidity for peptide[251, 252]. Together, these can

influence multiple downstream signaling events after engagement, including the rate of calcium flux and the phosphorylation of Lck, LAT, and ERK proteins[253, 254]. These alterations to intracellular signaling pathways impact the differentiation of responding T cells. In murine studies with LCMV Cl13 and tumors, T cell clones with low affinity are enriched for Tpex and effector-like Tex cells, while high affinity T cell clones preferentially progress to terminal Tex cells[255, 256, 257]. Since clonal trajectories of responding T cells correlate with TCR signaling affinity, it is important to note that our studies solely utilized P14 $CD8^+$ T cells, which are high affinity TCR transgenic T cells specific for the LCMV GP_{33-41} peptide. Therefore, the characterization of HMGB2's role in regulating $CD8^+$ T cell differentiation may be unique to this high affinity T cell clone, especially if HMGB2 expression is directly regulated by TCR signaling as we are proposing. It is possible that HMGB2 regulation of $CD8^+$ T cell epigenetic and transcriptional programs are dependent on TCR affinity, TCR signal strength, and/or activation of specific intracellular pathways. Diminished TCR signals associated with lower affinity T cell clones may impact HMGB2, and thus dampen or prevent its regulation of $CD8^+$ T cell differentiation. The opposite could also be true where HMGB2 plays a more critical role in low affinity T cell clones, especially since they preferentially progress to Tpex cells, which we found are regulated by HMGB2. Thus, the role of HMGB2 in $CD8^+$ T cell differentiation may depend on the affinity of T cell clones. We could determine to what extent this may be true by utilizing virus-specific $CD8^+$ T cells with various affinities, including T cells specific for either altered GP_{33-41} peptides or a subdominant peptide like $GP_{276-286}$. Since TCR signal strength determines the clonal behavior of responding T cells to chronic infections, it is

important to understand if HMGB2 is regulated by TCR affinity and how this may impact the role we discovered for HMGB2 in $CD8^+$ T cell differentiation.

Another limitation of our study was we sorted all transferred P14 T cells without considering specific subtypes for our secondary infection studies. For example, after 30dpi Arm infection, we sorted all live, WT and *Hmgb2*$^{-/-}$ memory T cells and transferred them into new mice. We then observed a deficiency in the ability of the *Hmgb2*$^{-/-}$ memory T cells to re-expand with secondary Arm infection. However, we had previously characterized a significant decrease in *Hmgb2*$^{-/-}$ Tcm cells at 30dpi Arm compared to WT and did not account for this when normalizing overall numbers of memory WT and *Hmgb2*$^{-/-}$ T cells for co-transfer in the secondary infection study. Therefore, the inability of the memory *Hmgb2*$^{-/-}$ T cells to re-expand could be explained by the significantly decreased frequencies of Tcm cells compared to WT and not by an intrinsic deficiency in proliferation and/or self-renewal. The same is true for our exhausted T cell secondary infection studies, where we sorted all live, WT and *Hmgb2*$^{-/-}$ exhausted T cells at 30dpi Cl13 and did not account for the significantly decreased frequencies of *Hmgb2*$^{-/-}$ Tpex cells before co-transfer into LCMV Arm infected mice. Therefore, the diminished *Hmgb2*$^{-/-}$ Tpex population may explain the inability of these cells to expand with reinfection as opposed to an intrinsic defect in their proliferation and/or self-renewal capacity. A more appropriate way to investigate the role of HMGB2 on memory and exhausted T cell re-expansion would be to normalize the subpopulations within our transferred cells and then evaluate their function, with an emphasis on the Tcm and Tpex populations during LCMV Arm and Cl13 infection, respectively.

Prior to this study, there was no characterization of HMGB2's role within mammalian $CD8^+$ T cells, so it remains unclear whether our findings may translate to humans. Although the sequence of HMGB2 is highly conserved between mammals, it is unknown whether its post-translational modifications follow a similar pattern. HMGB2 undergoes acetylation, phosphorylation, and methylation, but much of what is known regarding HMGB2 post-translational modifications comes from characterization of HMGB1[258]. Consequently, the pattern of these modifications in mammalian species and how they may influence HMGB2 localization and function are poorly understood. Thus, the role of HMGB2 in murine $CD8^+$ T cell differentiation may be different than its role in humans, depending on the conservation and/or divergence of its post-translational modifications.

Finally, while immunology research using mouse models has been instrumental in advancing our understanding of the immune system, there are some limitations when it comes to studying human immunology. Gene expression between mice and humans is highly conserved, but the regulatory patterns have diverged significantly. There are vast differences in the DNA binding patterns of many transcription factors between mice and humans, with potential impacts on overall cellular functions and regulatory mechanisms[259, 260]. The divergence of transcription factor binding sites between species may impact how, or if, HMGB2 impacts the differentiation of $CD8^+$ T cells in humans. Importantly, there has not been complete characterization of the conserved transcription factor binding patterns, and thus it is unclear to what extent the binding sites of specific transcription factors, including TCF-1 and TOX, are influenced by species. Additionally, since HMGB2 does not bind DNA with sequence specificity, the binding sites of HMGB2

in mammalian cells may also differ depending on species-specific chromatin structure and/or epigenetic regulation at these loci. Since we are hypothesizing HMGB2 co-regulates murine CD8$^+$ T cell differentiation with specific transcription factors, not knowing whether their binding sites are conserved prevents us from fully understanding if our findings will translate to humans.

Genes with conserved expression patterns in mice and humans are mainly associated with organelle compartments, RNA processing, and metabolic processes, while genes with divergent expression are associated with extracellular matrix, signaling receptors, and immune responses[261]. The regulation of genes involved in immune function tend to be species-specific, especially because they are frequently targeted by adaptive selection[262, 263]. There is also increasing evidence for species-specific *cis*-regulatory elements near immune function genes, correlating with extensive differences in mouse and human immune systems[261]. For example, mice and humans have known discrepancies in their balance of leukocyte subsets[264], T cell signaling components (ZAP70, γ-chain)[265, 266, 267], Th1/Th2 differentiation[268], and antigen presentation[269]. Since our studies primarily focused on CD8$^+$ T cells, and there's increased divergence of transcriptional regulatory sequences at immune related genes, it is unclear whether HMGB2's regulation of the epigenetic signature and transcriptional program of murine CD8$^+$ T cells will translate to humans. Specifically, HMGB2 may regulate the accessibility of species-specific *cis*-regulatory elements, and consequently, how it functions in CD8$^+$ T cell differentiation may differ between mice and humans.

Overall, our work investigating HMGB2 provides important insight into the epigenetic mechanisms underlying T cell differentiation. We showed that HMGB2

promotes the differentiation and recall function of Tcm cells following acute viral infection. In exhausted $CD8^+$ T cells, HMGB2 increases the accessibility and expression of genes required for Tpex cell differentiation and persistence, both in chronic viral infection and tumors. Our findings are an exciting contribution to TCF-1 mediated regulation of memory and exhausted T cell stemness, showing HMGB2 is an indispensable partner for recall capacity and maintenance of anti-viral T cells. We reveal modulation of HMGB2 may be a new avenue for improving immunotherapy strategies and provide the foundation for future impactful projects investigating the mechanisms by which HMGB2 modulates the transcriptional networks and chromatin architecture of T cells.

References

1. Kaech, S.M. & Cui, W. Transcriptional control of effector and memory CD8+ T cell differentiation. *Nat Rev Immunol* **12**, 749-761 (2012).

2. Chang, J.T., Wherry, E.J. & Goldrath, A.W. Molecular regulation of effector and memory T cell differentiation. *Nat Immunol* **15**, 1104-1115 (2014).

3. Obar, J.J. & Lefrancois, L. Memory CD8+ T cell differentiation. *Ann N Y Acad Sci* **1183**, 251-266 (2010).

4. Harty, J.T. & Badovinac, V.P. Shaping and reshaping CD8+ T-cell memory. *Nat Rev Immunol* **8**, 107-119 (2008).

5. Nayar, R. *et al.* Graded levels of IRF4 regulate CD8+ T cell differentiation and expansion, but not attrition, in response to acute virus infection. *J Immunol* **192**, 5881-5893 (2014).

6. Nowyhed, H.N., Huynh, T.R., Thomas, G.D., Blatchley, A. & Hedrick, C.C. Cutting Edge: The Orphan Nuclear Receptor Nr4a1 Regulates CD8+ T Cell Expansion and Effector Function through Direct Repression of Irf4. *J Immunol* **195**, 3515-3519 (2015).

7. Danilo, M., Chennupati, V., Silva, J.G., Siegert, S. & Held, W. Suppression of Tcf1 by Inflammatory Cytokines Facilitates Effector CD8 T Cell Differentiation. *Cell Rep* **22**, 2107-2117 (2018).

8. Joshi, N.S. *et al.* Inflammation Directs Memory Precursor and Short-Lived Effector CD8(+) T Cell Fates via the Graded Expression of T-bet Transcription Factor. *Immunity* **27**, 281-295 (2007).

9. Kim, M.T. & Harty, J.T. Impact of Inflammatory Cytokines on Effector and Memory CD8+ T Cells. *Front Immunol* **5**, 295 (2014).

10. Abdelsamed, H.A. *et al.* Human memory CD8 T cell effector potential is epigenetically preserved during in vivo homeostasis. *J Exp Med* **214**, 1593-1606 (2017).

11. Cui, W., Liu, Y., Weinstein, J.S., Craft, J. & Kaech, S.M. An interleukin-21-interleukin-10-STAT3 pathway is critical for functional maturation of memory CD8+ T cells. *Immunity* **35**, 792-805 (2011).

12. Siegel, A.M. *et al.* A critical role for STAT3 transcription factor signaling in the development and maintenance of human T cell memory. *Immunity* **35**, 806-818 (2011).

13. Hamilton, S.E. & Jameson, S.C. Effective effector generation of CD8+ T cells and NK cells: A need for T-bet and ZEB-too. *J Exp Med* **212**, 1990 (2015).

14. Palazon, A., Goldrath, A.W., Nizet, V. & Johnson, R.S. HIF transcription factors, inflammation, and immunity. *Immunity* **41**, 518-528 (2014).

15. Ladle, B.H. *et al.* De novo DNA methylation by DNA methyltransferase 3a controls early effector CD8+ T-cell fate decisions following activation. *Proc Natl Acad Sci U S A* **113**, 10631-10636 (2016).

16. Carty, S.A. *et al.* The Loss of TET2 Promotes CD8(+) T Cell Memory Differentiation. *J Immunol* **200**, 82-91 (2018).

17. Gray, S.M., Amezquita, R.A., Guan, T., Kleinstein, S.H. & Kaech, S.M. Polycomb Repressive Complex 2-Mediated Chromatin Repression Guides Effector CD8(+) T Cell Terminal Differentiation and Loss of Multipotency. *Immunity* **46**, 596-608 (2017).

18. Scott-Browne, J.P. *et al.* Dynamic Changes in Chromatin Accessibility Occur in CD8+ T Cells Responding to Viral Infection. *Immunity* **45**, 1327-1340 (2016).

19. Kaech, S.M., Wherry, E.J. & Ahmed, R. Effector and memory T-cell differentiation: implications for vaccine development. *Nat Rev Immunol* **2**, 251-262 (2002).

20. Kalia, V., Sarkar, S., Gourley, T.S., Rouse, B.T. & Ahmed, R. Differentiation of memory B and T cells. *Curr Opin Immunol* **18**, 255-264 (2006).

21. Kaech, S.M. *et al.* Selective expression of the interleukin 7 receptor identifies effector CD8 T cells that give rise to long-lived memory cells. *Nat Immunol* **4**, 1191-1198 (2003).

22. Pearce, E.L. & Shen, H. Making sense of inflammation, epigenetics, and memory CD8+ T-cell differentiation in the context of infection. *Immunol Rev* **211**, 197-202 (2006).

23. Wilson, C.B., Makar, K.W., Shnyreva, M. & Fitzpatrick, D.R. DNA methylation and the expanding epigenetics of T cell lineage commitment. *Semin Immunol* **17**, 105-119 (2005).

24. Kaech, S.M., Hemby, S., Kersh, E. & Ahmed, R. Molecular and functional profiling of memory CD8 T cell differentiation. *Cell* **111**, 837-851 (2002).

25. Roberts, A.D., Ely, K.H. & Woodland, D.L. Differential contributions of central and effector memory T cells to recall responses. *J Exp Med* **202**, 123-133 (2005).

26. Wherry, E.J. *et al.* Lineage relationship and protective immunity of memory CD8 T cell subsets. *Nat Immunol* **4**, 225-234 (2003).

27. Lanzavecchia, A. & Sallusto, F. Understanding the generation and function of memory T cell subsets. *Curr Opin Immunol* **17**, 326-332 (2005).

28. Masopust, D., Vezys, V., Marzo, A.L. & Lefrancois, L. Preferential localization of effector memory cells in nonlymphoid tissue. *Science* **291**, 2413-2417 (2001).

29. Hamann, D. *et al.* Phenotypic and functional separation of memory and effector human CD8+ T cells. *J Exp Med* **186**, 1407-1418 (1997).

30. Sallusto, F., Lenig, D., Forster, R., Lipp, M. & Lanzavecchia, A. Two subsets of memory T lymphocytes with distinct homing potentials and effector functions. *Nature* **401**, 708-712 (1999).

31. Masopust, D. *et al.* Dynamic T cell migration program provides resident memory within intestinal epithelium. *J Exp Med* **207**, 553-564 (2010).

32. Gebhardt, T. *et al.* Memory T cells in nonlymphoid tissue that provide enhanced local immunity during infection with herpes simplex virus. *Nat Immunol* **10**, 524-530 (2009).

33. Bouneaud, C., Garcia, Z., Kourilsky, P. & Pannetier, C. Lineage relationships, homeostasis, and recall capacities of central- and effector-memory CD8 T cells in vivo. *J Exp Med* **201**, 579-590 (2005).

34. Sheridan, B.S. & Lefrancois, L. Regional and mucosal memory T cells. *Nat Immunol* **12**, 485-491 (2011).

35. Jameson, S.C. & Masopust, D. Diversity in T cell memory: an embarrassment of riches. *Immunity* **31**, 859-871 (2009).

36. Mueller, S.N., Gebhardt, T., Carbone, F.R. & Heath, W.R. Memory T cell subsets, migration patterns, and tissue residence. *Annual Review of Immunology* **31**, 137-161 (2013).

37. Tussey, L., Speller, S., Gallimore, A. & Vessey, R. Functionally distinct CD8+ memory T cell subsets in persistent EBV infection are differentiated by migratory receptor expression. *Eur J Immunol* **30**, 1823-1829 (2000).

38. Gerlach, C. *et al.* The Chemokine Receptor CX3CR1 Defines Three Antigen-Experienced CD8 T Cell Subsets with Distinct Roles in Immune Surveillance and Homeostasis. *Immunity* **45**, 1270-1284 (2016).

39. Kaech, S.M. & Wherry, E.J. Heterogeneity and cell-fate decisions in effector and memory CD8+ T cell differentiation during viral infection. *Immunity* **27**, 393-405 (2007).

40. Delpoux, A. *et al.* Continuous activity of Foxo1 is required to prevent anergy and maintain the memory state of CD8(+) T cells. *J Exp Med* **215**, 575-594 (2018).

41. Hess Michelini, R., Doedens, A.L., Goldrath, A.W. & Hedrick, S.M. Differentiation of CD8 memory T cells depends on Foxo1. *J Exp Med* **210**, 1189-1200 (2013).

42. Marcel, N. & Hedrick, S.M. A key control point in the T cell response to chronic infection and neoplasia: FOXO1. *Curr Opin Immunol* **63**, 51-60 (2020).

43. Utzschneider, D.T. *et al.* Active Maintenance of T Cell Memory in Acute and Chronic Viral Infection Depends on Continuous Expression of FOXO1. *Cell Rep* **22**, 3454-3467 (2018).

44. Abdel-Hakeem, M.S. *et al.* Epigenetic scarring of exhausted T cells hinders memory differentiation upon eliminating chronic antigenic stimulation. *Nat Immunol* **22**, 1008-1019 (2021).

45. Kim, M.V., Ouyang, W., Liao, W., Zhang, M.Q. & Li, M.O. The transcription factor Foxo1 controls central-memory CD8+ T cell responses to infection. *Immunity* **39**, 286-297 (2013).

46. Wang, D. *et al.* The Transcription Factor Runx3 Establishes Chromatin Accessibility of cis-Regulatory Landscapes that Drive Memory Cytotoxic T Lymphocyte Formation. *Immunity* **48**, 659-674 e656 (2018).

47. Liu, Z. *et al.* Cutting Edge: Transcription Factor BCL6 Is Required for the Generation, but Not Maintenance, of Memory CD8(+) T Cells in Acute Viral Infection. *J Immunol* **203**, 323-327 (2019).

48. Lee, P.P. *et al.* A critical role for Dnmt1 and DNA methylation in T cell development, function, and survival. *Immunity* **15**, 763-774 (2001).

49. Akondy, R.S. *et al.* Origin and differentiation of human memory CD8 T cells after vaccination. *Nature* **552**, 362-367 (2017).

50. Russ, B.E. *et al.* Distinct epigenetic signatures delineate transcriptional programs during virus-specific CD8(+) T cell differentiation. *Immunity* **41**, 853-865 (2014).

51. Youngblood, B. *et al.* Effector CD8 T cells dedifferentiate into long-lived memory cells. *Nature* **552**, 404-409 (2017).

52. Siddiqui, I. *et al.* Intratumoral Tcf1(+)PD-1(+)CD8(+) T Cells with Stem-like Properties Promote Tumor Control in Response to Vaccination and Checkpoint Blockade Immunotherapy. *Immunity* **50**, 195-211 e110 (2019).

53. Zhao, D.M. *et al.* Constitutive activation of Wnt signaling favors generation of memory CD8 T cells. *J Immunol* **184**, 1191-1199 (2010).

54. Zhou, X. & Xue, H.H. Cutting edge: generation of memory precursors and functional memory CD8+ T cells depends on T cell factor-1 and lymphoid enhancer-binding factor-1. *J Immunol* **189**, 2722-2726 (2012).

55. Zhou, X. *et al.* Differentiation and persistence of memory CD8(+) T cells depend on T cell factor 1. *Immunity* **33**, 229-240 (2010).

56. Jeannet, G. *et al.* Essential role of the Wnt pathway effector Tcf-1 for the establishment of functional CD8 T cell memory. *Proc Natl Acad Sci U S A* **107**, 9777-9782 (2010).

57. Shan, Q. *et al.* The transcription factor Runx3 guards cytotoxic CD8(+) effector T cells against deviation towards follicular helper T cell lineage. *Nat Immunol* **18**, 931-939 (2017).

58. Johnson, J.L. *et al.* Lineage-Determining Transcription Factor TCF-1 Initiates the Epigenetic Identity of T Cells. *Immunity* **48**, 243-257 e210 (2018).

59. Xing, S. *et al.* Tcf1 and Lef1 transcription factors establish CD8(+) T cell identity through intrinsic HDAC activity. *Nat Immunol* **17**, 695-703 (2016).

60. Shan, Q. *et al.* Tcf1 preprograms the mobilization of glycolysis in central memory CD8(+) T cells during recall responses. *Nat Immunol* **23**, 386-398 (2022).

61. Moskophidis, D., Lechner, F., Pircher, H. & Zinkernagel, R.M. Virus persistence in acutely infected immunocompetent mice by exhaustion of antiviral cytotoxic effector T cells. *Nature* **362**, 758-761 (1993).

62. Gallimore, A. *et al.* Induction and exhaustion of lymphocytic choriomeningitis virus-specific cytotoxic T lymphocytes visualized using soluble tetrameric major histocompatibility complex class I-peptide complexes. *J Exp Med* **187**, 1383-1393 (1998).

63. Zajac, A.J. *et al.* Viral immune evasion due to persistence of activated T cells without effector function. *J Exp Med* **188**, 2205-2213 (1998).

64. Tang, L., Zhang, Y., Hu, Y. & Mei, H. T Cell Exhaustion and CAR-T Immunotherapy in Hematological Malignancies. *Biomed Res Int* **2021**, 6616391 (2021).

65. Wherry, E.J. & Kurachi, M. Molecular and cellular insights into T cell exhaustion. *Nat Rev Immunol* **15**, 486-499 (2015).

66. Wherry, E.J. T cell exhaustion. *Nat Immunol* **12**, 492-499 (2011).

67. Schietinger, A. & Greenberg, P.D. Tolerance and exhaustion: defining mechanisms of T cell dysfunction. *Trends Immunol* **35**, 51-60 (2014).

68. Tan, A., Koh, S. & Bertoletti, A. Immune Response in Hepatitis B Virus Infection. *Cold Spring Harb Perspect Med* **5**, a021428 (2015).

69. Wherry, E.J., Blattman, J.N., Murali-Krishna, K., van der Most, R. & Ahmed, R. Viral Persistence Alters CD8 T-Cell Immunodominance and Tissue Distribution and Results in Distinct Stages of Functional Impairment. *J Virol* **77**, 4911-4927 (2003).

70. Crawford, A. & Wherry, E.J. The diversity of costimulatory and inhibitory receptor pathways and the regulation of antiviral T cell responses. *Curr Opin Immunol* **21**, 179-186 (2009).

71. Jamieson, B.D., Butler, L.D. & Ahmed, R. Effective clearance of a persistent viral infection requires cooperation between virus-specific Lyt2+ T cells and nonspecific bone marrow-derived cells. *J Virol* **61**, 3930-3937 (1987).

72. Matloubian, M., Concepcion, R.J. & Ahmed, R. CD4+ T cells are required to sustain CD8+ cytotoxic T-cell responses during chronic viral infection. *J Virol* **68**, 8056-8063 (1994).

73. Jin, X. *et al.* Dramatic rise in plasma viremia after CD8(+) T cell depletion in simian immunodeficiency virus-infected macaques. *J Exp Med* **189**, 991-998 (1999).

74. Schmitz, J.E. *et al.* Control of viremia in simian immunodeficiency virus infection by CD8+ lymphocytes. *Science* **283**, 857-860 (1999).

75. Bengsch, B. *et al.* Bioenergetic Insufficiencies Due to Metabolic Alterations Regulated by the Inhibitory Receptor PD-1 Are an Early Driver of CD8(+) T Cell Exhaustion. *Immunity* **45**, 358-373 (2016).

76. Chapman, N.M., Boothby, M.R. & Chi, H. Metabolic coordination of T cell quiescence and activation. *Nat Rev Immunol* **20**, 55-70 (2020).

77. Pearce, E.L., Poffenberger, M.C., Chang, C.H. & Jones, R.G. Fueling immunity: insights into metabolism and lymphocyte function. *Science* **342**, 1242454 (2013).

78. Schurich, A. *et al.* Distinct Metabolic Requirements of Exhausted and Functional Virus-Specific CD8 T Cells in the Same Host. *Cell Rep* **16**, 1243-1252 (2016).

79. Ahmadzadeh, M. *et al.* Tumor antigen-specific CD8 T cells infiltrating the tumor express high levels of PD-1 and are functionally impaired. *Blood* **114**, 1537-1544 (2009).

80. Baitsch, L. *et al.* Exhaustion of tumor-specific CD8(+) T cells in metastases from melanoma patients. *J Clin Invest* **121**, 2350-2360 (2011).

81. Fourcade, J. *et al.* Upregulation of Tim-3 and PD-1 expression is associated with tumor antigen-specific CD8+ T cell dysfunction in melanoma patients. *J Exp Med* **207**, 2175-2186 (2010).

82. Huang, A.C. *et al.* T-cell invigoration to tumour burden ratio associated with anti-PD-1 response. *Nature* **545**, 60-65 (2017).

83. Lee, P.P. *et al.* Characterization of circulating T cells specific for tumor-associated antigens in melanoma patients. *Nat Med* **5**, 677-685 (1999).

84. Mumprecht, S., Schurch, C., Schwaller, J., Solenthaler, M. & Ochsenbein, A.F. Programmed death 1 signaling on chronic myeloid leukemia-specific T cells results in T-cell exhaustion and disease progression. *Blood* **114**, 1528-1536 (2009).

85. Fraietta, J.A. *et al.* Determinants of response and resistance to CD19 chimeric antigen receptor (CAR) T cell therapy of chronic lymphocytic leukemia. *Nat Med* **24**, 563-571 (2018).

86. Riches, J.C. *et al.* T cells from CLL patients exhibit features of T-cell exhaustion but retain capacity for cytokine production. *Blood* **121**, 1612-1621 (2013).

87. Matsuzaki, J. *et al.* Tumor-infiltrating NY-ESO-1-specific CD8+ T cells are negatively regulated by LAG-3 and PD-1 in human ovarian cancer. *Proc Natl Acad Sci U S A* **107**, 7875-7880 (2010).

88. Bengsch, B. *et al.* Deep immune profiling by mass cytometry links human T and NK cell differentiation and cytotoxic molecule expression patterns. *J Immunol Methods* **453**, 3-10 (2018).

89. Zhang, Y., Huang, S., Gong, D., Qin, Y. & Shen, Q. Programmed death-1 upregulation is correlated with dysfunction of tumor-infiltrating CD8+ T lymphocytes in human non-small cell lung cancer. *Cell Mol Immunol* **7**, 389-395 (2010).

90. Gandhi, M.K. *et al.* Expression of LAG-3 by tumor-infiltrating lymphocytes is coincident with the suppression of latent membrane antigen-specific CD8+ T-cell function in Hodgkin lymphoma patients. *Blood* **108**, 2280-2289 (2006).

91. Baitsch, L., Fuertes-Marraco, S.A., Legat, A., Meyer, C. & Speiser, D.E. The three main stumbling blocks for anticancer T cells. *Trends Immunol* **33**, 364-372 (2012).

92. Dolina, J.S., Van Braeckel-Budimir, N., Thomas, G.D. & Salek-Ardakani, S. CD8(+) T Cell Exhaustion in Cancer. *Front Immunol* **12**, 715234 (2021).

93. Angelosanto, J.M., Blackburn, S.D., Crawford, A. & Wherry, E.J. Progressive loss of memory T cell potential and commitment to exhaustion during chronic viral infection. *J Virol* **86**, 8161-8170 (2012).

94. Philip, M. *et al.* Chromatin states define tumour-specific T cell dysfunction and reprogramming. *Nature* **545**, 452-456 (2017).

95. Beltra, J.C. *et al.* Developmental Relationships of Four Exhausted CD8(+) T Cell Subsets Reveals Underlying Transcriptional and Epigenetic Landscape Control Mechanisms. *Immunity* **52**, 825-841 e828 (2020).

96. Chu, T. & Zehn, D. Charting the Roadmap of T Cell Exhaustion. *Immunity* **52**, 724-726 (2020).

97. Chen, Z. *et al.* TCF-1-Centered Transcriptional Network Drives an Effector versus Exhausted CD8 T Cell-Fate Decision. *Immunity* **51**, 840-855.e845 (2019).

98. Wu, T. *et al.* The TCF1-Bcl6 axis counteracts type I interferon to repress exhaustion and maintain T cell stemness. *Sci Immunol* **1** (2016).

99. Menner, A.J. *et al.* Id3 Controls Cell Death of 2B4+ Virus-Specific CD8+ T Cells in Chronic Viral Infection. *J Immunol* **195**, 2103-2114 (2015).

100. Utzschneider, D.T. *et al.* Early precursor T cells establish and propagate T cell exhaustion in chronic infection. *Nature Immunology* **21**, 1256-1266 (2020).

101. Yao, C. *et al.* BACH2 enforces the transcriptional and epigenetic programs of stem-like CD8(+) T cells. *Nat Immunol* **22**, 370-380 (2021).

102. Im, S.J. *et al.* Defining CD8+ T cells that provide the proliferative burst after PD-1 therapy. *Nature* **537**, 417-421 (2016).

103. He, R. *et al.* Follicular CXCR5- expressing CD8(+) T cells curtail chronic viral infection. *Nature* **537**, 412-428 (2016).

104. Kurtulus, S. *et al.* Checkpoint Blockade Immunotherapy Induces Dynamic Changes in PD-1(-)CD8(+) Tumor-Infiltrating T Cells. *Immunity* **50**, 181-194 e186 (2019).

105. Leong, Y.A. *et al.* CXCR5(+) follicular cytotoxic T cells control viral infection in B cell follicles. *Nat Immunol* **17**, 1187-1196 (2016).

106. Utzschneider, D.T. *et al.* T Cell Factor 1-Expressing Memory-like CD8(+) T Cells Sustain the Immune Response to Chronic Viral Infections. *Immunity* **45**, 415-427 (2016).

107. Hudson, W.H. *et al.* Proliferating Transitory T Cells with an Effector-like Transcriptional Signature Emerge from PD-1(+) Stem-like CD8(+) T Cells during Chronic Infection. *Immunity* **51**, 1043-1058 e1044 (2019).

108. Raju, S. *et al.* Identification of a T-bet(hi) Quiescent Exhausted CD8 T Cell Subpopulation That Can Differentiate into TIM3(+)CX3CR1(+) Effectors and Memory-like Cells. *J Immunol* **206**, 2924-2936 (2021).

109. Belk, J.A., Daniel, B. & Satpathy, A.T. Epigenetic regulation of T cell exhaustion. *Nat Immunol* **23**, 848-860 (2022).

110. Jiang, W. *et al.* Exhausted CD8+T Cells in the Tumor Immune Microenvironment: New Pathways to Therapy. *Front Immunol* **11**, 622509 (2020).

111. Miller, B.C. *et al.* Subsets of exhausted CD8 + T cells differentially mediate tumor control and respond to checkpoint blockade. *Nature Immunology* **20**, 326-336 (2019).

112. Bengsch, B. *et al.* Epigenomic-Guided Mass Cytometry Profiling Reveals Disease-Specific Features of Exhausted CD8 T Cells. *Immunity* **48**, 1029-1045 e1025 (2018).

113. Pritykin, Y. *et al.* A unified atlas of CD8 T cell dysfunctional states in cancer and infection. *Mol Cell* **81**, 2477-2493 e2410 (2021).

114. Gennert, D.G. *et al.* Dynamic chromatin regulatory landscape of human CAR T cell exhaustion. *Proc Natl Acad Sci U S A* **118** (2021).

115. Giles, J.R. *et al.* Human epigenetic and transcriptional T cell differentiation atlas for identifying functional T cell-specific enhancers. *Immunity* **55**, 557-574 e557 (2022).

116. Sen, D.R. *et al.* The epigenetic landscape of T cell exhaustion. *Science* **354**, 1165-1169 (2016).

117. Pauken, K.E. *et al.* Epigenetic stability of exhausted T cells limits durability of reinvigoration by PD-1 blockade. *Science* **354**, 1160-1165 (2016).

118. Youngblood, B. *et al.* Chronic virus infection enforces demethylation of the locus that encodes PD-1 in antigen-specific CD8(+) T cells. *Immunity* **35**, 400-412 (2011).

119. Ghoneim, H.E. *et al.* De Novo Epigenetic Programs Inhibit PD-1 Blockade-Mediated T Cell Rejuvenation. *Cell* **170**, 142-157 e119 (2017).

120. Pauken, K.E. *et al.* Epigenetic stability of exhausted T cells limits durability of reinvigoration by PD-1 blockade. *Science* **354**, 1160-1165 (2016).

121. Utzschneider, D.T. *et al.* T cells maintain an exhausted phenotype after antigen withdrawal and population reexpansion. *Nature Immunology* **14**, 603-610 (2013).

122. Doering, T.A. *et al.* Network analysis reveals centrally connected genes and pathways involved in CD8+ T cell exhaustion versus memory. *Immunity* **37**, 1130-1144 (2012).

123. Paley, M.A. *et al.* Progenitor and terminal subsets of CD8+ T cells cooperate to contain chronic viral infection. *Science* **338**, 1220-1225 (2012).

124. Martinez, G.J. *et al.* The transcription factor NFAT promotes exhaustion of activated CD8(+) T cells. *Immunity* **42**, 265-278 (2015).

125. Scott, A.C. *et al.* TOX is a critical regulator of tumour-specific T cell differentiation. *Nature* **571**, 270-274 (2019).

126. Alfei, F. *et al.* TOX reinforces the phenotype and longevity of exhausted T cells in chronic viral infection. *Nature* **571**, 265-269 (2019).

127. Khan, O. *et al.* TOX transcriptionally and epigenetically programs CD8 + T cell exhaustion. *Nature* **571**, 211-218 (2019).

128. Kao, C. *et al.* Transcription factor T-bet represses expression of the inhibitory receptor PD-1 and sustains virus-specific CD8+ T cell responses during chronic infection. *Nat Immunol* **12**, 663-671 (2011).

129. Agnellini, P. *et al.* Impaired NFAT nuclear translocation results in split exhaustion of virus-specific CD8+ T cell functions during chronic viral infection. *Proc Natl Acad Sci U S A* **104**, 4565-4570 (2007).

130. Escobar, G., Mangani, D. & Anderson, A.C. T cell factor 1: A master regulator of the T cell response in disease. *Sci Immunol* **5** (2020).

131. Jadhav, R.R. *et al.* Epigenetic signature of PD-1+ TCF1+ CD8 T cells that act as resource cells during chronic viral infection and respond to PD-1 blockade. *Proc Natl Acad Sci U S A* **116**, 14113-14118 (2019).

132. Shan, Q. *et al.* Ectopic Tcf1 expression instills a stem-like program in exhausted CD8(+) T cells to enhance viral and tumor immunity. *Cell Mol Immunol* **18**, 1262-1277 (2021).

133. Wang, Y. *et al.* The Transcription Factor TCF1 Preserves the Effector Function of Exhausted CD8 T Cells During Chronic Viral Infection. *Front Immunol* **10**, 169 (2019).

134. Brummelman, J. *et al.* High-dimensional single cell analysis identifies stem-like cytotoxic CD8+ T cells infiltrating human tumors. *The Journal of Experimental Medicine* **215**, 2520-2535 (2018).

135. Sade-Feldman, M. *et al.* Defining T Cell States Associated with Response to Checkpoint Immunotherapy in Melanoma. *Cell* **175**, 998-1013.e1020 (2018).

136. Seo, H. *et al.* TOX and TOX2 transcription factors cooperate with NR4A transcription factors to impose CD8+ T cell exhaustion. *PNAS* **116**, 12410-12415 (2019).

137. Yao, C. *et al.* Single-cell RNA-seq reveals TOX as a key regulator of CD8 + T cell persistence in chronic infection. *Nature Immunology* **20**, 890-901 (2019).

138. Zeng, Z., Wei, F. & Ren, X. Exhausted T cells and epigenetic status. *Cancer Biol Med* **17**, 923-936 (2020).

139. Wang, X. *et al.* TOX promotes the exhaustion of antitumor CD8(+) T cells by preventing PD1 degradation in hepatocellular carcinoma. *J Hepatol* **71**, 731-741 (2019).

140. Shin, H. & Wherry, E.J. CD8 T cell dysfunction during chronic viral infection. *Current Opinion in Immunology* **19**, 408-415 (2007).

141. Virgin, H.W., Wherry, E.J. & Ahmed, R. Redefining chronic viral infection. *Cell* **138**, 30-50 (2009).

142. Hensel, N. *et al.* Memory-like HCV-specific CD8(+) T cells retain a molecular scar after cure of chronic HCV infection. *Nat Immunol* **22**, 229-239 (2021).

143. Yates, K.B. *et al.* Epigenetic scars of CD8(+) T cell exhaustion persist after cure of chronic infection in humans. *Nat Immunol* **22**, 1020-1029 (2021).

144. Anderson, A.C., Joller, N. & Kuchroo, V.K. Lag-3, Tim-3, and TIGIT: Co-inhibitory Receptors with Specialized Functions in Immune Regulation. *Immunity* **44**, 989-1004 (2016).

145. McLane, L.M., Abdel-Hakeem, M.S. & Wherry, E.J. CD8 T Cell Exhaustion During Chronic Viral Infection and Cancer. *Annual Review of Immunology* **37**, 457-495 (2019).

146. Mahoney, K.M., Rennert, P.D. & Freeman, G.J. Combination cancer immunotherapy and new immunomodulatory targets. *Nat Rev Drug Discov* **14**, 561-584 (2015).

147. Pauken, K.E. & Wherry, E.J. Overcoming T cell exhaustion in infection and cancer. *Trends in Immunology* **36**, 265-276 (2015).

148. Postow, M.A. *et al.* Nivolumab and ipilimumab versus ipilimumab in untreated melanoma. *N Engl J Med* **372**, 2006-2017 (2015).

149. Ribas, A. & Wolchok, J.D. Cancer immunotherapy using checkpoint blockade. *Science* **359**, 1350-1355 (2018).

150. Sharma, P., Hu-Lieskovan, S., Wargo, J.A. & Ribas, A. Primary, Adaptive, and Acquired Resistance to Cancer Immunotherapy. *Cell* **168**, 707-723 (2017).

151. June, C.H. & Sadelain, M. Chimeric Antigen Receptor Therapy. *N Engl J Med* **379**, 64-73 (2018).

152. Sadelain, M., Riviere, I. & Riddell, S. Therapeutic T cell engineering. *Nature* **545**, 423-431 (2017).

153. Park, J.H. *et al.* Long-Term Follow-up of CD19 CAR Therapy in Acute Lymphoblastic Leukemia. *N Engl J Med* **378**, 449-459 (2018).

154. Schuster, S.J. *et al.* Chimeric Antigen Receptor T Cells in Refractory B-Cell Lymphomas. *N Engl J Med* **377**, 2545-2554 (2017).

155. Delgoffe, G.M. *et al.* The role of exhaustion in CAR T cell therapy. *Cancer Cell* **39**, 885-888 (2021).

156. Kouro, T., Himuro, H. & Sasada, T. Exhaustion of CAR T cells: potential causes and solutions. *J Transl Med* **20**, 239 (2022).

157. Prinzing, B. *et al.* Deleting DNMT3A in CAR T cells prevents exhaustion and enhances antitumor activity. *Sci Transl Med* **13**, eabh0272 (2021).

158. Wang, Y. *et al.* Low-dose decitabine priming endows CAR T cells with enhanced and persistent antitumour potential via epigenetic reprogramming. *Nat Commun* **12**, 409 (2021).

159. Štros, M., Launholt, D. & Grasser, K.D. The HMG-box: a versatile protein domain occurring in a wide variety of DNA-binding proteins. *Cell. Mol. Life Sci.* **64**, 2590 (2007).

160. Johns, E.W. *The HMG chromosomal proteins*. Academic Press: London ; New York, 1982, pp 43-45, 59-60.

161. Vaccari, T., Beltrame, M., Ferrari, S. & Bianchi, M.E. Hmg4, a new member of the Hmg1/2 gene family. *Genomics* **49**, 247-252 (1998).

162. Štros, M. HMGB proteins: interactions with DNA and chromatin. *Biochim Biophys Acta* **1799**, 101-113 (2010).

163. Calogero, S. *et al.* The lack of chromosomal protein Hmg1 does not disrupt cell growth but causes lethal hypoglycaemia in newborn mice. *Nat Genet* **22**, 276-280 (1999).

164. Ronfani, L. *et al.* Reduced fertility and spermatogenesis defects in mice lacking chromosomal protein Hmgb2. *Development* **128**, 1265-1273 (2001).

165. Bianchi, M.E., Beltrame, M. & Paonessa, G. Specific recognition of cruciform DNA by nuclear protein HMG1. *Science* **243**, 1056-1059 (1989).

166. Hamada, H. & Bustin, M. Hierarchy of binding sites for chromosomal proteins HMG 1 and 2 in supercoiled deoxyribonucleic acid. *Biochemistry* **24**, 1428-1433 (1985).

167. Isackson, P.J., Fishback, J.L., Bidney, D.L. & Reeck, G.R. Preferential affinity of high molecular weight high mobility group non-histone chromatin proteins for single-stranded DNA. *J Biol Chem* **254**, 5569-5572 (1979).

168. Lange, S.S. & Vasquez, K.M. HMGB1: the jack-of-all-trades protein is a master DNA repair mechanic. *Mol Carcinog* **48**, 571-580 (2009).

169. Thomas, J.O. & Travers, A.A. HMG1 and 2, and related 'architectural' DNA-binding proteins. *Trends in Biochemical Sciences* **26**, 167-174 (2001).

170. Becker, N.A., Kahn, J.D. & Maher, L.J., 3rd. Eukaryotic HMGB proteins as replacements for HU in E. coli repression loop formation. *Nucleic Acids Res* **36**, 4009-4021 (2008).

171. Stros, M., Stokrova, J. & Thomas, J.O. DNA looping by the HMG-box domains of HMG1 and modulation of DNA binding by the acidic C-terminal domain. *Nucleic Acids Res* **22**, 1044-1051 (1994).

172. Zirkel, A. *et al.* HMGB2 Loss upon Senescence Entry Disrupts Genomic Organization and Induces CTCF Clustering across Cell Types. *Mol Cell* **70**, 730-744 e736 (2018).

173. Kimura, A., Matsuda, T., Sakai, A., Murao, N. & Nakashima, K. HMGB2 expression is associated with transition from a quiescent to an activated state of adult neural stem cells. *Dev Dyn* **247**, 229-238 (2018).

174. Zhang, C. *et al.* Latexin regulation by HMGB2 is required for hematopoietic stem cell maintenance. *1* **105**, 573-584 (2020).

175. Benavides Damm, T. & Egli, M. Calcium's role in mechanotransduction during muscle development. *Cell. Physiol. Biochem.* **33**, 249-272 (2014).

176. Ronfani, L. *et al.* Reduced fertility and spermatogenesis defects in mice lacking chromosomal protein Hmgb2. *Development* **128**, 1265-1273 (2001).

177. Abraham, A.B. *et al.* Members of the high mobility group B protein family are dynamically expressed in embryonic neural stem cells. *Proteome Sci* **11**, 18 (2013).

178. Agrawal, A. & Schatz, D.G. RAG1 and RAG2 form a stable postcleavage synaptic complex with DNA containing signal ends in V(D)J recombination. *Cell* **89**, 43-53 (1997).

179. Aidinis, V. *et al.* The RAG1 homeodomain recruits HMG1 and HMG2 to facilitate recombination signal sequence binding and to enhance the intrinsic DNA-bending activity of RAG1-RAG2. *Mol Cell Biol* **19**, 6532-6542 (1999).

180. van Gent, D.C., Hiom, K., Paull, T.T. & Gellert, M. Stimulation of V(D)J cleavage by high mobility group proteins. *EMBO J* **16**, 2665-2670 (1997).

181. Kwon, J., Imbalzano, A.N., Matthews, A. & Oettinger, M.A. Accessibility of nucleosomal DNA to V(D)J cleavage is modulated by RSS positioning and HMG1. *Mol Cell* **2**, 829-839 (1998).

182. Travers, A.A. Priming the nucleosome: a role for HMGB proteins? *EMBO Rep* **4**, 131-136 (2003).

183. Bonaldi, T. *et al.* Monocytic cells hyperacetylate chromatin protein HMGB1 to redirect it towards secretion. *EMBO J* **22**, 5551-5560 (2003).

184. Muller, S., Ronfani, L. & Bianchi, M.E. Regulated expression and subcellular localization of HMGB1, a chromatin protein with a cytokine function. *J Intern Med* **255**, 332-343 (2004).

185. Nemeth, M.J. *et al.* Hmgb3: an HMG-box family member expressed in primitive hematopoietic cells that inhibits myeloid and B-cell differentiation. *Blood* **102**, 1298-1306 (2003).

186. Duff, M.O. *et al.* Genome-wide identification of zero nucleotide recursive splicing in Drosophila. *Nature* **521**, 376-379 (2015).

187. Fagerberg, L. *et al.* Analysis of the human tissue-specific expression by genome-wide integration of transcriptomics and antibody-based proteomics. *Mol Cell Proteomics* **13**, 397-406 (2014).

188. Syed, N. *et al.* Silencing of high-mobility group box 2 (HMGB2) modulates cisplatin and 5-fluorouracil sensitivity in head and neck squamous cell carcinoma. *Proteomics* **15**, 383-393 (2015).

189. Fu, D. *et al.* HMGB2 is associated with malignancy and regulates Warburg effect by targeting LDHB and FBP1 in breast cancer. *Cell Communication and Signaling* **16**, 8 (2018).

190. Redmond, A.M. *et al.* Genomic interaction between ER and HMGB2 identifies DDX18 as a novel driver of endocrine resistance in breast cancer cells. *Oncogene* **34**, 3871-3880 (2015).

191. Shin, Y.J. *et al.* High-mobility group box 2 (HMGB2) modulates radioresponse and is downregulated by p53 in colorectal cancer cell. *Cancer Biol Ther* **14**, 213-221 (2013).

192. Cui, G., Cai, F., Ding, Z. & Gao, L. HMGB2 promotes the malignancy of human gastric cancer and indicates poor survival outcome. *Hum Pathol* **84**, 133-141 (2019).

193. Li, H., Zhang, H. & Wang, Y. Centromere protein U facilitates metastasis of ovarian cancer cells by targeting high mobility group box 2 expression. *Am J Cancer Res* **8**, 835-851 (2018).

194. Qiu, X. *et al.* Identification of HMGB2 associated with proliferation, invasion and prognosis in lung adenocarcinoma via weighted gene co-expression network analysis. *BMC Pulm Med* **22**, 310 (2022).

195. Williams, M.A. & Bevan, M.J. Effector and memory CTL differentiation. *Annu Rev Immunol* **25**, 171-192 (2007).

196. Martin, M.D. & Badovinac, V.P. Defining Memory CD8 T Cell. *Front Immunol* **9**, 2692 (2018).

197. Ahmed, R. & Gray, D. Immunological memory and protective immunity: understanding their relation. *Science* **272**, 54-60 (1996).

198. Sarkar, S. *et al.* Functional and genomic profiling of effector CD8 T cell subsets with distinct memory fates. *J Exp Med* **205**, 625-640 (2008).

199. Milner, J.J. *et al.* Delineation of a molecularly distinct terminally differentiated memory CD8 T cell population. *Proc Natl Acad Sci U S A* **117**, 25667-25678 (2020).

200. Jameson, S.C. & Masopust, D. Understanding Subset Diversity in T Cell Memory. *Immunity* **48**, 214-226 (2018).

201. Dominguez, C.X. *et al.* The transcription factors ZEB2 and T-bet cooperate to program cytotoxic T cell terminal differentiation in response to LCMV viral infection. *J Exp Med* **212**, 2041-2056 (2015).

202. Kallies, A., Xin, A., Belz, G.T. & Nutt, S.L. Blimp-1 transcription factor is required for the differentiation of effector CD8(+) T cells and memory responses. *Immunity* **31**, 283-295 (2009).

203. Mollo, S.B., Ingram, J.T., Kress, R.L., Zajac, A.J. & Harrington, L.E. Virus-specific CD4 and CD8 T cell responses in the absence of Th1-associated transcription factors. *J Leukoc Biol* **95**, 705-713 (2014).

204. Omilusik, K.D. *et al.* Transcriptional repressor ZEB2 promotes terminal differentiation of CD8+ effector and memory T cell populations during infection. *J Exp Med* **212**, 2027-2039 (2015).

205. Omilusik, K.D. *et al.* Sustained Id2 regulation of E proteins is required for terminal differentiation of effector CD8(+) T cells. *J Exp Med* **215**, 773-783 (2018).

206. Rutishauser, R.L. *et al.* Transcriptional repressor Blimp-1 promotes CD8(+) T cell terminal differentiation and represses the acquisition of central memory T cell properties. *Immunity* **31**, 296-308 (2009).

207. Banerjee, A. *et al.* Cutting edge: The transcription factor eomesodermin enables CD8+ T cells to compete for the memory cell niche. *J Immunol* **185**, 4988-4992 (2010).

208. Ji, Y. *et al.* Repression of the DNA-binding inhibitor Id3 by Blimp-1 limits the formation of memory CD8+ T cells. *Nat Immunol* **12**, 1230-1237 (2011).

209. Yang, C.Y. *et al.* The transcriptional regulators Id2 and Id3 control the formation of distinct memory CD8+ T cell subsets. *Nat Immunol* **12**, 1221-1229 (2011).

210. Ueda, T. & Yoshida, M. HMGB proteins and transcriptional regulation. *Biochimica et Biophysica Acta (BBA) - Gene Regulatory Mechanisms* **1799**, 114-118 (2010).

211. Mallik, R., Kundu, A. & Chaudhuri, S. High mobility group proteins: the multifaceted regulators of chromatin dynamics. *Nucleus* **61**, 213-226 (2018).

212. Wherry, E.J. *et al.* Molecular signature of CD8+ T cell exhaustion during chronic viral infection. *Immunity* **27**, 670-684 (2007).

213. Chen, X., Zhang, B., Wang, T., Bonni, A. & Zhao, G. Robust principal component analysis for accurate outlier sample detection in RNA-Seq data. *BMC Bioinformatics* **21**, 269 (2020).

214. Corces, M.R. *et al.* An improved ATAC-seq protocol reduces background and enables interrogation of frozen tissues. *Nat Methods* **14**, 959-962 (2017).

215. Olive, P.L. & Banath, J.P. The comet assay: a method to measure DNA damage in individual cells. *Nat Protoc* **1**, 23-29 (2006).

216. Mah, L.J., El-Osta, A. & Karagiannis, T.C. gammaH2AX: a sensitive molecular marker of DNA damage and repair. *Leukemia* **24**, 679-686 (2010).

217. Chen, Y., Zander, R., Khatun, A., Schauder, D.M. & Cui, W. Transcriptional and Epigenetic Regulation of Effector and Memory CD8 T Cell Differentiation. *Front Immunol* **9**, 2826 (2018).

218. Korinfskaya, S., Parameswaran, S., Weirauch, M.T. & Barski, A. Runx Transcription Factors in T Cells-What Is Beyond Thymic Development? *Front Immunol* **12**, 701924 (2021).

219. Quigley, M., Huang, X. & Yang, Y. STAT1 signaling in CD8 T cells is required for their clonal expansion and memory formation following viral infection in vivo. *J Immunol* **180**, 2158-2164 (2008).

220. Yuzefpolskiy, Y., Baumann, F.M., Kalia, V. & Sarkar, S. Early CD8 T-cell memory precursors and terminal effectors exhibit equipotent in vivo degranulation. *Cell Mol Immunol* **12**, 400-408 (2015).

221. Barber, D.L. *et al.* Restoring function in exhausted CD8 T cells during chronic viral infection. *Nature* **439**, 682-687 (2006).

222. Franco, F., Jaccard, A., Romero, P., Yu, Y.R. & Ho, P.C. Metabolic and epigenetic regulation of T-cell exhaustion. *Nat Metab* **2**, 1001-1012 (2020).

223. Speiser, D.E. *et al.* T cell differentiation in chronic infection and cancer: functional adaptation or exhaustion? *Nat Rev Immunol* **14**, 768-774 (2014).

224. Kallies, A., Zehn, D. & Utzschneider, D.T. Precursor exhausted T cells: key to successful immunotherapy? *Nat Rev Immunol* **20**, 128-136 (2020).

225. Lau, J.S.Y. *et al.* The impact of immune checkpoint therapy on the latent reservoir in HIV-infected individuals with cancer on antiretroviral therapy. *AIDS* **35**, 1631-1636 (2021).

226. Rutishauser, R.L. *et al.* TCF-1 regulates HIV-specific CD8+ T cell expansion capacity. *JCI Insight* **6** (2021).

227. Wong, W.K. *et al.* The Interplay Between Epigenetic Regulation and CD8(+) T Cell Differentiation/Exhaustion for T Cell Immunotherapy. *Front Cell Dev Biol* **9**, 783227 (2021).

228. Das, S. & Johnson, D.B. Immune-related adverse events and anti-tumor efficacy of immune checkpoint inhibitors. *J Immunother Cancer* **7**, 306 (2019).

229. Mo, Y. *et al.* MicroRNA-329 upregulation impairs the HMGB2/beta-catenin pathway and regulates cell biological behaviors in melanoma. *J Cell Physiol* **234**, 23518-23527 (2019).

230. Lou, N., Zhu, T., Qin, D., Tian, J. & Liu, J. High-mobility group box 2 reflects exacerbated disease characteristics and poor prognosis in non-small cell lung cancer patients. *Ir J Med Sci* (2021).

231. Li, H. *et al.* Dysfunctional CD8 T Cells Form a Proliferative, Dynamically Regulated Compartment within Human Melanoma. *Cell* **181**, 747 (2020).

232. Kaczanowska, S. *et al.* Genetically engineered myeloid cells rebalance the core immune suppression program in metastasis. *Cell* **184**, 2033-2052 e2021 (2021).

233. Kramer, A., Green, J., Pollard, J., Jr. & Tugendreich, S. Causal analysis approaches in Ingenuity Pathway Analysis. *Bioinformatics* **30**, 523-530 (2014).

234. Chen, Z. *et al.* TCF-1-Centered Transcriptional Network Drives an Effector versus Exhausted CD8 T Cell-Fate Decision. *Immunity* **51**, 840-855 e845 (2019).

235. Aliahmad, P. *et al.* TOX provides a link between calcineurin activation and CD8 lineage commitment. *J Exp Med* **199**, 1089-1099 (2004).

236. Laurent, B. *et al.* High-mobility group protein HMGB2 regulates human erythroid differentiation through trans-activation of GFI1B transcription. *Blood* **115**, 687-695 (2010).

237. Abraham, A.B. *et al.* Aberrant neural stem cell proliferation and increased adult neurogenesis in mice lacking chromatin protein HMGB2. *PLoS One* **8**, e84838 (2013).

238. Fang, Y. *et al.* High mobility group box 2 regulates skeletal muscle development through ribosomal protein S6 kinase 1. *FASEB J* **34**, 12367-12378 (2020).

239. Taniguchi, N. *et al.* Chromatin protein HMGB2 regulates articular cartilage surface maintenance via beta-catenin pathway. *Proc Natl Acad Sci U S A* **106**, 16817-16822 (2009).

240. Tabana, Y., Moon, T.C., Siraki, A., Elahi, S. & Barakat, K. Reversing T-cell exhaustion in immunotherapy: a review on current approaches and limitations. *Expert Opin Ther Targets* **25**, 347-363 (2021).

241. Zhang, Z. *et al.* T Cell Dysfunction and Exhaustion in Cancer. *Front Cell Dev Biol* **8**, 17 (2020).

242. Xing, S. *et al.* Tcf1 and Lef1 are required for the immunosuppressive function of regulatory T cells. *J Exp Med* **216**, 847-866 (2019).

243. Shan, Q. *et al.* Tcf1 and Lef1 provide constant supervision to mature CD8(+) T cell identity and function by organizing genomic architecture. *Nat Commun* **12**, 5863 (2021).

244. Blattman, J.N., Wherry, E.J., Ha, S.J., van der Most, R.G. & Ahmed, R. Impact of epitope escape on PD-1 expression and CD8 T-cell exhaustion during chronic infection. *J Virol* **83**, 4386-4394 (2009).

245. Kurachi, M. *et al.* Optimized retroviral transduction of mouse T cells for in vivo assessment of gene function. *Nat Protoc* **12**, 1980-1998 (2017).

246. Zebley, C.C. & Youngblood, B. Mechanisms of T cell exhaustion guiding next-generation immunotherapy. *Trends Cancer* **8**, 726-734 (2022).

247. Trebak, M. & Kinet, J.P. Calcium signalling in T cells. *Nat Rev Immunol* **19**, 154-169 (2019).

248. Sofiadis, K. *et al.* HMGB1 coordinates SASP-related chromatin folding and RNA homeostasis on the path to senescence. *Mol Syst Biol* **17**, e9760 (2021).

249. Yu, B. *et al.* Epigenetic landscapes reveal transcription factors that regulate CD8(+) T cell differentiation. *Nat Immunol* **18**, 573-582 (2017).

250. Lewis, S.A. *et al.* Ethanol Consumption Induces Nonspecific Inflammation and Functional Defects in Alveolar Macrophages. *Am J Respir Cell Mol Biol* **67**, 112-124 (2022).

251. King, C.G. *et al.* T cell affinity regulates asymmetric division, effector cell differentiation, and tissue pathology. *Immunity* **37**, 709-720 (2012).

252. Zehn, D., Lee, S.Y. & Bevan, M.J. Complete but curtailed T-cell response to very low-affinity antigen. *Nature* **458**, 211-214 (2009).

253. Daniels, M.A. *et al.* Thymic selection threshold defined by compartmentalization of Ras/MAPK signalling. *Nature* **444**, 724-729 (2006).

254. Stefanova, I. *et al.* TCR ligand discrimination is enforced by competing ERK positive and SHP-1 negative feedback pathways. *Nat Immunol* **4**, 248-254 (2003).

255. Burger, M.L. *et al.* Antigen dominance hierarchies shape TCF1(+) progenitor CD8 T cell phenotypes in tumors. *Cell* **184**, 4996-5014 e4926 (2021).

256. Daniel, B. *et al.* Divergent clonal differentiation trajectories of T cell exhaustion. *Nat Immunol* **23**, 1614-1627 (2022).

257. Shakiba, M. *et al.* TCR signal strength defines distinct mechanisms of T cell dysfunction and cancer evasion. *J Exp Med* **219** (2022).

258. Starkova, T., Polyanichko, A., Tomilin, A.N. & Chikhirzhina, E. Structure and Functions of HMGB2 Protein. *Int J Mol Sci* **24** (2023).

259. Breschi, A., Gingeras, T.R. & Guigo, R. Comparative transcriptomics in human and mouse. *Nat Rev Genet* **18**, 425-440 (2017).

260. Cheng, Y. *et al.* Principles of regulatory information conservation between mouse and human. *Nature* **515**, 371-375 (2014).

261. Yue, F. *et al.* A comparative encyclopedia of DNA elements in the mouse genome. *Nature* **515**, 355-364 (2014).

262. King, D.C. *et al.* Finding cis-regulatory elements using comparative genomics: some lessons from ENCODE data. *Genome Res* **17**, 775-786 (2007).

263. Ponting, C.P. The functional repertoires of metazoan genomes. *Nat Rev Genet* **9**, 689-698 (2008).

264. Doeing, D.C., Borowicz, J.L. & Crockett, E.T. Gender dimorphism in differential peripheral blood leukocyte counts in mice using cardiac, tail, foot, and saphenous vein puncture methods. *BMC Clin Pathol* **3**, 3 (2003).

265. Chu, D.H. *et al.* Pre-T cell receptor signals are responsible for the down-regulation of Syk protein tyrosine kinase expression. *J Immunol* **163**, 2610-2620 (1999).

266. Elder, M.E. *et al.* Distinct T cell developmental consequences in humans and mice expressing identical mutations in the DLAARN motif of ZAP-70. *J Immunol* **166**, 656-661 (2001).

267. Fischer, A. *et al.* Naturally occurring primary deficiencies of the immune system. *Annu Rev Immunol* **15**, 93-124 (1997).

268. Farrar, J.D. *et al.* Selective loss of type I interferon-induced STAT4 activation caused by a minisatellite insertion in mouse Stat2. *Nat Immunol* **1**, 65-69 (2000).

269. Pober, J.S., Kluger, M.S. & Schechner, J.S. Human endothelial cell presentation of antigen and the homing of memory/effector T cells to skin. *Ann N Y Acad Sci* **941**, 12-25 (2001).